Università degli Studi di Milano

Dipartimento della Salute

Laboratori di Farmacologia, Polo Universitario S. Paolo

Dottorato di Ricerca in

Fisiopatologia, Farmacologia, Clinica e Terapia

delle Malattie Metaboliche (XXV ciclo)

Effects of GMG-43AC on adipocyte differentiation in the culture of 3T3-L1 cells

Settore scientifico disciplinare: **BIO-14**

Coordinatore del Corso di Dottrato: **Chiar.mo Prof. A. Gorio**

Docente Guida: **Chiar.mo Prof. A. Gorio**

Tesi di dottorato di: **Hebda Danuta Maria**

Matr. n° R08825

Anno accademico 2011-2012

alla mia famiglia

e a Paolo

Index

1. SUMMARY

In recent decades, obesity has become a prominent health problem in many countries. It is closely linked to cardiovascular disease, type 2 diabetes mellitus and metabolic syndrome, resulting in increasing morbidity and mortality. Hence, it is necessary to develop effective prevention and treatment of obesity.

In this study, we examined whether GMG-43AC, the new experimental drug of Giuliani Sp. A. (Milano, Italy), could inhibit the differentiation induced by a hormone mixture (IBMX, DEX and insulin) or troglitazone of 3T3-L1 preadipocytes, and further explored the possible mechanism of action. 3T3-L1 cells constitute one of the most popular *in vitro* models for the investigation of adipogenesis. To achieve the goals proposed in this research project it was necessary to set up: a) the differentiation protocol for 3T3-L1 cells; b) the colorimetric technique for detecting adipocytes droplets, and c) the quantification assay for accumulated triglycerides. In our experimental conditions droplets of triglycerides accumulated in differentiated 3T3-L1 cells were highly positive to the Oil Red O staining.

As evidenced by Oil Red O staining, GMG-43AC dose-dependent inhibited triglycerides synthesize and accumulate at concentrations of 500, 1000 and 2000 µM.

Studies in adipogenic cell lines have shown that the differentiation of preadipocytes into adipocytes is accompanied by changes in gene expression: e.g., a dramatic increase in the expression of the CCAAT/enhancer-binding proteins C/EBPβ and C/EBPδ followed by the expression C/EBPα and the nuclear hormone receptor peroxisome proliferator-activated receptor γ (PPARγ).

At the molecular level, the expression of transcription factors, C/EBPβ, PPARγ and C/EBPα, was reduced by GMG-43AC during adipogenesis. After treatment for 10 days, the mRNA levels of adipocyte-specific genes, such as FABP-4 and leptin, were also down-regulated by GMG-43AC in a dose-dependent manner. Furthermore, the exposure to GMG-43AC during the initial 48 hours of adipocyte differentiation markedly reduced C/EBPβ levels in a dose-dependent manner with the exception of the dose 300 µM.

Moreover, we investigated the capability of GMG-43AC to revert the adipocyte differentiation process induced by hormone stimulants or troglitazone. We observed that GMG-43AC was able to revert the adipocyte phenotype in fully differentiated adipocytes. The reverting effect of GMG-43AC treatment can be observed from concentrations of 500 µM or greater. Interestingly, the drug left in the culture medium for the period of 14 days

became more effective in the reversion of differentiation with respect to the treatment for 7 days. The accurate molecular mechanisms that regulate loss of accumulated triglycerides in fully differentiated adipocytes are still unclear and will be investigated in the near future.

Thus, GMG-43AC has the potential to be an innovative product for the prevention and treatment of obesity.

2. INTRODUCTION

2.1. Introduction to obesity

Obesity is one of the world's greatest public health challenges, contributing to morbidity and mortality through the increased risk for many chronic diseases, including type 2 diabetes, hypertension, dyslipidemia, coronary artery disease, stroke, osteoarthritis and certain forms of cancer (Youngson NA et al., 2012). Obesity is a multifactorial disorder and it is most commonly caused by a combination of excessive food energy intake, lack of physical activity, and genetic susceptibility, although a few cases are caused primarily by alterations, endocrine disorders, medication or psychiatric illness (Hossain P et al., 2007).

Body weight regulation depends on the interaction between genetic, environmental and psychosocial factors. The prevalence of obesity is increasing worldwide at an alarming rate, which indicates that the primary cause of the excessive energy storage lies in environmental and behavioural changes rather than in genetic modifications. The factors that influence body weight regulation ultimately act by a chronic modification of the energy balance equation:

Energy stored = energy intake - energy lost in feces and urine - energy expenditure

Obesity is a problem of imbalance between energy intake and expenditure. Cellular events can cause obesity only if they affect energy balance (Fig.1). This means that changes in the expression of genes which control the differentiation and the development of adipocytes are not primarily responsible for the gain in body weight. A minor imbalance between energy intake and energy expenditure may lead to severe obesity: if energy intake exceeds energy expenditure by 5% every day, this results in a gain of 5 kg fat mass over one year, and to morbid obesity over several years (Jéquier E, 2002).

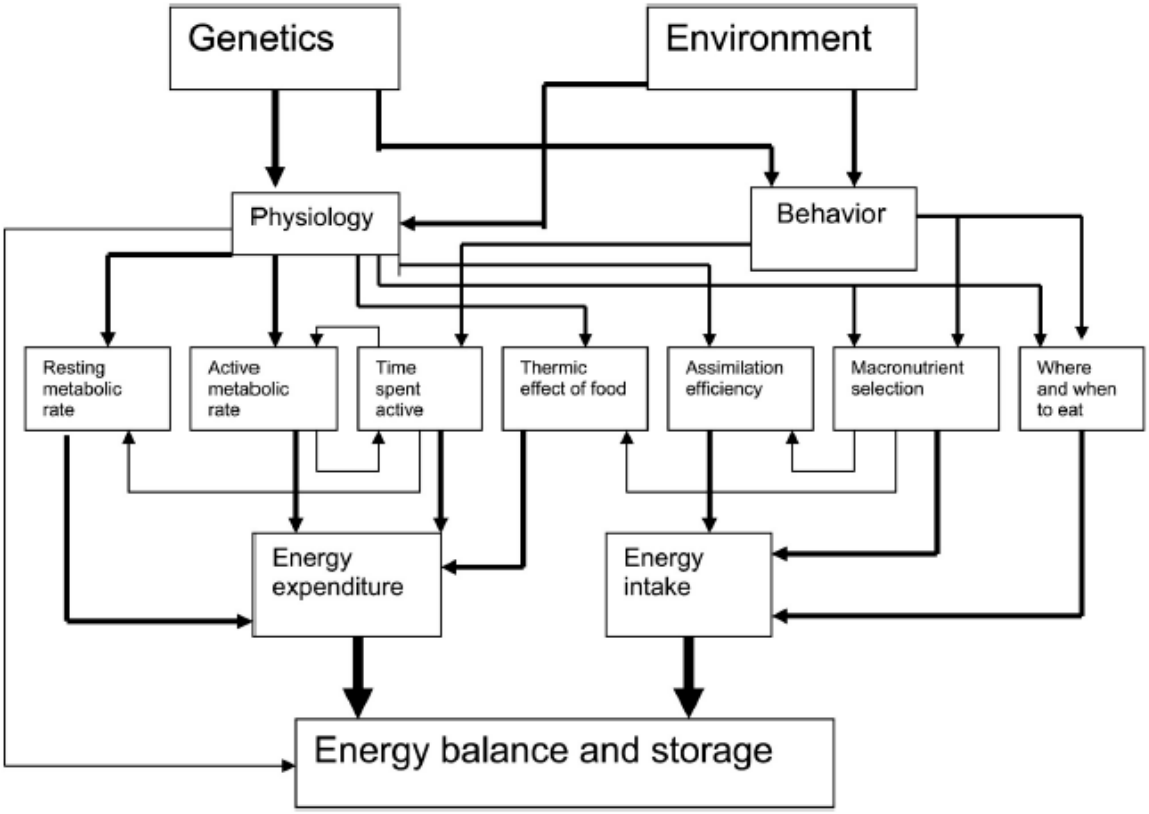

Fig. 1 **The major causal linkages among genetics, environmental effects, physiology, behaviour, and energy balance** (from Speakman JM, 2004).

The increase in the prevalence of obesity has been observed worldwide, and will most likely continue to be an important risk factor for the health of all populations, in particular of those in developing countries (Day FR et al., 2011). Over the past 20 years, the rate of obesity has tripled in developing countries. Obesity has become recognized as one of the major health problems threatening the world today, along with malnourishment and infectious diseases. The International Obesity Task Force and the World Health Organization (WHO) report over 1.1 billion adults worldwide are overweight, 312 million of whom are obese. In addition, over 155 million children are overweight or obese worldwide; 42 million of these children are under the age of 5. The areas of the world at greatest risk due to due to increasing prevalence are the Middle East, Pacific Islands, Southeast Asia, and China. Obesity is highly prevalent in the middle-income countries of Eastern Europe, Latin America, and Asia, where obesity is the fifth most common cause of disease, ranking just below malnourishment (Hossain P et al., 2007; Haidar YM et al., 2011).

2.1.1. Effects of obesity

Obesity's health risks include a long list of debilitating but not life-threatening diseases like respiratory difficulties, osteoarthritis, skin problems, infertility, etc. Increased body fat leads to adverse metabolic effects on blood pressure, insulin resistance, and cholesterol levels. The major obesity-associated conditions stem from these metabolic effects: cardiovascular disease, type 2 diabetes, cancers (particularly colorectal, breast, prostate, endometrial, kidney, and gallbladder), and gallbladder disease (Hossain P et al., 2007; Haidar YM et al., 2011).

The risk of cardiovascular disease is considerably greater among obese people, and this group has an incidence of hypertension that is greater in comparison to people of normal bodyweight (Hossain P et al., 2007).

The increase in the prevalence of type 2 diabetes is closely linked to the upsurge in obesity. About 90% of type 2 diabetes cases can be attributed to excess weight. Furthermore, obesity-related metabolic syndrome causes impaired glucose tolerance in 197 million people worldwide. This number is expected to increase to 420 million by 2025, with the most prominent increase in developing countries (Hossain P et al., 2007; Haidar YM et al., 2011).

Obesity, diabetes, and hypertension also affect the kidneys. Diabetic nephropathy develops in about one third of patients with diabetes, and its incidence is sharply increasing in the developing world. The WHO Multinational Study of Vascular Disease in Diabetes showed that proteinuria was associated with an increased risk of death from chronic kidney disease or cardiovascular disease, as well as of death from any cause (Hossain P et al., 2007).

2.1.2. Childhood obesity

Childhood obesity is a global problem, but the prevalence is higher in developed countries, particularly the United States. Changing diet and decreasing physical activity are believed to be the two most important factors in causing the recent increase in the rates. Worldwide, the childhood obesity prevalence in 2010 was 6.7%. Interestingly, in both developed and developing countries, the prevalence of overweight girls is greater than overweight boys, particularly among adolescents: 70% of obese adolescents become obese adults. This has led many observers to view childhood obesity as the root of the obesity problem, and also its most potentially tractable element (Haidar YM et al., 2011).

2.1.3. Etiology

Rising incomes, increasing urban populations, diets high in fats and simple sugars, and a shift toward less physically demanding jobs are some of the societal changes resulting in increased obesity. Less physical activity is promoted by automated transport, labor-saving technology in the home and workplace, television, and computer games. These changes in the social environment promote excessive food intake and decreased physical activity, leading to obesity. Studies in humans have shown that a high-fat diet (>35% of calories from fat) leads to increased energy intake, efficiency of body fat gain, and obesity (Haidar YM et al., 2011).

2.1.4. Genetics

Numerous studies have confirmed the contribution of genetics in the obesity epidemic. Ten percent of morbidly obese children come from consanguineous families, suggesting that other forms of genetic links are present (Friedman JM, 2003; Haidar YM et al., 2011). There are clear genetic elements in obesity. Genetic polymorphisms, causing decreased or nonfunctional levels of leptin or malfunctioning mutations in the leptin receptor, result in an abnormally high appetite and obesity beginning in childhood (Haidar YM et al., 2011).

Obesity is a problem of imbalance between energy intake and expenditure. The expansion of the prevalence of obesity reflects changes that have occurred in our behaviour (activity and food intake) that are dependent on the changing environment rather than the effects of population genetics. Moreover, the susceptibility of individuals to obesity is differential. Whatever environment or time period we choose, we find a mix of obese and lean people. These differences may reside in the microstructure of the environment experienced by each individual or may depend on genetic differences. An important point to recognize is that genetics and environmental factors exert their effects on energy balance and obesity via effects on our behaviour and physiology (Fig. 1). There is no direct link between our genes and our body weight or fatness. This is frequently misunderstood as is evidenced by discussions about whether obesity is caused by our genes or our behaviour. Behaviour and genes are different levels of the same causal framework. Consequently, although we might say that obesity has a large genetic component to it, this doesn't mean that the obese have somehow miraculously deposited enormous quantities of body fat without eating too much food, or expending too little energy, or doing both (Speakman JM, 2004).

2.1.5. Energy homeostasis

Energy homeostasis is controlled by neurons in the hypothalamus that regulate both appetite and metabolism. Endocrine signals such as glucose, insulin, free fatty acids, and leptin send messages about the body's energy state to the hypothalamus, thus controlling the firing of these neurons (Haidar YM et al., 2011). Leptin is a 167-amino acid peptide hormone encoded by the obesity (ob) gene and secreted by white adipocytes. Leptin is the satiety hormone, providing negative feedback to the hypothalamus to control appetite and energy expenditure (Feng H et al., 2012). The blood concentration of leptin is increased in obese individuals. Circulating leptin can cross the blood–brain barrier and bind to receptors (LEPR) in the brain, where it acts to decrease food intake and promote energy expenditure. With weight loss, circulating leptin decreases, leading to increased appetite and decreased energy expenditure. Variation among individuals may explain why some people seem protected against becoming overweight despite living in the same environment and consuming the same food as the obese. The leptin system also helps explain why it is more difficult to lose weight than to gain. Genetic deficiency of leptin or its receptors results in abnormally high appetite followed by the extent of fat stores. The consequent extreme hyperphagia and reduced energy expenditure produce massive obesity (Haidar YM et al., 2011; Feng H et al., 2012).

2.2. GMG-43AC features

GMG-43AC is a new experimental drug from Giuliani Sp.A (Milano, Italy). GMG-43AC is a white powder with molecular weight at 237.22 gr/l. It is soluble in DMSO (dimethyl sulfoxide) (up to 0.1-1 gr/ml) and also in water (up to 1-10 gr/l).

Calculated physic-chemical proprieties:

Conditions:

- Temperature 25^0C
- Pressure 760 mmHg
- Vapour pressure -12.56 log(atm)
- Boiling point 350.7^0C
- Water diffusion $6.06x10^{-6}cm^2/sec$

- Density 1.19 g/cm^3
- Refractive index 1.53
- Electron affinity -0.24 eV
- Heat of vaporization 34,97 Kcal/mol
- Air diffusion 0.044 cm^2/sec
- Volume 199.3 cm^3/mol
- Polarizability 24.44 Å^3
- logP (octanol/water) 1,79

Solvent	Henry constant log(atm/(mol/l))	Activity coefficient log	Solubility log(mole fraction)	Solubility log(mole/l)
Water	-9.58	3.69	-4.72	-2.98
DMSO	-14.32	1.65	-1.03	0.12
n-Octanol	-10.96	1.36	-2.39	-1.59
Tetrahydrofuran	-11.24	1.37	-2.40	-1.32
Ethyl ether	-10.92	1.60	-2.63	-1.64
Acetone	-12.20	0.47	-1.33	-0.18
N,N-Dimethylformamide	-12.56	0.05	-1.03	-0.06
Chloroform	-9.89	2.74	-3.77	-2.67
Methanol	-10.94	1.97	-3.00	-1.62
Ethanol	-11.04	1.72	-2.75	-1.51
Cyclohexane	-7.37	5.12	-6.15	-5.19
1,2-Dichloroethane	-9.95	2.67	-3.71	-2.61
1,2-Dichlorobenzene	-8.73	3.73	-4.77	-3.82
Toluene	-9.46	3.04	-4.07	-3.10
Acetonitrile	-13.32	0.52	-1.03	0.24
Dioxane	-11.18	1.41	-2.44	-1.38

Table 1. **Physic-chemical proprieties of GMG-43AC.**

2.3. Introduction to adipogenesis

The adipocytes play a critical role in energy balance. Adipogenesis is a hyperplasia process of adipose cells. It begins with a common multipotent precursor cell, that progressively goes through four sequential phases (Fig. 2): preconfluent proliferation; growth arrest; clonal expansion and terminal differentiation (Gregoire FM et al., 1998; Hansen JB et al., 1999; Prusty B et al, 2002; Fève B, 2005).

A confluence, induction of differentiation by appropriate treatment leads to cell shape changes. The preadipocyte converts to a spherical shape, accumulates lipid droplets, and

progressively acquires the morphological and biochemical characteristics of a mature adipocyte. During adipocyte differentiation cell morphology, cytoskeletal components and the level and type of extracellular matrix components (ECM) change (Gregoire FM et al., 1998; Fève B, 2005).

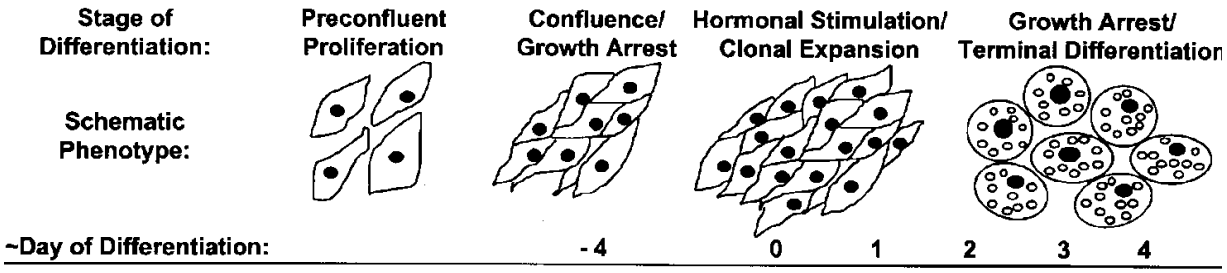

***Fig. 2* Summary of in vitro adipocyte differentiation** (from Cowherd RM et al., 1999).

Adipogenesis starts when cells stop growing as a consequence of contact inhibition. In the clonal expansion phase cells can re-enter in the cell cycle and divide once or twice. This phase occurs after confluent cells are treated with differentiation-inducing agents (see: part 1.3.1.). The last phase of adipogenesis is the terminal differentiation. In this phase the preadipocyte takes on the characteristics of the mature adipocyte - it acquires the machinery that is necessary for lipid transport and synthesis, insulin sensitivity and the secretion of adipocyte-specific proteins. During the terminal phase of differentiation, activation of the transcriptional cascade leads to increased activity and mRNA levels for enzymes involved in triacylglycerol synthesis and degradation. Glucose transporters, insulin receptor numbers, and insulin sensitivity also increase. Synthesis of adipocyte-secreted products including leptin, adipsin, resistin, etc.

Several cellular models are available to study adipogenesis that involve almost all stages of development, such as embryonic stem cells and mouse embryo fibroblasts. The cellular and molecular mechanism of adipocyte differentiation has been studied by using preadipocyte culture systems. Various preadipocyte cell lines and primary cultures of adipose-derived stromal vascular precursor cells have been used. The most frequently employed murine cell lines are 3T3-L1 and 3T3-F442A. These were clonally isolated from Swiss 3T3 cells derived from 17- to 19-day mouse embryos. The most popular human model is represented by human

primary white adipocyte cells isolated from fat biopsies. *In vitro*-differentiated adipocytes have many characteristics of adipose cells *in vivo*. The 3T3-L1 mouse cells differentiate spontaneously when exposed to a hormonal cocktail composed of dexamethasone (DEX), 3-isobutyl-1-methylxanthine (IBMX), and high concentration of insulin (Gregoire FM et al., 1998; Prusty B et al., 2002; Fève B, 2005).

2.3.1. The role of dexamethasone, 3-isobutyl-1-methylxanthine, and insulin in 3T3-L1 adipocyte differentiation

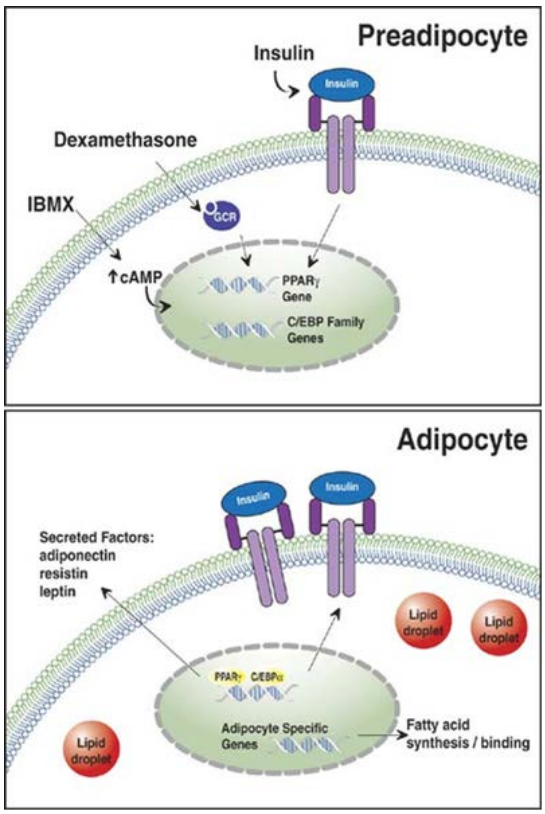

***Fig. 3* Stimulation of adipogenesis process in vitro.** Preadipocytes, such as 3T3-L1 cells (top panel), can be stimulated to undergo differentiation to adipocytes by addition of IBMX, dexamethasone and insulin. IBMX increases intracellular cAMP, dexamethasone binds to the glucocorticoid receptor and insulin binds to the insulin receptor. These three pathways culminate in activation of the PPARγ and C/EBP family genes. Adipocytes (lower panel) contain PPARγ and C/EBPα, which activate adipocyte-specific genes encoding secreted factors, insulin receptor, and proteins involved in the synthesis and binding of fatty acids that compose Oil Red O-stainable lipid droplets.

3T3-L1 cells (Fig. 3, top panel), can be stimulated to undergo differentiation to adipocytes by the addition of IBMX, dexamethasone and insulin. **Dexamethasone (DEX)** is a synthetic glucocorticoid. It has been demonstrated in 3T3-L1 cells that glucocorticoids induce expression of C/EBPδ. This increase may contribute to the formation of C/EBPβ-C/EBPδ heterodimer, which in turn may leads to PPARγ and C/EBPα expression. Moreover, DEX inhibits the transcription of protein Pref-1 *(preadipocyte factor-1)* which is the marker of preadipocytes and also the inhibitor of adipogenesis (Sul HS, 2009). **3-isobutyl-1-methylxanthine (IBMX)** is a xanthine derivative. IBMX is a phosphodiesterase inhibitor which raises intracellular cAMP level. This step is crucial for the induction of adipocyte differentiation. High level of cAMP actives *cAMP response element-binding* (CREB) and in consequence induces the expression of C/EBPβ. It was shown that IBMX accelerates the adipogenesis and slows the proliferation (Gregoire FM et al., 1998; Cowherd RM et al., 1999).

Insulin has a prominent and complex role in the development of adipose cells, serving as a growth or differentiation factor depending on the specific cell type. Insulin has marked effects on adipogenesis. In the early stages of adipogenesis, insulin functions predominantly through insulin growth factor-1 (IGF-1) receptor signalling. The IGF-1 and insulin receptors are tyrosine kinases that can activate the Ras-MAPK pathway. Insulin is a weak activator of ERK2 but is unable to activate ERK1, nevertheless, it is able to potentiate the phosphorylation of both of these kinase in the presence of IBMX and DEX (Prusty D et al., 2002). Preadipocytes express many more receptors for IGF-1 than for insulin, although this ratio shifts during differentiation proceeds (Hu E et al., 1996). From the metabolic point of view insulin stimulates the GLUT-4 translocation and glucose entries in adipose cells. Downstream components of the insulin/IGF1 signalling cascade are also crucially important for adipogenesis (Fig. 4). The loss of individual insulin-receptor substrate (IRS) proteins inhibits adipogenesis, with an order of importance of IRS1>IRS3>IRS2>IRS4. IRSs, in the early phase of differentiation, directly regulate the expression of PPARγ and C/EBPα by the activation of CREB. Moving down the insulin signalling cascade, inhibition of phosphatidylinositol-3 kinase (PI3K) as well as loss of AKT1/protein kinase B (PKB) or AKT2/PKB blocks adipogenesis (Garofalo RS et al., 2003; Xu J et al., 2004). Other downstream effectors of insulin action, such as mammalian target of rapamycin (mTOR), have also been shown to be involved in adipogenesis (Kim JE et al., 2004). Moreover, insulin inhibits the hormone sensitive lipase activity reducing the release of free fatty acids. Insulin acutely inhibits lipolysis via inhibition of the above cAMP-dependent pathway by PKB-dependent phosphorylation and activation of phosphodiesterase, which in turn lowers cAMP levels (Kershaw EE et al., 2006). At the same time, insulin inhibits GATA2 and GATA3 factors that act as differentiation inhibitors (Rosen ED et al., 2006).

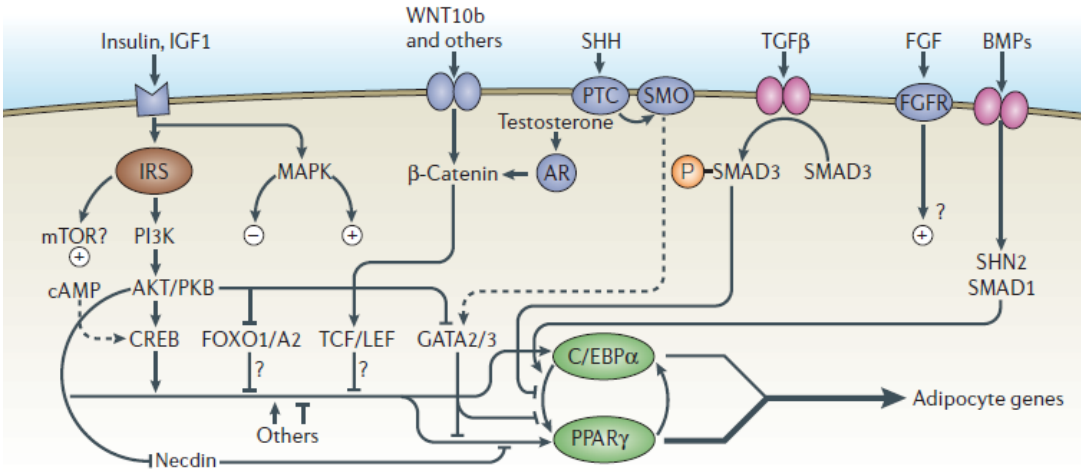

Fig. 4 **Regulation of adipogenesis by extracellular factors.** Signals from activators and repressors of adipogenesis are integrated in the nucleus by transcription factors that directly or indirectly regulate expression of peroxisome proliferator-activated receptor γ (PPARγ) and CCAAT-enhancer-binding protein α (C/EBPα). In the scheme it is emphasized the role of insulin/IGF-1 (from Rosen ED et al., 2006).

2.3.2. Key molecular factors in adipose differentiation process

The adipogenesis is accompanied by a dramatic increase in expression of adipocyte genes (Fig.5).

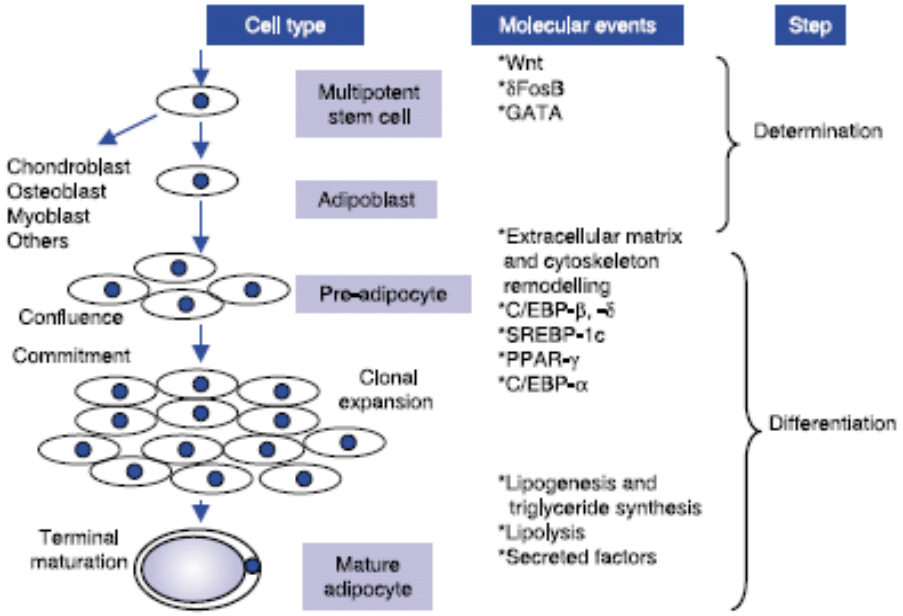

Fig. 5 **Representative scheme of adipocytes differentiation and molecular events that take place** (from Fève B et al., 2005).

At least two families of transcription factors, C/EBP (*CCAAT/enhancer binding protein*) and PPAR *(peroxisome proliferator-activated receptors)*, are induced early during adipocyte differentiation (Fig. 6). PPARγ is a member of a nuclear hormone receptor superfamily. There are 2 isoforms of PPARγ: γ1 and γ2. The isoform γ1 is found in the many different tissues such as heart, skeletal muscle, colon, small and large intestines, kidney, pancreas and spleen, while expression of PPARγ2 is predominantly localized to adipocytes (Cowherd RM et al., 1999; Berger J et al., 2002). PPARγ is crucial for adipogenesis and also is required for maintenance of the differentiated state. PPARγ is adipose specific and is expressed at low but detectable levels in preadipocytes (Gregoire F et al., 1998). Its expression rapidly increases after hormonal induction of differentiation. It is easily detectable during the second day of 3T3-L1 adipocyte differentiation (Fig. 6) Maximal levels of expression are noted in mature adipocytes. PPARγ regulates the expression of key genes involved in lipid and glucose metabolism or adipocyte differentiation, such as FABP-4, LPL, GLUT4. The genes regulated by PPARγ contain *PPAR response elements* (PPRE) (Rosen ED et al., 2006; Gregoire F et al., 1998; Rangwala SM et al., 2000). The function of PPARγ is regulated by phosphorylation. In particular, PPARγ2 is phosphorylated at serine 112 by MAP kinase. The phosphorylated form has a lower affinity for ligand than the non-phosphorylated form. This phenomenon has negative effect on differentiation process and on the transcription of the genes regulated by PPARγ (see part 2.3.3.) (Rangwala SM et al., 2000).

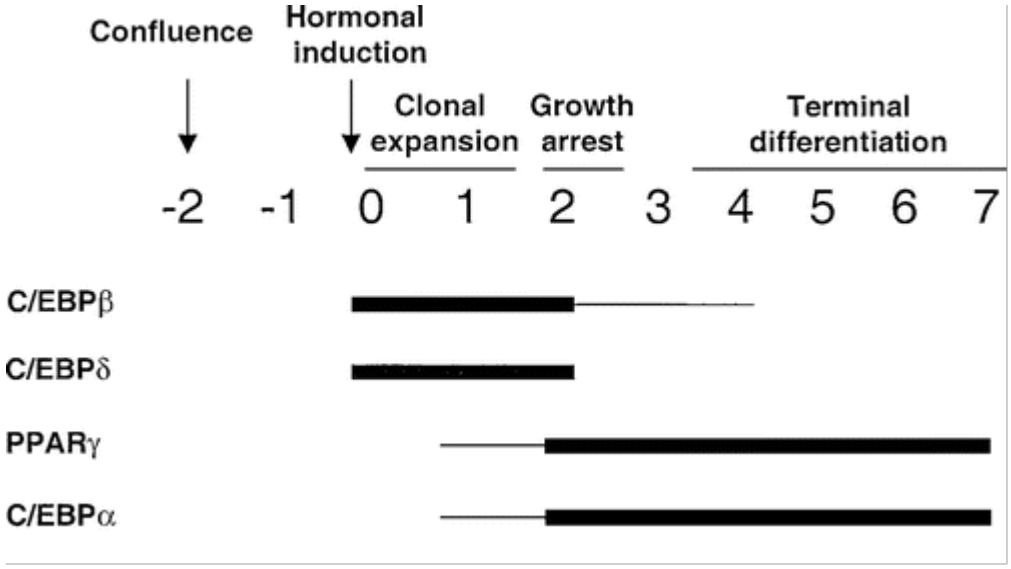

***Fig. 6* Timing of molecular factors expression during adipogenesis** (from Rangwala SM et al., 2000).

Another molecular factor implicated in adipogenesis is C/EBP that is able to bind to the CCAAT sequence localized in the promoter region of many genes. There are three main isoforms of C/EBP protein present in adipocytes: α, β e δ. Each isoform has a distinct temporal and spatial expression pattern during adipocyte differentiation (Fig. 6 and 7). During the initial phases of adipogenesis, C/EBPβ and C/EBPδ are induced in response to adipogenic hormones such as IBMX and DEX, respectively. C/EBPβ e C/EBPδ form a heterodimer that regulates the expression of PPARγ and C/EBPα (Fig. 7). The expression of PPARγ and C/EBPα take place at the end of the clonal expansion when the terminal differentiation phase begins with the accumulation of triacylglycerol droplets in the cytoplasmic compartment and synthesis of specific cellular factors named adipokines such as leptin, adiponectin, omentin, resistin, angiotensinogen. C/EBPα is necessary for the acquisition of insulin sensivity. C/EBPα induces expression of PPARγ or *vice versa* (positive feedback) (Cowherd RM et al., 1998; Gregoire F et al., 1998, Rosen ED et al., 2006).

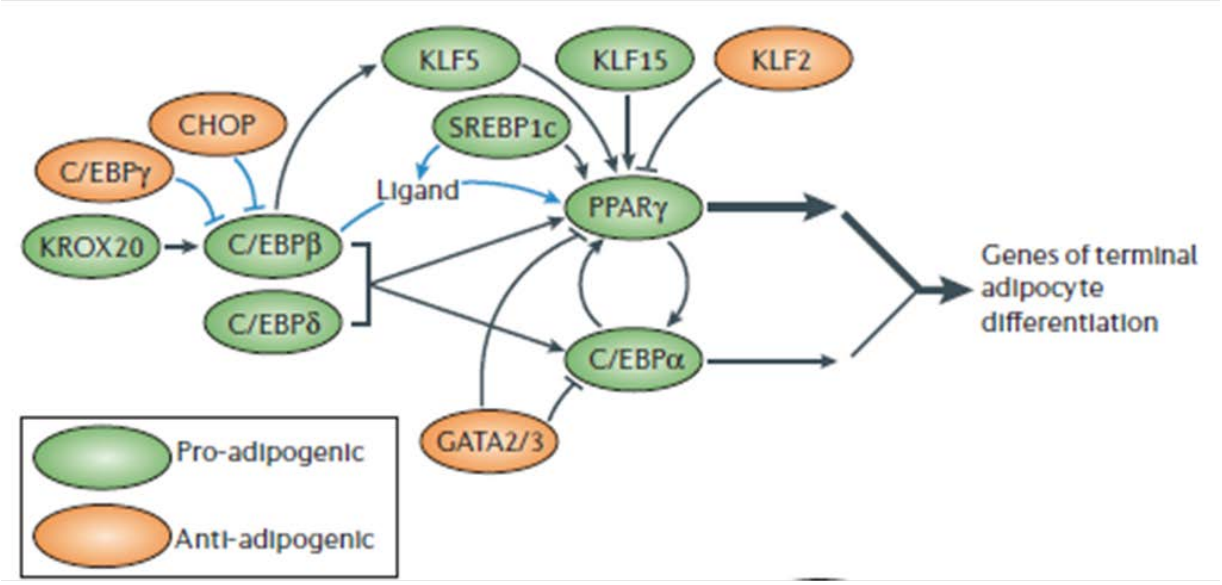

Fig. 7 **Schematic interaction between pro-adipogenic and anti-adipogenic factors** (from Rosen ED et al., 2006).

In addition to transcription factors, other signalling molecules such as Pref-1 (*preadipocyte factor-1)* regulate adipocyte differentiation (Sul HS et al., 2000). Pref-1 is an inhibitor of adipocyte differentiation and is synthesized as a plasma membrane protein containing six EGF repeats in the extracellular domain. Pref-1 is highly expressed in 3T3-L1 preadipocytes, but is not detectable in mature fat cells. DEX, a differentiation agent, inhibits Pref-1 transcription and thereby promotes adipogenesis. Downregulation of Pref-1 is required for

adipose conversion, and constitutive expression of Pref-1 inhibits adipogenesis. Conversely, decreasing Pref-1 levels by antisense Pref-1 transfection greatly enhances adipogenesis (Sul HS et al., 2000).

The most popular markers used to characterize adipogenesis are FABP-4 and leptin. FABP-4 is a carrier protein for fatty acids. This protein is also a marker for mature adipocytes (Wang M et al., 2009). Leptin is one of the most important adipose derived hormones (adipokine) and is primarily made and secreted by mature adipocytes (Gregoire F et al., 1998). Expression of *lipoprotein lipase* (LPL) mRNA is an early sign of adipocyte differentiation. LPL is secreted by mature adipocytes and plays a role in controlling lipid accumulation (Gregoire F et al., 1998).

2.3.3. Role of MAP kinases in adipogenesis regulation

The ERK, p38 and JNK *mitogen activated protein kinases* (MAPKs) are intracellular signalling pathways that play a pivotal role in many essential cellular processes such as proliferation and differentiation. MAPKs are activated by a large variety of stimuli and one of their major functions is to connect cell surface receptors to transcription factors in the nucleus, which consequently lead to gene regulation and long-term cellular responses. All modules comprise two additional protein kinases activated in series and lead to activation of a specific MAP kinase: a *MAP kinase kinase* (MAPKK), represented by MEK or MKK proteins, which phosphorylates a specific MAPK, and a *MAP kinase kinase kinase* (MAPKKK), represented by Raf and MEKK proteins, which phosphorylates a specific MAPKK (Fig. 8) (Bost F et al, 2005).

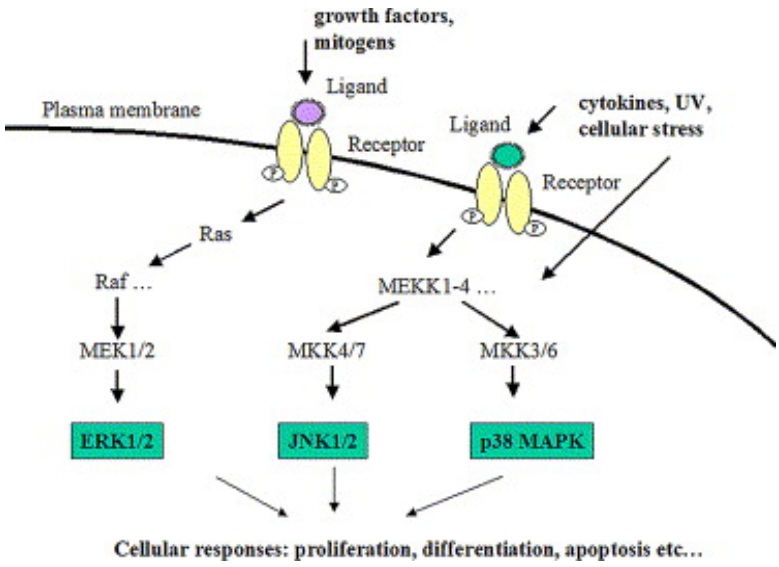

Fig. 8 **MAPKs signal transduction pathways** (from Bost F et al., 2005).

MAP kinases ERK1 and ERK2 are activated by phosphorylation on threonine and tyrosine residues by the dual specificity kinase MEK1. MEK1 induces translocation of ERK1 and ERK2 into the nucleus where they activate or repress a variety of transcription factor involved in growth and differentiation (Prusty D et al., 2002). ERKs are required for differentiation of 3T3-L1 fibroblasts to adipocytes, thereafter, this signal transduction pathway needs to be shut-off to proceed with adipocyte maturation. During the terminal differentiation, ERKs phophorylate PPARγ, decrease its transcriptional activity and inhibit adipocyte differentiation. The function of ERK in adipogenesis has to be time-regulated: during early phases of induction, ERK has to be turned on for a proliferative step, while later on, it has to be shut-off to avoid PPARγ phospshorylation. This hypothesis is in agreement with the fact that the adipocyte differentiation process of 3T3-L1 requires, at the beginning, a precise proliferative step, called mitotic clonal expansion (MCE), which takes place post-confluency. The MCE phase is initiated by adipogenic stimuli, such as insulin, which are known to activate the ERK pathway (Bost F et al., 2005). It was shown that insulin together with IBMX (MIX treatment) are principal regulators of MEK activity and promote adipose differentiation. On the contrary, the blockade of ERKs activity in 3T3-L1 cells by using specific inhibitors of MEK/ERK pathway (UO126 or PD98059) causes the inhibition of differentiation process (Prusty D et al., 2002). Furthermore, PPARγ expression is not detected during MCE, and progressively increases during terminal differentiation, when ERK activity is returned to a low level. It has also been shown that ERK activity is necessary for the expression of the crucial adipogenic regulators like C/EBPα, β and δ and PPARγ. ERK phosphorylation of C/EBPβ activates its

transcriptional activity (Bost F et al., 2005). Moreover, it has been shown that in the late phase of the differentiation process MEK/ERK pathway regulates the activation state of PPARγ causing its phosphorylation. This post-translational modification of the protein causes its degradation via ubiquitin/proteasome system (Burns KA et al., 2007). Other authors have shown that upon cellular stimulation MEK/ERK complex in the active state can translocate into the nucleus causing the phosphorylation of PPARγ and its export into the cytoplasm, where it is ubiquitinated and degradated (Fig. 9) (Burgermeister E et al., 2007).

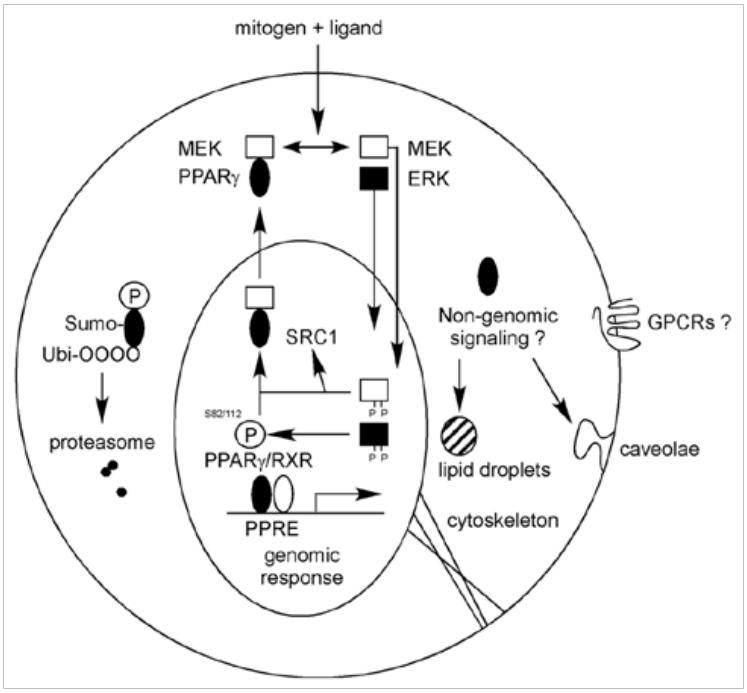

Fig. 9 **Mechanism of PPARγ down-regulation by MEKs/ERKs** (from Bost F et al., 2005).

2.4. Regulation of lipolysis in 3T3-L1 adipocytes

Lipolysis plays a central role in the regulation of energy balance. Lipolysis is the process in which triglycerides (TG) are hydrolyzed into glycerol and free fatty acids (FFA). This process releases FFA into bloodstream where they may be either re-esterified by the adipocyte or travel to other tissues and exert other effects throughout the body. FFA are an essential source of energy for many tissues. The control of lipolysis is complex and involves multiple players such as lipolytic (β-adrenergic agonists, ACTH, etc.) and anti-lipolytic (insulin, adenosine, etc.) hormones, their cognate receptors and signalling pathways, lipid droplet-associated proteins, such as perilipins, and *hormone-sensitive lipase* (HSL) which is the rate-

limiting enzyme responsible for mediating the hydrolysis of TG (Greenberg AS et al, 2001). The activity of HSL is well known to be regulated by reversible phosphorylation. Lipolytic stimuli increase lipolysis by activating adenylyl-cyclase and raising intracellular concentrations of *cyclic AMP* (cAMP), with resultant activation of *cAMP-dependent protein kinase* (PKA), which phosphorylates both perilipins and HSL. The phosphorylation of HSL is associated with an increase in hydrolytic activity of the enzyme and the translocation of HSL from the cytosol to the lipid droplet. In murine adipocytes, PKA phosphorylates HSL at several serine residues (563, 659, 660). In addition, HSL may be also phosphorylated by other kinases such as ERK1/2, which has been shown to activate HSL by phosphorylation on Ser^{600} (Greenberg AS et al, 2001; Fernández-Galilea M et al., 2012). Insulin acutely inhibits lipolysis, at least in part, via inhibition of the above cAMP-dependent pathway by PKB-dependent phosphorylation and activation of phosphodiesterase 3B, which in turn lowers cAMP levels (Fig. 10) (Kershaw EE et al., 2006).

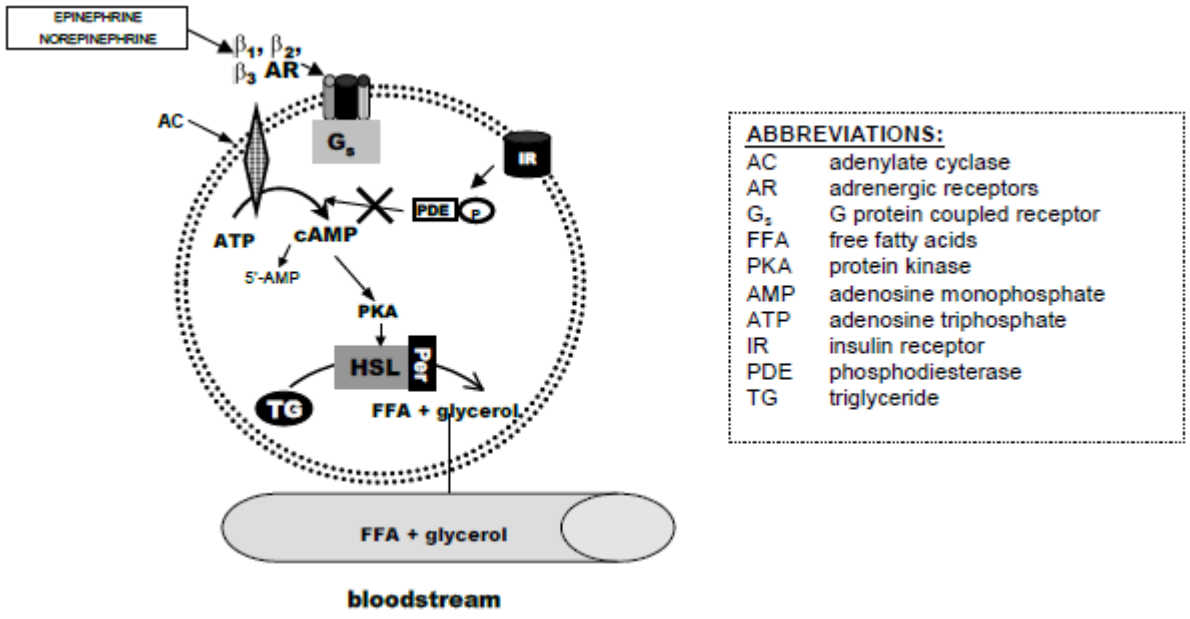

Fig. 10 **Overview of adipocyte lipolysis** (from Lipolysis Assay Kit for 3T3-L1 Cells: Glycerol Detection; ZENBIO).

3. Aim

The principal goal of this project was to evaluate the effect of GMG-43AC, the new experimental drug from Giuliani Sp.A (Milan, Italy), on adipocyte differentiation by using various differentiation schedules:

- differentiation induced by 3-isobutyl-1-methylxanthine (IBMX), dexamethasone (DEX) and insulin,
- differentiation induced by troglitazone and insulin.

The initial aim of this study was to set up the protocol of differentiation of 3T3-L1 cells and optimize protocols for the analysis of this phenomenon. Afterwards, the active concentrations of GMG-43AC were identified and the toxicity of the drug was assessed.

In particular, the specific objectives related to the study of the effects of GMG-43AC were to evaluate effects of this drug on adipogenesis through cell count and the measurement of triglycerides after staining with Oil Red O. The mechanism of the action of GMG-43AC was studied with molecular analysis conducted by:

- Western Blot - for the evaluation of protein factors involved in adipogenesis,
- Immunofluorescence – to verify the presence and localization of protein fundamental for adipogenesis,
- Real Time RT-PCR – to verify the gene expression crucial for adipocyte differentiation process.

The achievement of the objectives listed above will make possible to evaluate the potential effects of GMG-43AC on obesity by determining the effects of this drug on preadipocyte differentiation into adipocytes in 3T3-L1 cells.

4. MATERIALS AND METHODS

4.1. Materials and solutions

4.1.1. Materials

Insulin was purchased from SIGMA and dissolved in HCl 0.005N at the concentration of 10 mg/ml. Dexamethasone (DEX) was purchased from SIGMA and dissolved in DMSO at the concentration of 1 mM. 3-isobutil-1-metylxantine (IBMX) was purchased from SIGMA and dissolved in DMSO at the concentration of 0.5 M. PD98059 was purchased from SIGMA and dissolved in DMSO at the concentration of 6 mM. Troglitazone was purchased from SIGMA and dissolved in DMSO at the concentration of 10 μM. L-Thyroxine was purchased from SIGMA and dissolved in distilled water. Eutirox® was obtained from Bracco (Germany) and dissolved in distilled water. Caffeine was obtained from Giuliani Sp.A (Milano, Italy) and dissolved in distilled water at the concentration of 50 mM. GMG-43AC (levorotation isomer), RACEME and caffeine were obtained from Giuliani Sp.A (Milano, Italy) and were dissolved in DMSO at the concentration of 50 mM.

The final concentration of DMSO added to the growth medium was less than 0.001%.

4.1.2. Solutions

Electrode buffer 1X

192 mM Glycin (BDH; Manchester-UK)

0.1% SDS (SIGMA)

25 mM Tris (SIGMA)

Transfer buffer 1X

19 mM Glycin (BDH)

2.5 mM Tris Base (BIO-RAD)

2% Methanol (BDH)

Sample buffer 4X

0.25 M Tris-HCl (BDH) pH 6.8

36% Glycerol (SIGMA)

8% SDS (SIGMA)

0.2% Bromophenol blue (BIO-RAD)

20% ß-mercaptoetanol (SIGMA).

Ponceaus red

0.2% (w/v) Ponceau's (SIGMA)

3% (w/v) TCA (SIGMA)

3% sulfosalicylic acid (SIGMA)

TBS

20 mM Tris (SIGMA)

500 mM NaCl (SIGMA)

T-TBS 0.05%

20 mM Tris (SIGMA)

500 mM NaCl (SIGMA)

0.05% Tween20 (SIGMA)

Blocking buffer

5% not fat milk powder (SIGMA) in T-TBS 0.05%.

PBS 0.01 M

137 mM NaCl (SIGMA)

2.7 mM KCl (BDH)

1.47 mM KH_2PO_4 (BDH)

8.1 mM Na_2HPO_4 (BDH)

in dH_2O.

3T3-L1 maintenance medium

87% DMEM 1 g/l D-glucose (Euro Clone)

10% FBS (Euro Clone)

1% Penicillin G potassic salt (100 U/ml) (Euro Clone)

1% Streptomycin Sul fate (100 μg/ml) (Euro Clone)

1% Glutamine (Euro Clone)

3T3-L1 induction medium 1

87% DMEM 4,5 g/l D-glucose (Euro Clone)

10% FBS (Euro Clone)

0,5 mM IBMX (SIGMA)

1 μM DEX (SIGMA)

10 μg/ml insulin (SIGMA)

1% Penicillin G potassic salt (100 U/ml) (Euro Clone)

1% Streptomycin Sulfate (100 μg/ml) (Euro Clone)

1% Glutamine (Euro Clone)

3T3-L1 induction medium 2

87% DMEM 4,5 g/l D-glucose (Euro Clone)

10% FBS (Euro Clone)

10 μg/ml insulin (SIGMA)

1% Penicillin G potassic salt (100 U/ml) (Euro Clone)

1% Streptomycin Sul fate (100 μg/ml) (Euro Clone)

1% Glutamine (Euro Clone)

3T3-L1 maintenance differentiation medium

87% DMEM 4,5 g/l D-glucose (Euro Clone)

10% FBS (Euro Clone)

1% Penicillin G potassic salt (100 U/ml) (Euro Clone)

1% Streptomycin Sul fate (100 μg/ml) (Euro Clone)

1% Glutamine (Euro Clone)

RIPA buffer

40mM TRIS-HCl pH=7,5 (SIGMA)

150mM NaCl (SIGMA)

1% Triton X-100;

0,1% SDS (SIGMA);

0,5% sodium deoxycholate (SIGMA);

0,1mM EDTA with protease inhibitor cocktail.

in dH2O

plus protease inhibitors:

50 mM NaF (SIGMA)

1 mM NaVO3 (SIGMA)

4 mM PMSF (SIGMA)

1 M Benzamidine (SIGMA)

1 M NaN3 (SIGMA)

10 µg/ml Aprotinin (SIGMA)

10 µg/ml Leupeptin (SIGMA)

Oil Red O stock

0.5g Oil Red O (SIGMA)

in 100% isopropanol

4.2. Methods

4.2.1. Cell cultures and induction of differentiation in 3T3-L1 cells

Mouse embryo fibroblast 3T3-L1 cells were obtained from the American Type Culture Collection (ATCC-CL-173). The cell line was originally derived from Swiss mouse embryos at 17 to 19 days of age (Kehinde and Green, 1975). 3T3-L1 preadipocytes were cultured in Dulbecco's modified Eagle's medium (DMEM) (Euro Clone) containing 1g/l D-glucose, 10% heat-inactivated fetal bovine serum (FBS) supplemented with antibiotics at 37^0C in a humidified atmosphere containing 5% CO_2. The experimental conditions for achieving differentiation towards adipocyte and fat accumulation had been well described previously in Han KL et al., 2006; Kawaji A et al., 2010. Briefly, 2-3 days post-confluence (defined as *day 0*) cells were exposed to the adipocyte differentiating medium (DMEM) containing 4,5 g/l D-glucose, insulin (10 µg/ml SIGMA), dexamethasone (DEX; 1 µM SIGMA), and 3-isobutil-1-metylxantine (IBMX; 0.5 mM SIGMA) for 48 hours. Then, the differentiating medium was substituted with DMEM containing insulin (10 µg/ml) for further 48 hours (defined as *day 2*). The last period of differentiation was conducted keeping the cells in regular growth medium (DMEM 4,5 g/l D-glucose with 10% fetal bovine serum). In our experiments the differentiation process latest *8-10 days* (see scheme below).

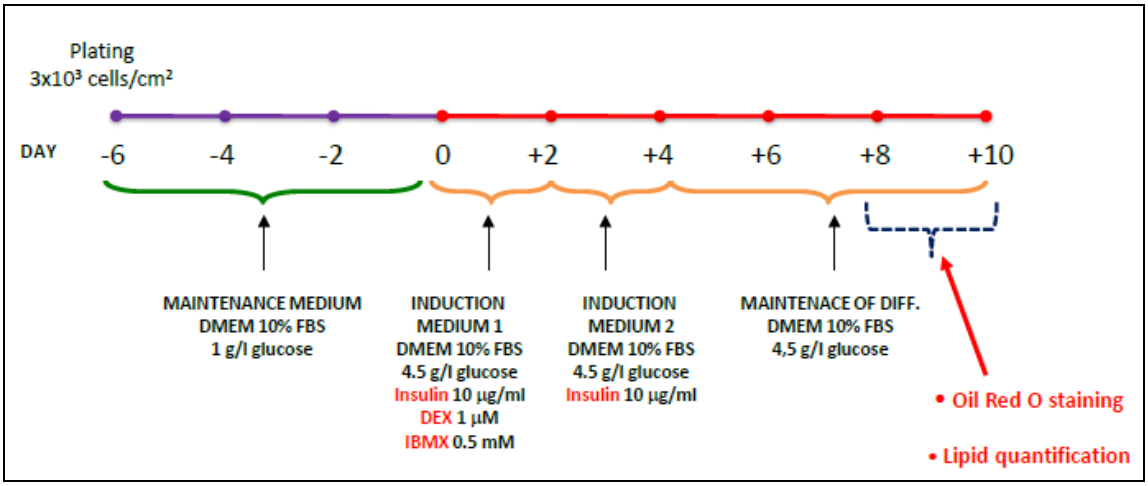

4.2.2. Evaluation of the effects of GMG-43AC on *in-vitro* induction of adipogenesis

GMG-43AC was diluted in DMSO and different quantities were added to the culture medium of 3T3-L1 cells to reach a final concentration ranging from 0.1 µM to 2000 µM. Cells were incubated with the drug in according to 4 different protocols as described below:

1. GMG-43AC was added to the medium at *day 0* of the differentiation process and maintained thereafter for the following *10 days* (scheme 1).

2. GMG-43AC was added to the medium at *day 0* and maintained for *48 hours* during the early differentiation process (scheme 2)

3. GMG-43AC was added to the medium at *day 2* and maintained for *48 hours* during the differentiation process (scheme 3)

4. GMG-43AC was added to the medium at *day 2* and maintained until the end of the differentiation process (*day 10*; scheme 4)

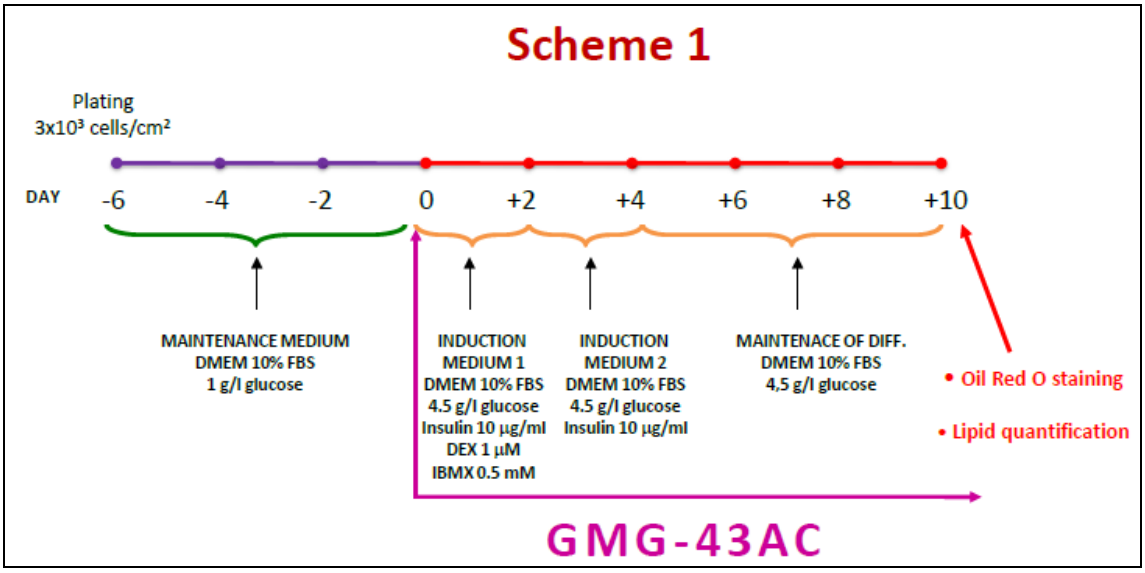
Scheme 1
Plating
3x10³ cells/cm²
DAY
-6
-4
-2
0
+2
+4
+6
+8
+10
MAINTENANCE MEDIUM
DMEM 10% FBS
1 g/l glucose
INDUCTION
MEDIUM 1
DMEM 10% FBS
4.5 g/l glucose
Insulin 10 µg/ml
DEX 1 µM
IBMX 0.5 mM
INDUCTION
MEDIUM 2
DMEM 10% FBS
4.5 g/l glucose
Insulin 10 µg/ml
MAINTENACE OF DIFF.
DMEM 10% FBS
4,5 g/l glucose
• Oil Red O staining
• Lipid quantification
GMG-43AC

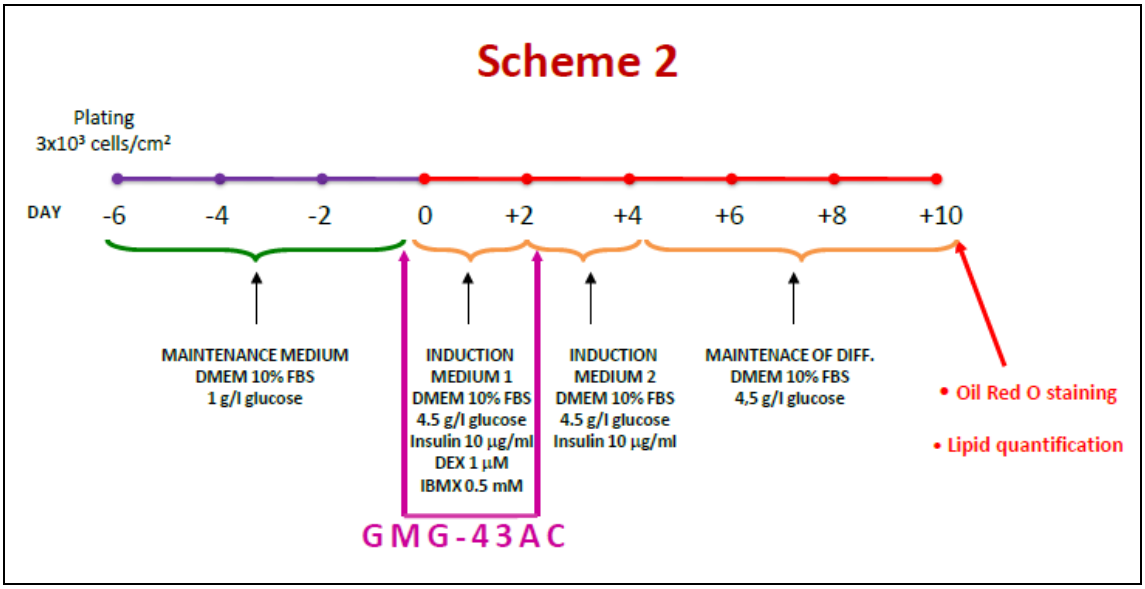
Scheme 2
Plating
3x10³ cells/cm²
DAY
-6
-4
-2
0
+2
+4
+6
+8
+10
MAINTENANCE MEDIUM
DMEM 10% FBS
1 g/l glucose
INDUCTION
MEDIUM 1
DMEM 10% FBS
4.5 g/l glucose
Insulin 10 µg/ml
DEX 1 µM
IBMX 0.5 mM
INDUCTION
MEDIUM 2
DMEM 10% FBS
4.5 g/l glucose
Insulin 10 µg/ml
MAINTENACE OF DIFF.
DMEM 10% FBS
4,5 g/l glucose
• Oil Red O staining
• Lipid quantification
GMG-43AC

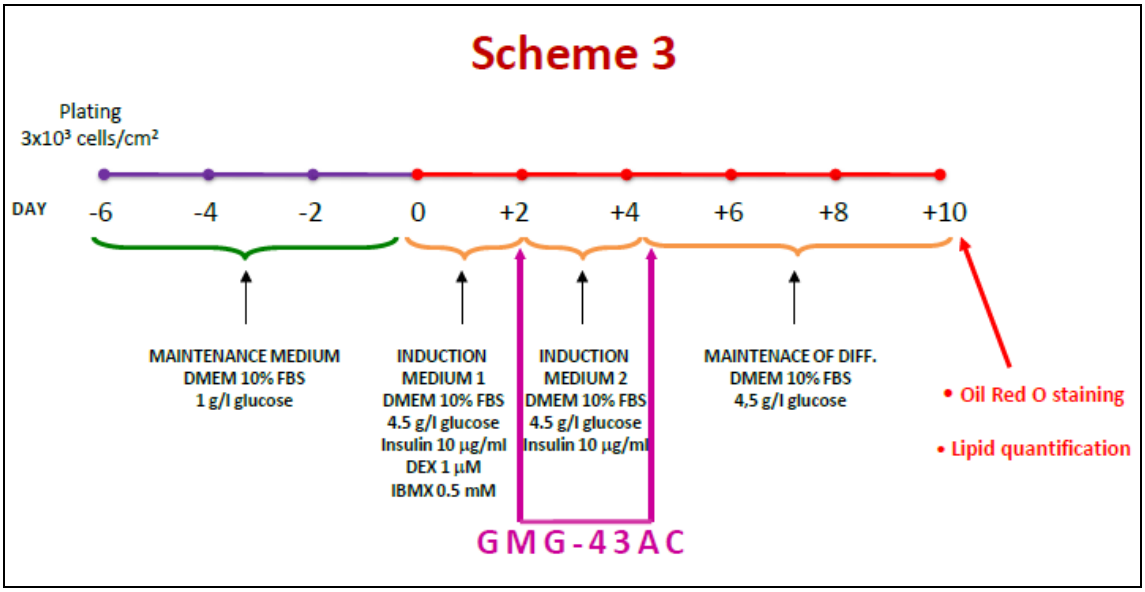
Scheme 3
Plating
3x10³ cells/cm²
DAY
-6
-4
-2
0
+2
+4
+6
+8
+10
MAINTENANCE MEDIUM
DMEM 10% FBS
1 g/l glucose
INDUCTION
MEDIUM 1
DMEM 10% FBS
4.5 g/l glucose
Insulin 10 µg/ml
DEX 1 µM
IBMX 0.5 mM
INDUCTION
MEDIUM 2
DMEM 10% FBS
4.5 g/l glucose
Insulin 10 µg/ml
MAINTENACE OF DIFF.
DMEM 10% FBS
4,5 g/l glucose
• Oil Red O staining
• Lipid quantification
GMG-43AC

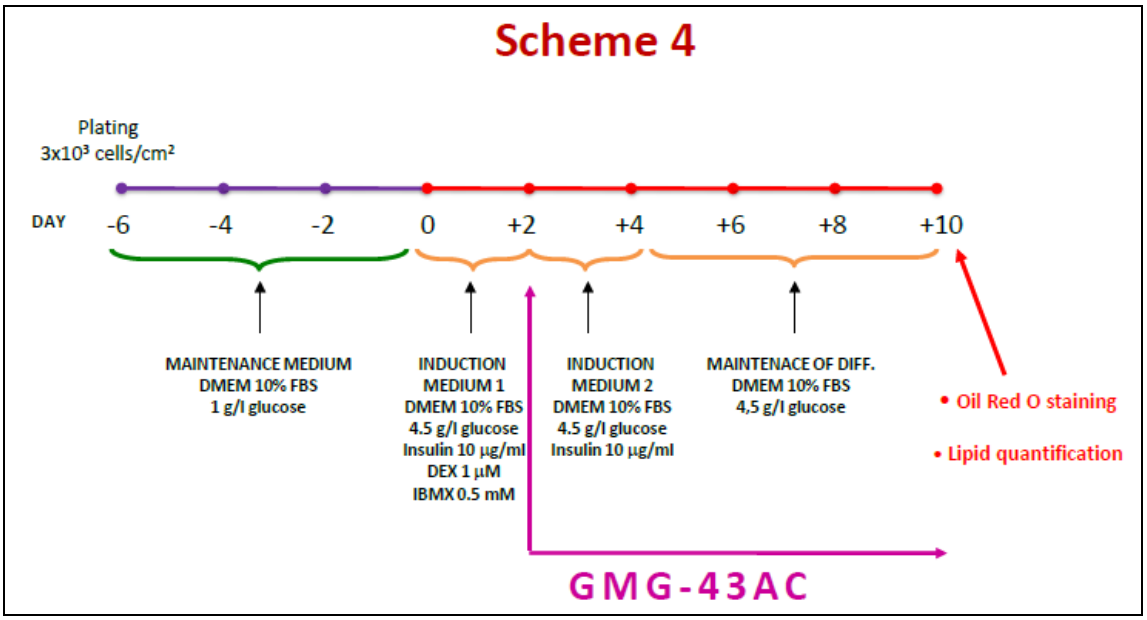
Scheme 4
Plating
3x10³ cells/cm²
DAY
-6
-4
-2
0
+2
+4
+6
+8
+10
MAINTENANCE MEDIUM
DMEM 10% FBS
1 g/l glucose
INDUCTION
MEDIUM 1
DMEM 10% FBS
4.5 g/l glucose
Insulin 10 µg/ml
DEX 1 µM
IBMX 0.5 mM
INDUCTION
MEDIUM 2
DMEM 10% FBS
4.5 g/l glucose
Insulin 10 µg/ml
MAINTENACE OF DIFF.
DMEM 10% FBS
4,5 g/l glucose
• Oil Red O staining
• Lipid quantification
GMG-43AC

4.2.3. Reversion of adipogenesis process by GMG-43AC

3T3-L1 were differentiated for 8 days as described before. The ability of GMG-43AC to revert the adipocyte differentiation process was evaluated at 2 different time points as presented on the schemes 5 and 6. GMG-43AC was added to the culture medium and maintained for the following 7 (scheme 5) or 14 days (scheme 6). The dosages of GMG-43AC tested in these experiments were 300 µM, 500 µM, 1000 µM and 2000 µM.

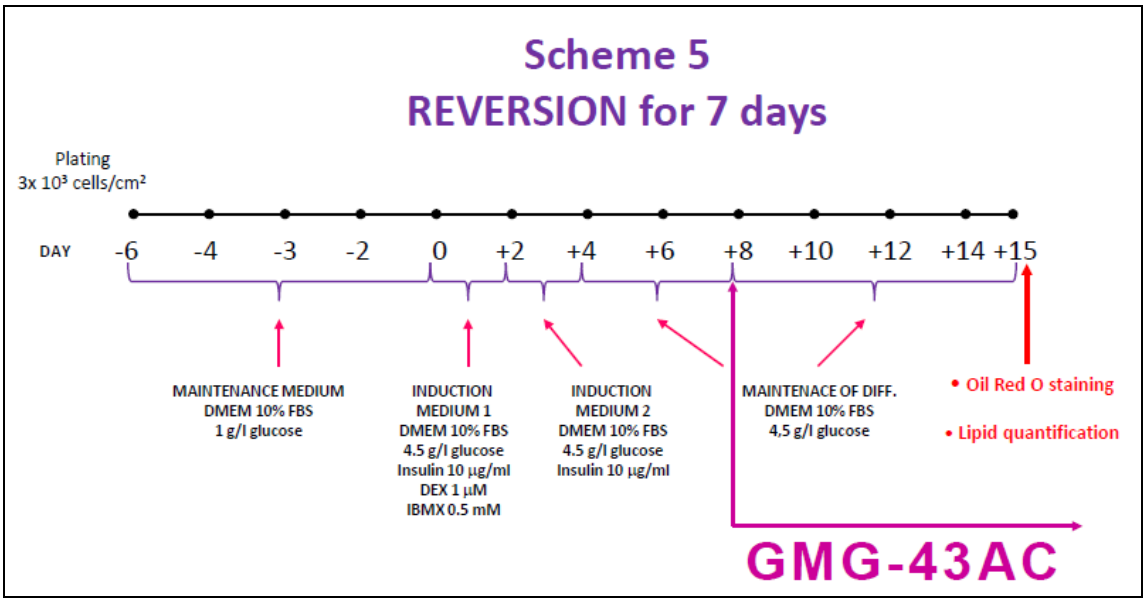

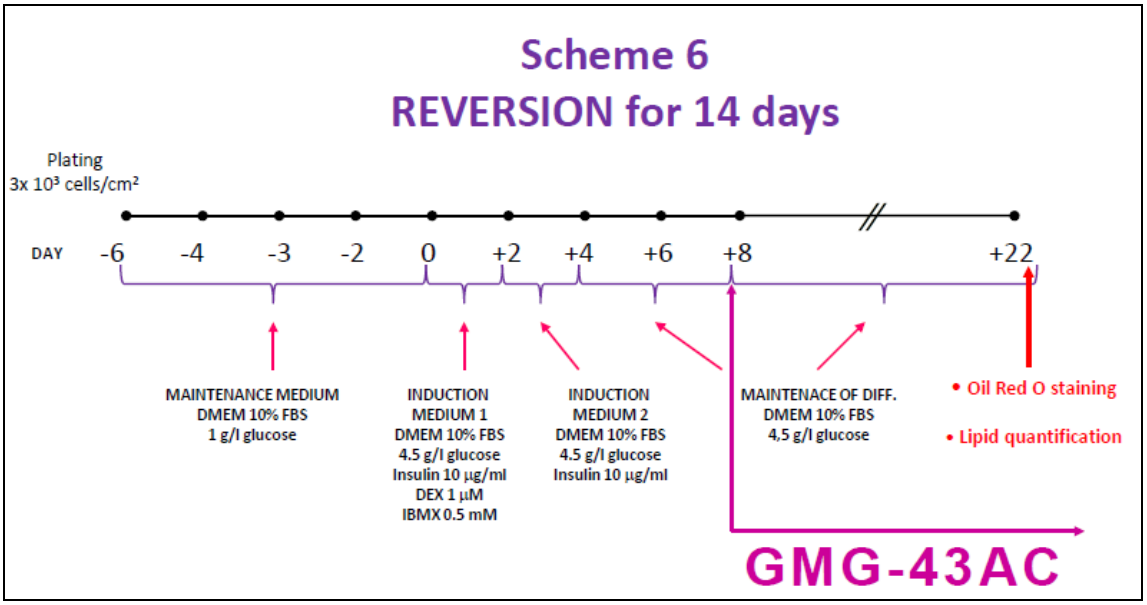

4.2.4. Evaluation of the actions of GMG-43AC in adipogenesis induced by troglitazone (10 µM)

Troglitazone, a potent inducer of adipocyte differentiation, was added at *day 0* to the growth medium containing insulin (10 µg/ml) at the final concentration of 10 µM as described by Su TZ et al., 1998; Han KL et al., 2006; Kim KJ et al., 2010, and maintained until the end of the differentiation process (day 10; see scheme below).

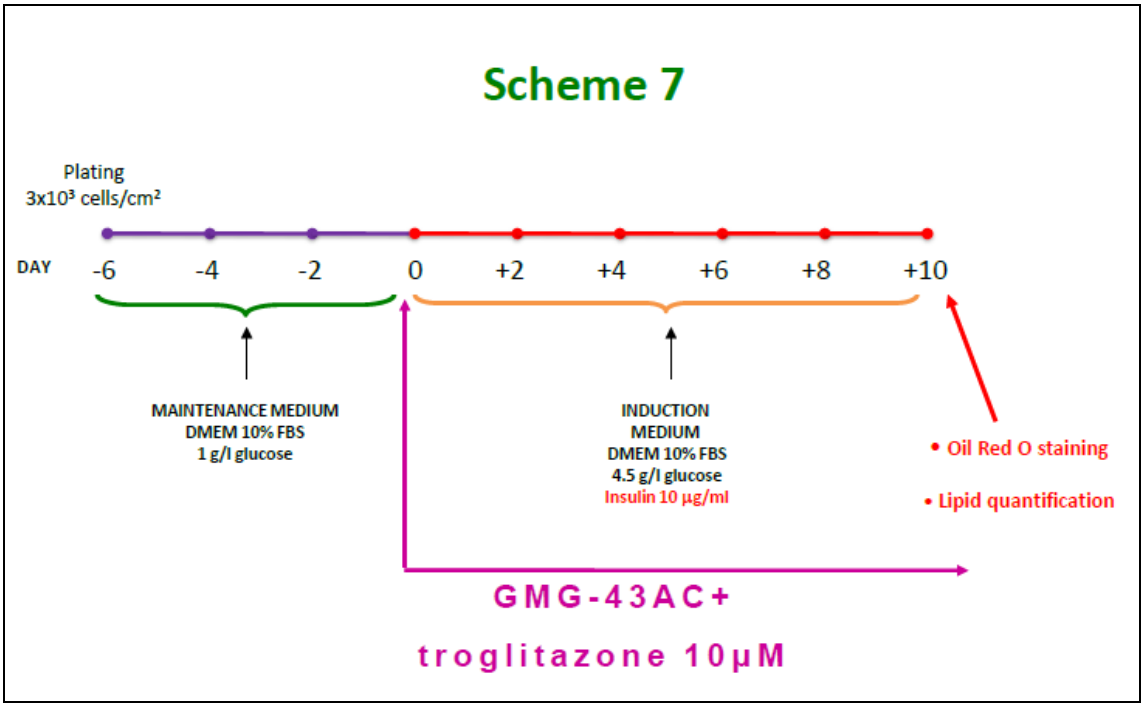

4.2.5. Evaluation of the actions of GMG-43AC in recovery of adipogenesis induced by troglitazone (5 µM)

3T3-L1 were differentiated in presence of troglitazone (5 µM) for 9 days as described before (see scheme 7). The ability of GMG-43AC to revert the adipocyte differentiation process was evaluated by adding the drug at day 9 to the culture medium and maintained for the following 7 or 14 days. The dosages of GMG-43AC tested in these experiments were 300 µM, 500 µM, 1000 µM and 2000 µM (see scheme 8).

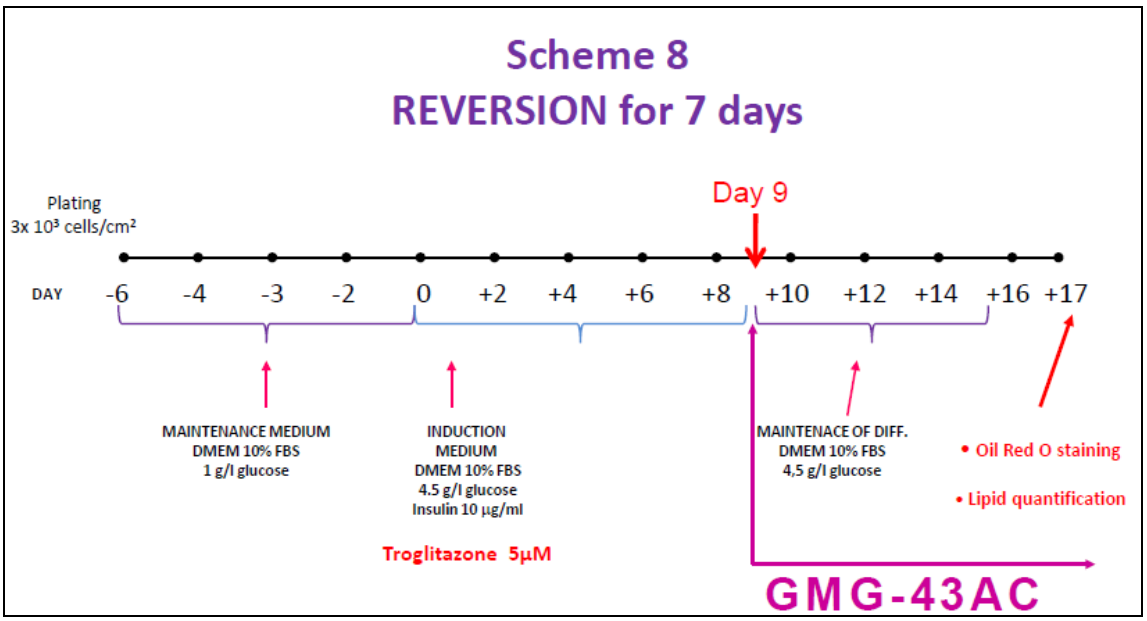

4.2.6. Evaluation of the actions of GMG-43AC, Raceme, caffeine, L-Thyroxine and Eutirox® in adipogenesis

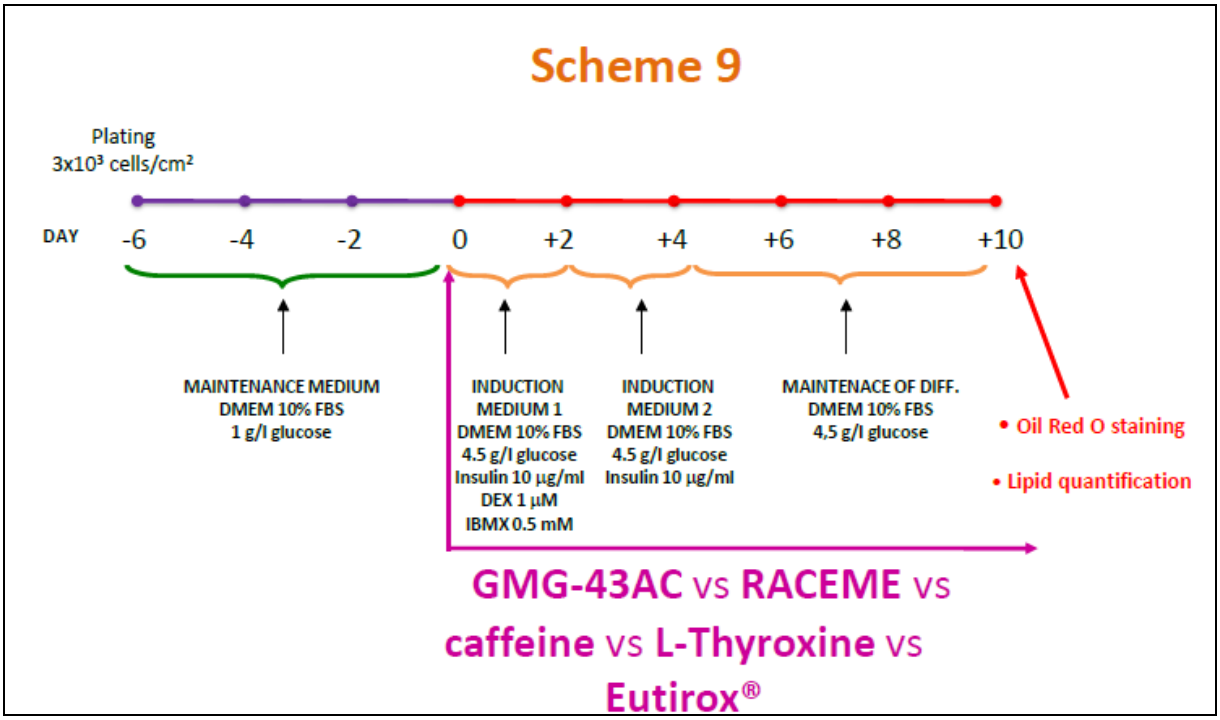

4.2.7. Comparison of the actions of GMG-43AC and PD98059 in adipogenesis

PD98059 is a MEK-1 specific inhibitor (Prusty D et al., 2002). It was dissolved in DMSO and added to the culture medium at the final concentrations of 10 µM and 30 µM at *day 2* and maintained until *day 4* (see schemes below). The effect on adipogenesis was evaluated at *day 4* or at *day 10* by triglycerides quantification and/or by counting adipocyte cells.

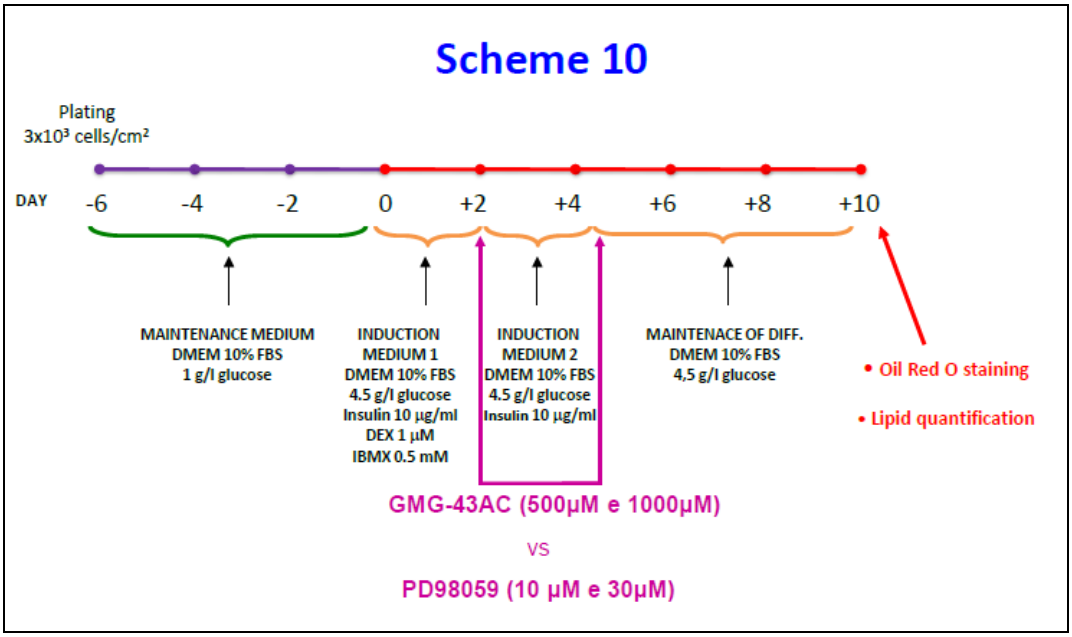

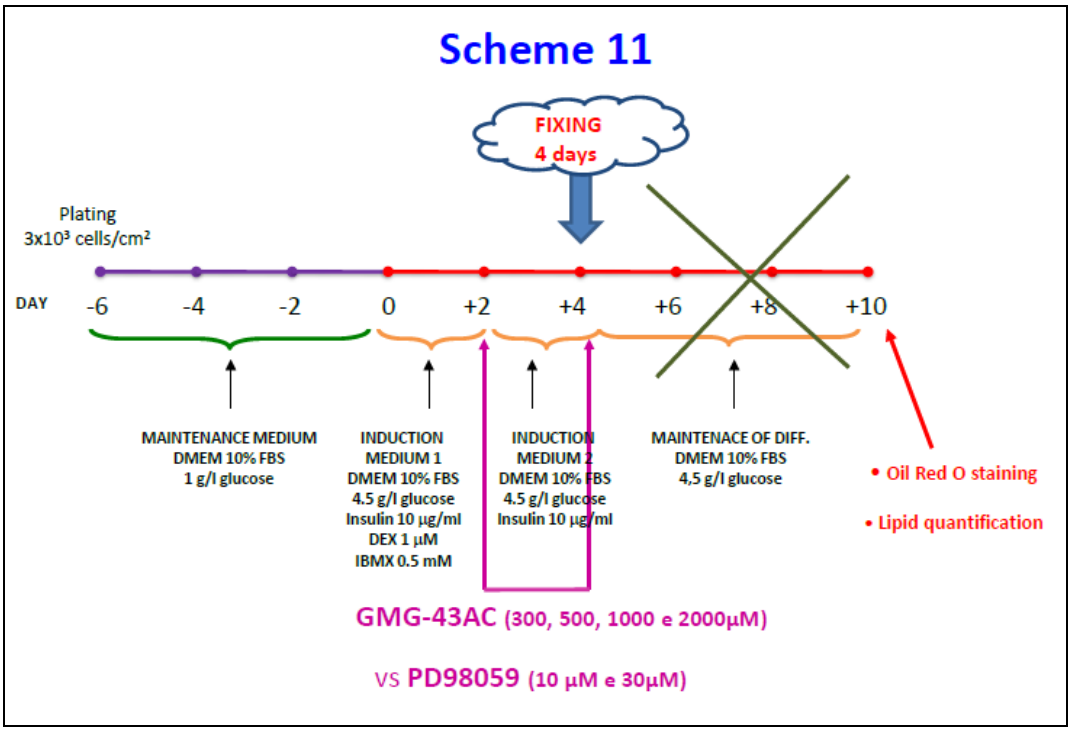

4.2.8. Oil Red O staining and quantification of lipid accumulation in adipocytes

Cells were cultured and differentiated in 6-wells or 48-wells plates on coverslips as described in section 2.2.1. Eight to ten days after the induction of differentiation, cells were rinsed twice with phosphate buffered saline (PBS), fixed with 4% fresh formalin in PBS for 1 hour and washed 2 times with PBS (5 min, RT). After that were stained with Oil Red O. Oil Red O staining is the standard technique utilized to visualize droplets of neutral lipid accumulated in cytoplasm (Koopman R et al., 2001). Briefly, this dye specifically interacts with triacylglycerol and stains droplets in red. Oil Red O preparation procedure and adipocyte staining procedure used were following:

- Prepare Oil Red O stock. Dissolve 0.5 g Oil Red O in 100 ml of isopropanol, stir overnight at room temperature and then filter with 0.45 µm and store at $+4^0$C.
- Prepare Oil Red O working solution. Dilute 6 parts of the stock stain with 4 parts of distilled water, allow to stand for 20 min, and filter with 0.20 µm. The stain does not keep, and should be made up fresh from the stock solution each time.
- Wash wells once with 60% isopropanol (5 min, RT).
- Let the wells dry completely.
- Add Oil Red O working solution for 15 min (do not touch walls of the wells).
- Remove all Oil Red O and immediately add H_2O, wash with H_2O 2 times and then wash under running tap water.
- Take pictures if desired.
- Remove all water and let dry.
- Elute Oil Red O by adding 100% isopropanol, incubate about 10 min.
- Pipet the isopropanol with Oil Red O up and down several times to be sure that all Oil Red O is in the solution.
- Transfer to 1.5 ml tubes.
- Measure OD at 500 nm, 0.5 sec reading.
- As blank use 100% isopropanol. As control use isopropanol from empty well stained as previously described.

The dye retained in the cells was evaluated with 2 different approaches:

1. by elution with 1,5 ml isopropanol for at least 10 min. Specific optical density was measured at 500 nm in spectrophotometer Bio UV/VIS® Parkin Helmer (UK).

2. by the counting of positive stained cells compared to all the cells indicated by hematoxilin (SIGMA) staining (5 min). Slides were photographed by using optical microscope Leica and digital camera Leica (German). Data was plotted reporting the percentage of positive cells as the mean of the quantification of at least 5 fields for each condition.

4.2.9. SDS Page, Western blotting and protein detection

Protein extraction

For protein analysis, cells were cultured in 25cm^2 Petri dishes as described before. At the end of the treatments, the plates were placed on ice, the media was removed and cells were rinsed twice with cold PBS. Protein extracts were obtained from the cells in RIPA buffer. Samples were incubated on ice for 30 min and centrifuged at 13,200 rpm at 4^{0}C for 20 min. After that the supernatants were collected. Protein concentration was measured at 595 nm by the Bradford method (Quick Start™ Bradford Protein Assay, BIO-RAD) using a spectrophotometer (MPT Reader DV990BVG).

Protein sample preparation for electrophoresis

60 μg of cell lysate was precipitated with 100% TCA (trichloroacetic acid) for 4 h at 4^{0}C. After that samples were centrifuged at 13,200 rpm at 4^{0}C for 20 min. After that the supernatans were removed and pellets were washed with cold acetone at 10,000 rpm at 4^{0}C for 5 min. Pellets were re-suspended SDS sample buffer 4X (INVITROGEN) containing 5% 2-β mercaptoethanol (70mM). In the case of TCA precipitation, Tris buffer is sometimes added to adjust pH if TCA residues are still present in sample resuspension. The samples are boiled for 5 min to fully denature the proteins and loaded onto the gel.

SDS Page

Sodium dodecyl sulfate-polyacrylamide gel electrophoresis (SDS-PAGE) is the most common analytical technique used to separate and characterize proteins, using a discontinuous polyacrylamide gel as support medium and SDS to denature the proteins. SDS (also called lauryl sulfate) is an anionic detergent bound by a polypeptide chain in proportion to its relative molecular mass. The negative charges on SDS destroy most of the complex structure of proteins, and are strongly attracted toward an anode in an electric field. Polyacrylamide gels restrain larger molecules from migrating as fast as smaller molecules. Because the charge-to-mass ratio is nearly the same among SDS-denatured polypeptides, the final separation of proteins is dependent almost entirely on the differences in relative molecular mass of polypeptides. In a gel of uniform density the relative migration distance of a protein (Rf) is negatively proportional to the log of its mass. If proteins of known mass are run simultaneously with the unknowns, the relationship between Rf and mass can be plotted, and the masses of unknown proteins estimated. Protein separation by SDS-PAGE can be used to estimate relative molecular mass, to determine the relative abundance of major proteins in a sample, and to determine the distribution of proteins among fractions. Acrylamide is the material of choice for preparing electrophoretic gels to separate proteins by size. Acrylamide mixed with bis-acrylamide forms a cross-linked polymer network when the polymerizing agent, ammonium persulfate, is added. The ammonium persulfate (AP) produces free radicals faster in the presence of TEMED (N,N,N,N'-tetramethylenediamine). The size of the pores in a gel is inversely related to the amount of acrylamide used. Very large polypeptides cannot penetrate far into a gel and thus their corresponding bands may be too compressed for resolution. Polypeptides below a particular size are not restricted at all by the gel, and regardless of mass they all move at the same pace along with the tracking dye. Gel concentration (%T) should be selected to resolve precisely proteins of interest. A typical gel of 7% acrylamide composition separates polypeptides with molecular mass between 45 and 200 kDa. There are two types of buffer systems used in PAGE electrophoresis: continuous and discontinuous systems. A continuous system has only a single separating gel and uses the same buffer in the tanks and the gel. In a discontinuous system, a non-restrictive large pore gel, called stacking gel, is layered on top of a separating gel called resolving gel. Each gel is made with a different buffer, and the tank buffers are different from the gel buffers. The stacking gel has a lower

concentration of acrylamide (larger pore size), lower pH and a different ionic content. This allows the proteins to be concentrated into a tight band before entering in the resolving gel. The resolving gel may consist of a constant acrylamide concentration or a gradient of acrylamide concentration (high percentage of acrylamide at the bottom of the gel and low percentage at the top). A gradient gel is prepared by mixing two different concentrations of acrylamide solution to form a gradient with decreasing concentrations of acrylamide. As the gradient forms, it is layered into a gel cassette. This latter gel is recommended for separation of a mixture of proteins with a greater molecular weight range.

In our experimental conditions, continuous gel was running under reducing and denaturant conditions. Gel preparation procedures and running conditions used are described in the following protocol:

- Assemble glass plate sandwich using two clean glass plates and two 1-mm spacers. Assemble the casting frame and stand as described by manufacturer.
- In a clean falcon, prepare the resolving gel solution, mixing the ingredients as described in table 2, remembering that AP and TEMED must be added at the end. Be careful not to generate bubbles.
- Pour the resolving gel to a level about 1 cm from the top. Wait 1 min, then layer the top of the gel with distilled water (this will help the gel to solidify quickly in the absence of air).
- Wait another 15-20 min for the gel to polymerize. Pour off the top layer of distilled water. Dry off as much of the water as possible, using absorbent paper.
- In a clean falcon, prepare the stacking gel as described in table 2, being careful not to generate bubbles.
- Pour the resolving gel till the space is full, then put in the appropriate comb. (The difference in the pH of the two layers is what causes the stacking of the proteins. Thus, if the proteins are not stacking properly check the pH of the buffers).
- Allow the top portion to solidify and then carefully remove the comb or store at 4°C in humidified condition, until use.
- Place gel in opposite side of apparatus (Mini-PROTEAN 3-Cell, Bio-Rad).
- Slowly add 1x Running buffer.
- Load samples and molecular weight marker.

- Run the gel at 60V until the blue dye overpass stacking phase, and then run it at 110 V until the blue dye reaches the bottom or runs off. At this time, the run is stopped, cables removed. The gel is removed from the cassette and can be processed for western blotting.

REAGENTS	Running gel (1x)		Stacking gel (1x)
Acrylamyde percentage	8%	10%	3%
dH_2O	6,75 ml	5,85 ml	3,3 ml
Lower Buffer pH=8.8	4,5 ml	4,5 ml	---
Upper Buffer pH=6.8	---	---	1,3 ml
40% acrylamide/bis-acrylamide solution	3,6 ml	4,5 ml	380 µl
TEMED	15 µl	15 µl	5 µl
AP (10%)	150 µl	150 µl	50 µl

Table 2. **Resolving and Stacking gel solution recipes.**

AP: ammonium persulfate (AP); TEMED: N,N,N,N'-tetramethylenediamine

Western blotting and protein detection

The term "blotting" refers to the transfer of biological samples from a gel to a membrane and their subsequent detection on the surface of the membrane. Western blotting was introduced by Towbin and colleagues [1989] and is now a routine technique for protein analysis. The specificity of the antibody-antigen interaction enables a single protein to be identified in the midst of a complex protein mixture. Western blotting is commonly used to identify a specific protein in a complex mixture and to obtain qualitative and semiquantitative data about that. The first step in a western blotting procedure is to separate the macromolecules using gel electrophoresis. Following electrophoresis, the separated molecules are transferred onto a second matrix, generally a nitrocellulose membrane. Next, the membrane is blocked to prevent any nonspecific binding of antibodies to the surface of the membrane. The transferred protein is completed with an enzyme-labeled antibody as a probe. An appropriate substrate is then added to the enzyme and together they produce a detectable product such as a chromogenic or fluorogenic precipitate on the membrane for colorimetric or

fluorimetric detection, respectively. The most sensitive detection methods use a chemiluminescent substrate that, when combined with the enzyme, produces light. This output can be captured using film, a CCD camera or a phosphorimager designed for chemiluminescent detection. Whatever substrate is used, the intensity of the signal correlates with the abundance of the antigen on the blotting membrane. In our experimental procedure, western blotting and protein detection protocols are the following:

- Cut a piece of nitrocellulose membrane (BIO-RAD). Wet the membrane in dH_2O.
- Pre-wet the sponges, filter papers (slightly bigger than gel) in 1x Transfer buffer. Assemble sandwich (sponge-paper-gel-membrane-paper-sponge) for the electroblotting apparatus (Mini Trans-Blot Electrophoretic Transfer Cell, Bio-Rad).
- Transfer for 1 hr at 100 V with a cold pack and prechilled buffer.
- After transfer is complete, turn off power supply and remove cathode plate of blotter. Remove transfer membrane and cut lower right corner of membrane to mark orientation of gel.
- Staining the membrane with Ponceau's dye and the gel with Coomassie Blue dye to verify the correct transfer.
- Remove Ponceau's staining, washing the membrane with dH_2O.
- Block the nitrocellulose membrane in TBS with 0,05% Tween-20 (v/v) (T-TBS), containing 5% slim milk (w/v) for at least 60 min on a rocking platform.
- Wash the nitrocellulose membrane 3 times in T-TBS for 10 min each on a rocking platform.
- Incubate the nitrocellulose membrane on a rocking platform with primary antibody diluted in T-TBS, overnight at 4°C.
- Wash the nitrocellulose membrane 3 times in T-TBS for 10 min each on a rocking platform.
- Incubate with secondary antibody horseradish peroxidase-conjugate diluted in T-TBS for 60-90 min on a rocking platform at room temperature.
- Wash the nitrocellulose membrane 3 times in T-TBS for 10 min each on a rocking platform.
- Wash the nitrocellulose membrane once in TBS to remove the excess of tween.

- Detect proteins by means of an enhanced chemiluminescence detection system (ECL^{TM}, Pierce).
- After incubation of 5 min with ECL, blots are placed in a sheet protector and exposed to Kodak X-Omat Blue Film (Blue X-ray Film) (Perkin Elmer) for different times. Several exposures allow better densitometric analysis.
- Autoradiography films are automated processed with an Automated x-ray film developer (Kodak M35A X-OMAT processor).

Primary antibodies used in experimental procedures:

- anti-MEK1/2 (dilution 1:1000 in T-TBS 0.05%) (Cell Signaling);
- anti-phopsho-MEK1/2 (dilution 1:1000 in T-TBS 0.05%) (Cell Signaling);
- anti-p42/44 MAPK (dilution 1:1000 in T-TBS 0.05%) (Cell Signaling);
- anti-phospho-p42/44 MAPK (ERK1/2) (dilution 1:1000 in T-TBS 0.05%) (Cell Signaling);
- anti-peroxisome proliferator-activated receptor-γ (PPARγ) (dilution 1:1000 in T-TBS 0.05%) (Cell Signaling);
- anti-adipocyte fatty acid-binding protein 4 (FABP-4) (dilution 1:1000 in T-TBS 0.05%) (Cell Signaling);
- anti-phospho peroxisome proliferator-activated receptor-γ (pPPARγ) (dilution 1:2.5 µg/ml in T-TBS 0.05%) (ABCAM);
- anti-RhoA (dilution 1:200 in T-TBS 0.05%) (Santa Cruz);
- anti-β-actin (dilution 1:1000 in T-TBS 0.05%) (SIGMA).

Secondary antibodies used in experimental procedures:

1. anti rabbit IgG-HRP (dilution 1:10.000 in T-TBS 0.05%) (Chemicon International).
2. anti mouse IgG-HRP (dilution 1:5.000 in T-TBS 0.05%) (Chemicon International).

Nitrocellulose membrane stripping

After visualizing protein of interest, it is possible to strip off the first set of protein probes so that different proteins on the blot may be detected using a second set of specific probes. When possible, this technique saves the time and resources that would be necessary to electrophorese another sample and transfer it to new sheet of

membrane. Stripping generally involves soaking the blot in a buffer that is sufficiently harsh to dissociate the affinity interactions between antibodies and the target sample protein that was transferred to the membrane.

In our experimental condition, the stripping protocol consists in:

- Wash abundantly the nitrocellulose membrane with T-TBS for 20 min on a rocking platform.
- Incubate the membrane with Restore Plus Western Blot Stripping Buffer (Thermo Scientific) for 10 min at room temperature on a rocking platform.
- Wash abundantly the nitrocellulose membrane with T-TBS for 20 min on a rocking platform.
- Return to membrane blocking and primary antibody incubation as previously described.

Densitometric analysis

Exposures of the same membrane for different times were acquired using GelDoc™ image capture system (Bio-Rad), following Manufacturer's instructions. The autoradiograms were quantified using Quantity One™ and Image J software. The data were then analyzed with suitable statistic methods.

Polyacrylamide gel staining

After western blotting procedure, gel staining allows to verify the correct loading of protein samples and the correct protein transfer to nitrocellulose membrane. A commonly used stain for detecting proteins in polyacrylamide gels is 0.1% Coomassie Blue dye in 50% methanol, 10% glacial acetic acid. Acidified methanol precipitates the proteins. Staining is usually performed overnight on a rocking platform. The dye penetrates the entire gel, and sticks permanently to the proteins. Excess dye is washed out by destaining procedure with acetic acid/methanol washes on a rocking platform. Destaining in two steps (first using 50% methanol, 10% acetic acid for 1-2 hours, and then using 7% methanol, 10% acetic methanol) provided a better efficiency. Finally, gels can be dried or photographed for later analysis.

4.2.10. Confocal microscopy

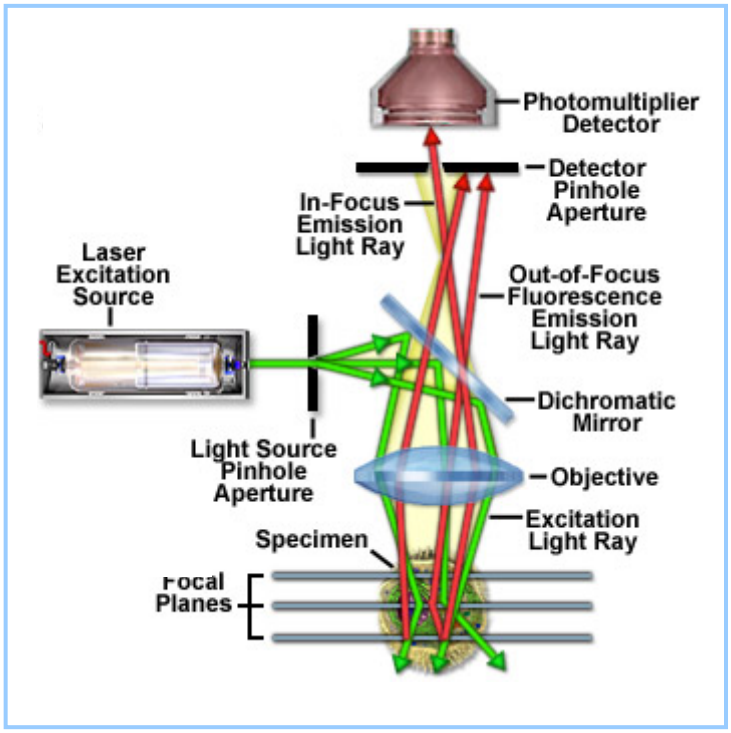

Confocal microscopy offers several advantages over conventional optical microscopy, including controllable depth of field, the elimination of image degrading out-of-focus information, and the ability to collect serial optical sections from thick specimens. The key to the confocal approach is the use of spatial filtering to eliminate out-of-focus light or flare in specimens that are thicker than the plane of focus. In recent years, there has been a tremendous explosion in the popularity of confocal microscopy, due in part to the relative ease with which extremely high-quality images can be obtained from specimens prepared for conventional optical microscopy. In a conventional widefield microscope, the entire specimen is bathed in light from a mercury or xenon source, and the image can be viewed directly by eye or projected onto an image capture device or photographic film. In contrast, the method of image formation in a confocal microscope is fundamentally different. Illumination is achieved by scanning one or more focused beams of light, usually from a laser or arc-discharge source, across the specimen. This point of illumination is brought to focus in the specimen by the objective lens, and laterally scanned using some form of scanning device under computer control. The sequences of points of light from the specimen are detected by a photomultiplier tube (PMT) through a pinhole (or in some cases, a slit), and the output from the PMT is built into an image and displayed by the computer (Fig. 11). Although unstained specimens can be viewed using light reflected back from the specimen, they usually are labelled with one or more fluorescent probes.

Specimen Preparation and Imaging

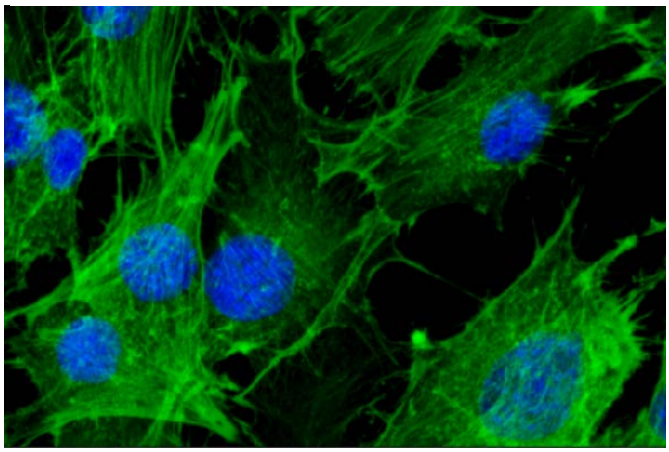

Fig. 11 Confocal microscopy image of actin immunostaining. Actin staining was performed in 3T3-L1 cells, previously fixed on slide with paraformaldehyde. In green, actin labelling; in blue, nuclei staining with DAPI dye. Immunofluorescence image assessed with confocal microscopy TSC SP2 Leica.

The procedures for preparing and imaging specimens in the confocal microscope are largely derived from those that have been developed over many years for use with the conventional wide field microscope. In the biomedical sciences, a major application of confocal microscopy involves imaging either fixed (Fig. 11) or living cells and tissues that have usually been labelled with one or more fluorescent probes. A large number of fluorescent probes are available that, when incorporated in relatively simple protocols, specifically stain certain cellular organelles and structures. Among the plethora of available probes are dyes that label nuclei, the Golgi apparatus, the endoplasmic reticulum, and mitochondria, and also dyes such as fluorescently labelled phalloidins that target polymerized actin in cells. Regardless of the specimen preparation protocol employed, a primary benefit of the way in which confocal microscopy is carried out is the flexibility in image display and analysis that results from the simultaneous collection of multiple images, in digital form, into a computer.

Critical aspects of Confocal microscopy

Quantitative three-dimensional imaging in fluorescence microscopy is often complicated by artefacts due to specimen preparation (*e.g.* autofluorescence problems, retractile structures presence, presence or absence of highly stained structures, immersion oil, coverslip thickness etc.), controllable and uncontrollable experimental variables, or configuration problems with the microscope (*e.g.* optical component alignment, objective magnification, bleaching artefacts, aberrations, quantum efficiency, and the specimen embedding medium).

In our experimental conditions, slides were photographed using a 40x objective lens and 1x zoom (Leica, Wetzlar, Germany) with confocal microscope Leica SP2 microscope with He/Kr and Ar lasers (Leica).

Immunofluorescence in 3T3-L1 cells

For all immunofluorescence experiments, cells were grown and differentiated in chamber-slides (Lab-Tek®) or onto glass coverslips as described before. Then cells were fixed with 2% (for 10 min) and 4% (successive 10 min) paraformaldehyde in PBS.

After cell fixation, the protocol used is the following:

- Wash three times with PBS for 5 min.
- Incubate in saturation solution consists of 4% bovine serum albumin (BSA), 0.3% Triton X-100 in PBS pH=7.5 for 40 min to block unspecific binding of the antibodies.
- Incubate in 1:10 saturation solution to permeabilize the cell membranes, 20 min at room temperature.
- Incubate with primary antibody in 1:10 saturation solution, over night at 4^0C.
- Wash three times with PBS for 5 min.
- Incubate with secondary antibody in 1:10 saturation solution, 60 min at room temperature.
- Wash three times with PBS for 5 min.
- Incubate in 0.2 mg/ml 4',6'-diamidino-2-phenyl-indole (DAPI) for 2 min.
- Wash two times with PBS for 10 min.
- Mount in Fluorsave (Chemion).

Primary antibodies:

- Anti-PPARγ (dilution 1:200, Cell Signaling)
- Anti-C/EBPα (dilution 1:50, Cell Signaling)
- Anti-FABP-4 (diluition 1:200, Cell Signaling)
- Anti-Leptin (dilution 5 μg/ml, ABCAM)
- Anti-C/EBPβ (dilution 1/200, Santa Cruz)

- Anti-C/EBPδ (dilution 1/200, Santa Cruz)
- Anti- RhoA (dilution 1/200, Santa Cruz)

Labelled secondary antibodies:

- Alexa Fluor® 488 donkey anti- Rabbit IgG (H+L) (INVITROGEN)
- Alexa Fluor® 546 Goat Anti-Rabbit IgG (H+L) (INVITROGEN)
- Alexa Fluor® 546 Donkey Anti-Goat IgG (H+L) (INVITROGEN)

Actin immunofluorescent labelling in 3T3-L1 cells

The phallotoxin had been isolated in 1937 from the deadly *Amanita phalloides* mushroom by Feodor Lynen and coll. The phallotoxin is bicyclic peptide that differ by two amino acid residues. It can be used interchangeably in most applications and bind competitively to the same sites in F-actin. Fluorescent phallotoxin stains F-actin at nanomolar concentrations, this providing convenient probes for labelling, identifying, and quantitating F-actin in tissue sections or cell cultures. It has been reported that phallotoxins are unable to bind to monomeric G-actin.

For these experiments, 3T3-L1 cells were grown and differentiated onto glass coverslips as previously described. Cells were fixed in 3.7% formaldehyde solution in PBS for 10 min at room temperature and then permeabilized with a cold solution of acetone (-20^0C) for 5 min.

Preparing the stock solution:

- The vial contents should be dissolved in 1.5 mL methanol to yield a final concentration of 200 units/mL, which is equivalent to approximately 6.6 µM.

  One unit of phallotoxin is defined as the amount of material used to stain one microscope slide of fixed cells and is equivalent to 5 µL of methanolic stock solution for the fluorescent phallotoxins.

- Dilute 5 µL methanolic stock solution into 200 µL PBS for each coverslip to be stained. To reduce nonspecific background staining with these conjugates, add 1% BSA to the staining solution.

When staining more than one coverslip, adjust volumes accordingly. For a stronger signal, use 2 or 3 units per coverslip.

- Place the staining solution on the coverslip for 20 minutes at room temperature. To avoid evaporation, keep the coverslips inside a covered container during the incubation.
- Wash two or more times with PBS.
- Incubate in 0.2 mg/ml 4',6'-diamidino-2-phenyl-indole (DAPI) for 2 min.
- Wash two times with PBS for 10 min.
- Mount in Fluorsave (Chemion).

4.2.11. RNA extraction

Real-time RT-PCR analysis

For these experiments, cells were grown and differentiated in 25cm^2 Petri dishes as described before. Total RNA was isolated by using TRI Reagent® (SIGMA) in accordance with the manufacturer's instructions. In briefly, the procedure used was the following:

- Add 1 ml of TRI Reagent directly on the culture dish. After addition of the reagent, the cell lysate should be passed several times through a pipette to form a homogenous lysate.
- Phase Separation: To ensure complete dissociation of nucleoprotein complexes, allow samples to stand for 5 minutes at room temperature. Add 0.2 ml of chloroform per ml of TRI Reagent used. Cover the sample tightly, shake vigorously for 15 seconds, and allow to stand for 15 min at room temperature. Centrifuge the resulting mixture at 12,000 x g for 15 minutes at 4°C.

  Centrifugation separates the mixture into 3 phases: a red organic phase (containing protein), an interphase (containing DNA), and a colourless upper aqueous phase (containing RNA).
- Transfer the aqueous phase to a fresh tube and add 0.5 ml of isopropanol per ml of TRI Reagent used in Sample Preparation and mix. Allow the sample to stand for 10 min at room temperature. Centrifuge at 12,000 x g for 10 min at 4°C. The RNA precipitate will form a pellet on the side and bottom of the tube.

- Remove the supernatant and wash the RNA pellet by adding 1 ml of 75% ethanol per 1 ml of TRI Reagent used in Sample Preparation. Vortex the sample and then centrifuge at 7,500 x g for 5 min at 4°C.
- Briefly dry the RNA pellet for 5–10 minutes by air-drying. Do not let the RNA pellet dry completely, as this will greatly decrease its solubility. Add an appropriate volume of 0.5% SDS water, or to the RNA pellet. To facilitate dissolution, mix by repeated pipetting with a micropipette at 55–60 °C for 10 min.

The RNA quality was verify by running it onto 1% agarose gel and the amount of RNA in the sample was quantified spectrophotometrically. The ratio between A260/A280 was calculated to verify RNA purity. 100 ng/sample was used for cDNA synthesis.

Degradation of genomic DNA and reverse transcription-PCR (RT-PCR)

The degradation of contaminating genomic DNA from RNA samples was performed with DNase I (RNase-free) (New England BioLabs) according to manufacturer's instructions. In briefly, the procedure used was the following:

- Resuspend 1 µg RNA in 1X DNase I Reaction Buffer to a final volume of 10 µ.
- Add 1 unit of DNase I, mix thoroughly and incubate at 37^0C for 10 min.
- Add 0.5 M EDTA to a final concentration of 5 mM. EDTA should be added to a final concentration of 5 mM to protect RNA from being degraded during enzyme inactivation.
- Heat inactivate at 75^0C for 10 min.

The synthesis of single-strand cDNA was carried out on 1 µg of RNA template, using iScript™ Reverse Transcription Supermix for RT-qPCR (BIO-RAD) following the manufacturer's instructions.

Component	Volume per reaction
5X iScript reverse transcription supermix	4 µl
RNA template (1 µg total RNA)	11 µl
Nuclease-free water	5 µl
Total volume	20 µl

Reaction protocol:

Priming	5 min at 25^0C
Reverse transcription	30 min at 42^0C
RT inactivation	5 min at 85^0C

Retrotrascription samples are stored at -20°C, until their use for real time RT-PCR.

Real Time RT-PCR

Real-time RT-PCR quantities the initial amount of the template most specifically, sensitively and reproducibly, and is a preferable alternative to other forms of quantitative RT-PCR that detect the amount of final amplified product at the end-point (Freeman WM et al., 1999). Real-time PCR monitors the fluorescence emitted during the reaction as an indicator of amplicon production during each PCR cycle as opposed to the endpoint detection (Higuchi R et al., 1993), eliminating post-PCR processing of PCR products. This helps to increase throughput and to reduce the chances of carryover contamination. In comparison to conventional RT-PCR, real-time PCR also offers a much wider dynamic range of up to 10^7-fold (compared to 1000-fold in conventional RT-PCR). The real-time PCR system is based on the detection and quantitation of a fluorescent report (Livak KJ et al., 1995). This signal increases in direct proportion to the amount of PCR product in a reaction. By recording the amount of fluorescence emission at each cycle, it is possible to monitor the PCR reaction during exponential phase where the first significant increase in the amount of PCR product correlates to the initial amount of target template. The higher the starting copy number of the nucleic acid target, the sooner a significant increase in fluorescence is observed. Currently four different chemistries, TaqMan®, Molecular Beacons, Scorpions® and SYBR® Green (BIO-RAD), are available for real-time PCR. All of these chemistries allow detection of PCR products via the generation of a fluorescent signal. TaqMan probes, Molecular Beacons and Scorpions depend on Förster Resonance Energy Transfer (FRET) to generate the fluorescence signal via the coupling of a fluorogenic dye molecule and a quencher moiety to the same or different oligonucleotide substrates. SYBR Green is a fluorogenic dye that exhibits little fluorescence when in solution, but emits a strong fluorescent signal upon binding to double-stranded DNA. The threshold cycle or C_t value (Fig. 12) is the point when the system begins to detect the increase in the signal

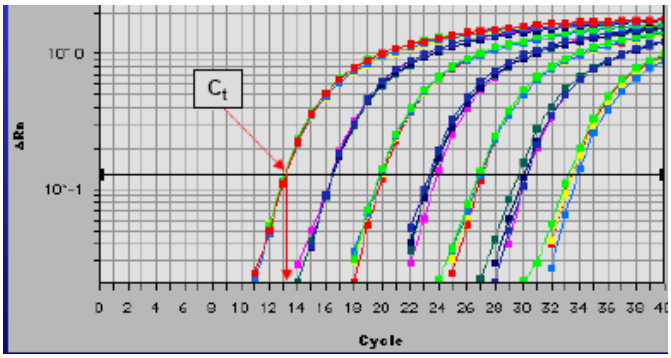

Fig. 12 **Real time RT-PCR curves and C_t values.**

associated with an exponential growth of PCR product during the log-linear phase. This phase provides the most useful information about the reaction and the slope of the log-linear phase is a reflection of the amplification efficiency. The efficiency (Eff) of the reaction can be calculated by the formula: $Eff=10^{(-1/slope)} - 1$. The efficiency of the PCR should be 90 - 100% (–3.6 > slope > –3.1). A number of variables can affect the efficiency of the PCR. These include length of the amplicon, secondary structure and primer quality. The C_t is an important parameter for quantitation. The higher the initial amount of genomic DNA, the sooner accumulated product is detected in the PCR process, and the lower is the C_t value. The threshold should be placed above any baseline activity and within the exponential increase phase. Some software allows determination of the cycle threshold (C_t) by a mathematical analysis of the growth curve. This provides better run-to-run reproducibility. Two strategies are commonly employed to quantify the real-time RT-PCR data: the **standard curve method** (absolute quantification) and the **comparative Ct method** (relative quantification).

In the **standard curve method**, a standard curve is first constructed from an RNA of known concentration. This curve is then used as a reference standard for extrapolating quantitative information for mRNA targets of unknown concentrations, thus generating absolute copy number data. In addition to RNA, other nucleic acid samples can be used to construct the standard curve, including purified plasmid dsDNA, *in vitro* generated ssDNA or any cDNA sample expressing the target gene. Spectrophotometric measurements at 260 nm can be used to assess the concentration of these DNAs, which can then be converted to a copy number value based on the molecular weight of the sample used. However, cDNA plasmids are the preferred standards for standard curve quantitation. The **comparative C_t method** involves comparing the C_t values of the samples of interest with a control or calibrator such as a non-treated sample or RNA from normal tissue. The C_t values of both the calibrator and the samples of interest are normalized to an appropriate endogenous housekeeping gene. The comparative C_t method is also known as the $2^{-\Delta\Delta Ct}$ method (Livak KJ et al., 2001), where

$\Delta\Delta C_t = \Delta C_{t,sample} - \Delta C_{t,reference}$. $\Delta C_{t,sample}$ is the C_t value for any sample normalized to the endogenous housekeeping gene and $\Delta C_{t,\ reference}$ is the C_t value for the calibrator also normalized to the endogenous housekeeping gene. For the $\Delta\Delta C_t$ calculation to be valid, the amplification efficiencies of the target and the endogenous reference must be approximately equal. This can be established by looking at how ΔC_t varies with template dilution. If the plot of cDNA dilution versus delta C_t is close to zero, it implies that the efficiencies of the target and housekeeping genes are very similar. This quantification method is described in the Applied Biosystems User Bulletins #2 and #5. Relative gene expression comparisons work best when the expression of the chosen internal control is abundant and remains constant among the samples. By using an invariant endogenous control as an active reference, quantitation of an mRNA target can be normalised for differences in the amount of total RNA added to each reaction. For this purpose, the most common choices are 18S RNA, GAPDH (glyceraldehyde-3-phosphate dehydrogenase) and β-actin.

Real-time PCR requires an instrumentation platform that consists of a thermal cycler, a computer, optics for fluorescence excitation and emission collection, data acquisition, and analysis software. These machines, available from several manufacturers, differ in sample capacity (some are 96-well standard format, others process fewer samples or require specialized glass capillary tubes), method of excitation (some use lasers, others broad spectrum light sources with tuneable filters), and overall sensitivity.

In our experimental conditions, Real-time PCR was performed in an MJ Opticon 2 using iQ™ SYBR Green supermix (BIO-RAD) following the manufacturer's instructions. 18S rRNA was used as reference housekeeping gene for normalization. We performed an analysis using the ΔΔCt, this procedure can be used since we have determined previously that the replication efficiencies (slopes of the calibration or standard curves) for the genes of interest and housekeeping gene are very close. All the amplification reactions were performed in duplicate. The primers were designed using Oligo Perfect® Designer Software (INVITROGEN). The nucleotide sequences of the primers were:

Gene Name	Forward primer	Reverse primer
C/EBPβ	CGCCTACCTGGGCTACCA	GACAGCTGCTCCACCTTCTTC
C/EBPδ	ATACCTCAGACCCCGACAGC	ATGCTTTCCCGTGTTCCTTC
C/EBPα	GAAGGTGCTGGAGTTGACCA	AGGAAGCAGGAATCCTCCAA
PPARγ	GTGGGGATGTCTCACAATGC	TGATCTCTTGCACGGCTTCT
FABP-4	ACGGCCCTGCAGAACTATCT	AAGGTTCACAAACGCGACAG
Pref-1	TTTCAACAAGGAGGCTGGTG	TCTAAGGGTTGCGGTGTGAG
Leptin	TGTGCACCTGAGGGTAGAGG	CCCTGGACAACCTTGGAGAT
HSL	GCTTCTCCCTCTCGTCTGCT	CAGACACACTCCTGCGCATA
18S rRNA	ACCGCGGTTCTATTTTGTTG	GACAAATCGCTCCACCAACT

Table 3. **The nucleotide sequences of the primers used for the experiments.**
C/EBPα, β and δ, CCAAT/enhancer-binding protein; **PPARγ**, peroxisome proliferative-activated receptor, gamma; **FABP-4**, fatty acid binding protein; **Pref-1**, preadipocyte factor-1; **HSL**, hormone-sensitive lipase; **18S rRNA**, 18S ribosomal RNA. 18S rRNA was used as the internal control.

Real Time RT PCR conditions

Amplification reactions were performed in 96-well standard plate. Each sample was analysed in duplicate. Reaction mix for all primers was prepared adding 2 μl of cDNA sample (dilution 1:10) to the following mix:

- 1.2 μl of *primer forward* (10 μM)
- 1.2 μl of *primer reverse* (10 μM)
- 10.6 μl of Dnase and Rnase free water
- 15 μl of 2X iQ™ SYBR Green supermix

Amplification conditions were:

- 95°C for 10 min } 1 cycle
- 95°C for 15 sec
- 60°C for 30 sec } 40 cycles
- 75^0C for 30 sec

4.2.12. Lipolysis measurement

For these experiments, cells were cultured and differentiated in 96-wells as described before. Lipolytic activity of GMG-43AC was evaluated after 2 and 7 days of treatment (see scheme 1) and after 4 days of drug-induced reversion of adipogenesis process. Lipolysis was evaluated by measuring the amount of glycerol released into the growth medium. Lipolysis was assayed by means of a commercial Assay KIT for Glycerol Detection (Zen-Bio Inc, Research Triangle Park, NC) according to the manufacturer's instructions. Briefly, glycerol released to the medium was phosphorylated by adenosine triphosphate (ATP) forming glycerol-1-phosphate (G-1-P) and adenosine-5'-diphosphate (ADP) in the reaction catalyzed by glycerol kinase. G-1-P was then oxidized by glycerol phosphate oxidase to dihydroxyacetone phosphate (DAP) and hydrogen peroxide (H_2O_2). A quinoneimine dye was produced by the peroxidase catalyzed coupling of 4-aminoantipyrine (4-AAP) and sodium N-ethytl-N-(3-sulfopropyl)m-anisidine (ESPA) with H_2O_2. The increase in absorbance at 540nm was directly proportional to glycerol concentration of the sample and was measured in spectrophotometer Bio UV/VIS® Parkin Helmer (UK).

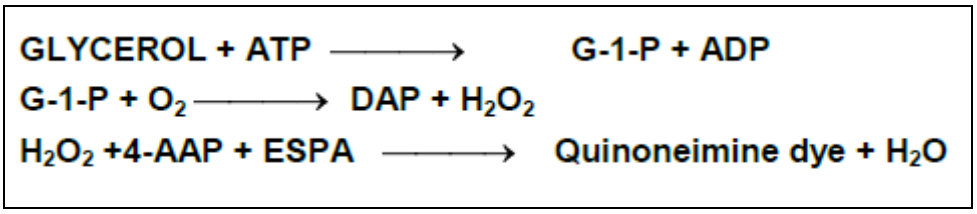

4.2.13. TUNEL assay

The cells were cultured and differentiated on 48-wells plates on coverslips as described before. 3T3-L1 were fixed with 4% for 15 min paraformaldehyde in PBS. TUNEL (Terminal deoxynucleotidyl transferase dUTP Nick End Labeling) is a common method for detecting DNA fragmentation that results from apoptotic signaling cascades. It measures the fragmented DNA of apoptotic cells by catalytically incorporating fluorescin-12-dUTP at 3'-OH DNA ends using the Terminal Deoxynucleotidyl Transferase enzyme (rTdT). The fluorescin-12-dUTP-labeled DNA can be visualized

directly by fluorescence microscopy. Nuclei were visualized after 2 min incubation with 0.2 mg/ml 4',6'-diamidino-2-phenyl-indole (DAPI). The apoptotic cells were visualized using TUNEL kit (ApoTag; Chemicon, Tamecula, CA) according to a standard protocol supplied by the manufacturer. Slides were photographed using fluorescence microscope Leica and digital camera Leica (German).

Statistical analysis

All data were expressed as means ± SEM. Differences between groups were examined for statistical significance using the unpaired Student's *t*-test. Multiple comparisons were analyzed by one-way analysis of variance (ANOVA) followed by Tukey post hoc test. Statistical significance was accepted at a level $P<0.05$.

5. RESULTS

5.1. The differentiation protocol for 3T3-L1 cells and Oil Red O staining

Adipogenesis is the process by which undifferentiated precursor cells differentiate into fat cells. This has become one of the most intensively studied developmental processes for at least two reasons: the increasing prevalence of obesity in our society has focused attention on many aspects of fat cell biology, and the availability of good cell culture models of adipocyte differentiation has permitted detailed studies not possible in other systems (Kui-Jin K et al., 2010). 3T3-L1 cells constitute one of the most popular *in vitro* models for the investigation of adipogenesis. These cells show fibroblast-like morphology with 3-4 protrusions and express receptors for growth factors such as insulin. Under certain stimulation, 3T3-L1 cells gradually become adipocytes and produce triglycerides accumulated in small and large droplets in cytoplasm (Fig.13).

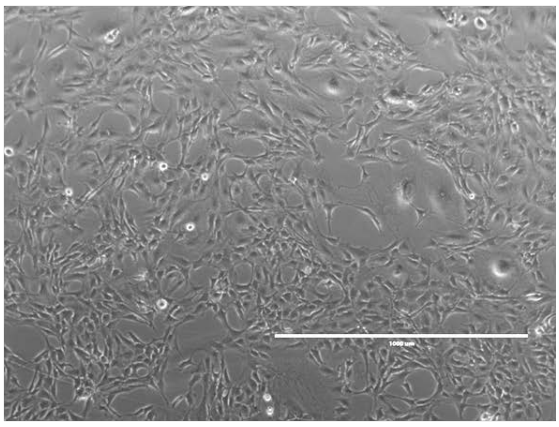

3T3-L1 preadipocytes

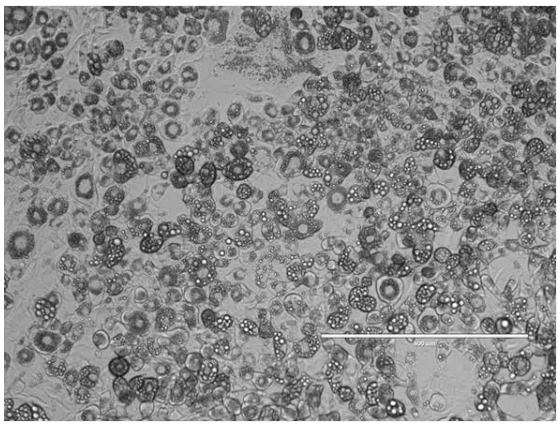

3T3-L1 adipocytes

Fig. 13 **3T3-L1 preadipocytes (left) and adipocytes (right).** Pictures were taken with EVOS® microscope (AMG, USA)

Studies in adipogenic cell lines have shown that the differentiation of preadipocytes into adipocytes is accompanied by changes in gene expression, e.g., a dramatic increase in the expression of the CCAAT/enhancer binding proteins C/EBPβ and C/EBPδ followed by the expression C/EBPα and the nuclear hormone receptor *peroxisome proliferator-activated receptor* γ (PPARγ) (Rosen ED et al., 2002; Kui-Jin K et al., 2010). These latter factors induce gene expression changes characteristic of mature adipocytes and remain elevated for the life of the cell. In the present model of the transcriptional cascade leading to adipogenesis, C/EBPβ and C/EBPδ induce low levels of PPARγ and

C/EBPα, which are then able to induce each other's expression in a positive feedback loop that promotes and maintains the differentiated state. This model is consistent with gain-of-function data showing that the addition of either PPARγ or C/EBPα can promote adipogenesis in fibroblast cell lines (Rosen ED et. al., 2002)

To achieve the goals proposed in this research project it was necessary to set up: a) the differentiation protocol for 3T3-L1 cells; b) the colorimetric technique for detecting adipocyte droplets, and c) the quantification assay for accumulated triglycerides.

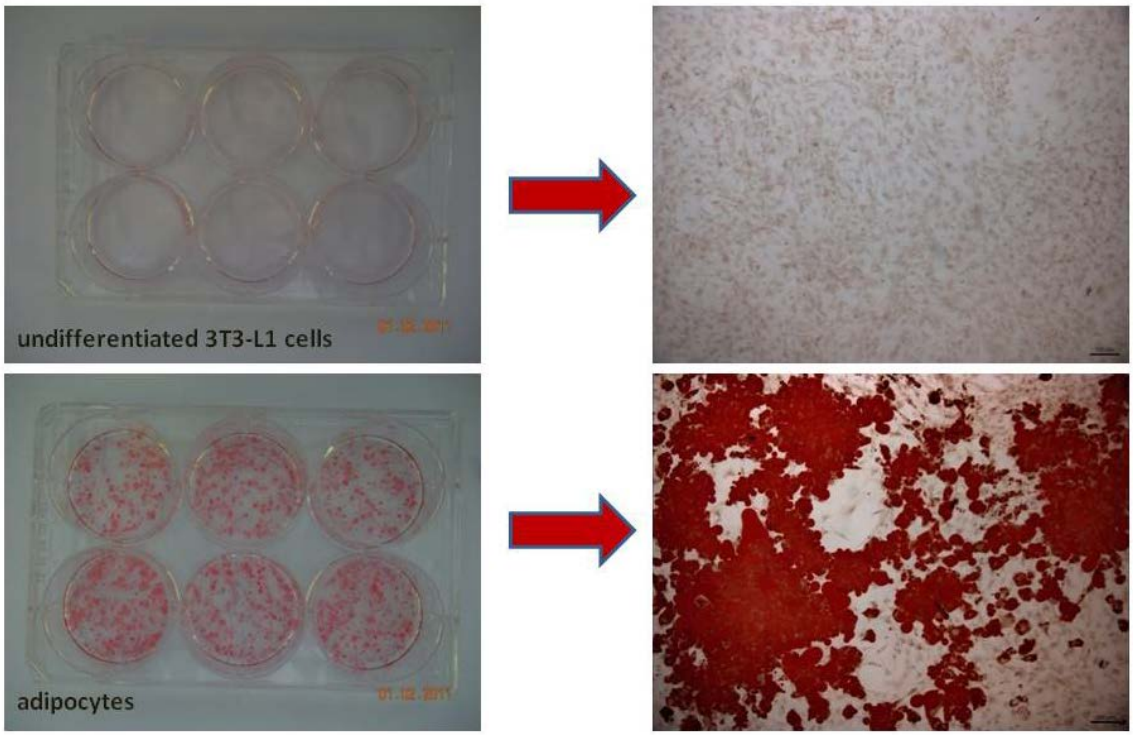

Fig. 14 **Oil Red O staining of undifferentiated 3T3-L1 cells (top) and adipocytes (bottom).**

In our experimental conditions droplets of triglycerides accumulated in differentiated 3T3-L1 cells were highly positive to the Oil Red O staining, which is shown in red in figure 14. The quantification of adipocytes and measurement of extracted Oil Red O at 500 nm are reported in figure 15.

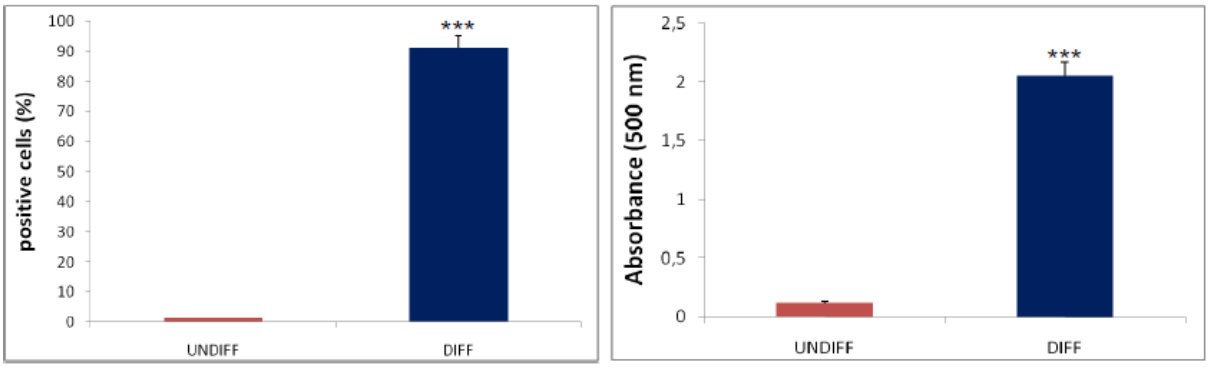

***Fig. 15* Oil Red O staining of undifferentiated 3T3-L1 cells and adipocytes.** Quantification of positive cells (left). Measurement of accumulated triglycerides (right). Each experimental condition was assayed in triplicate and the graph is referred to the means of at least eight independent experiments. Values are mean ± SEM. Significantly different from UNDIFF,*P<0.05, **P<0.01, ***P < 0.001.

5.2. GMG-43AC inhibition of lipid accumulation during 3T3-L1 differentiation in adipocyte promoting medium: results of scheme 1

5.2.1. Effects of GMG-43AC on lipid accumulation of adipocytes

To examine the role of GMG-43AC on adipocyte formation and lipid accumulation the drug was administrated to 3T3-L1 cells throughout the 10 days (see: materials and methods, scheme 1) and the effects were evaluated on *day 10*. Figure 16 shows a typical Oil Red O staining of lipid accumulation in differentiated adipocytes (Fig. 16, panel A). This process was significantly counteracted by the drug at the dosages beginning from 500 µM (Fig. 16, panel B and C).

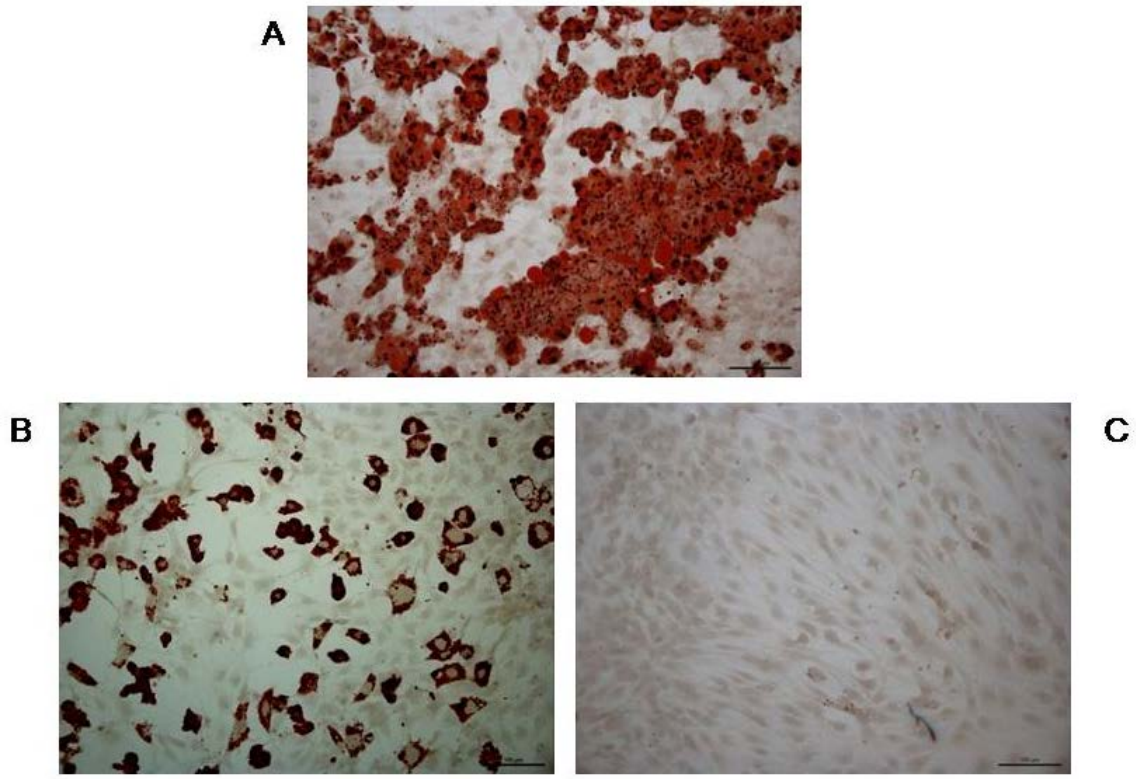

Fig. 16 *(A)* Oil Red O staining of adipocytes at day 10; (B) Oil Red O staining of adipocytes treated with 500 µM GMG-43AC at day 10 ; (C) Oil Red O staining of adipocytes treated with 1000 µM GMG-43AC at day 10.

Figure 17 shows the total count of differentiated cells positive to Oil Red O staining expressed as a percentage of the total number of cells. Almost 80% of the cells were positive to Oil Red O staining. According to the results, low concentrations of GMG-43AC (ranging from 0.1 µM to 300 µM) had no significant inhibitory effects on cell differentiation after 10 days of treatment. The inhibitory effects were observed with GMG-43AC concentrations of 500 µM and higher. These results were confirmed by measuring the absorbance at 500 nm of the triglycerides stained with Oil Red O and extracted from differentiated 3T3-L1 cells of the various experimental groups (Fig. 18).

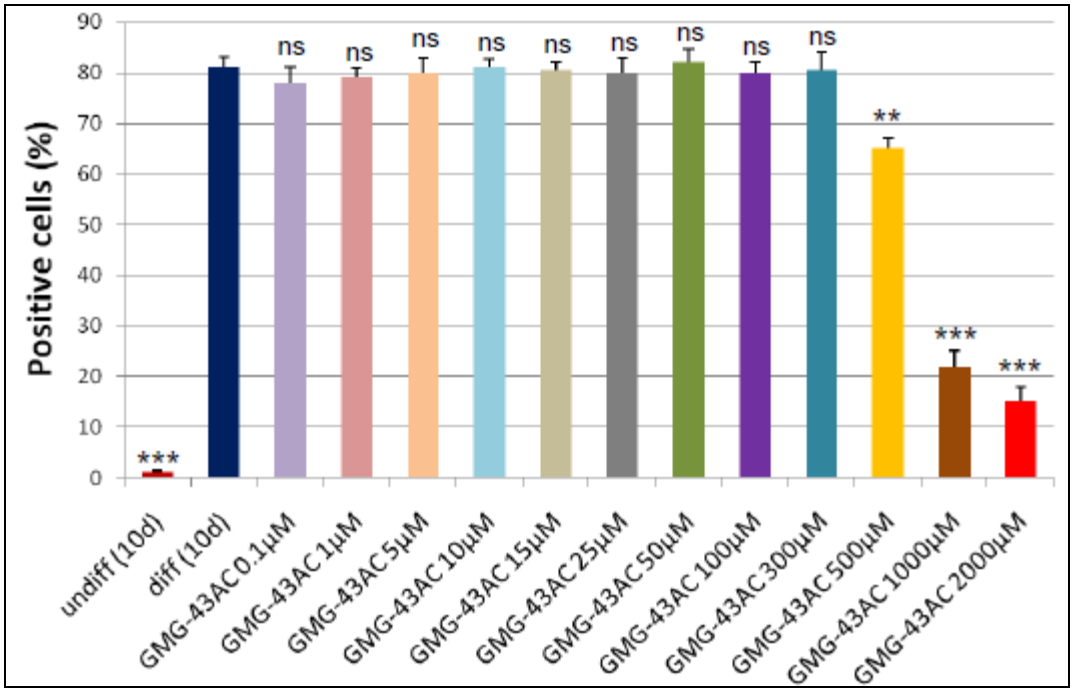

***Fig. 17* Oil Red O staining at *day 10* of undifferentiated 3T3-L1 cells and adipocytes (scheme 1 of treatment).** Percentage of positive cells in reference to total cell population. Reported values (mean± SEM) are the result of three independent experiments and for each experiment 5 fields were considered for each condition. Significantly different from DIFF, *P<0.005, **P<0.01, ***P<0.001.

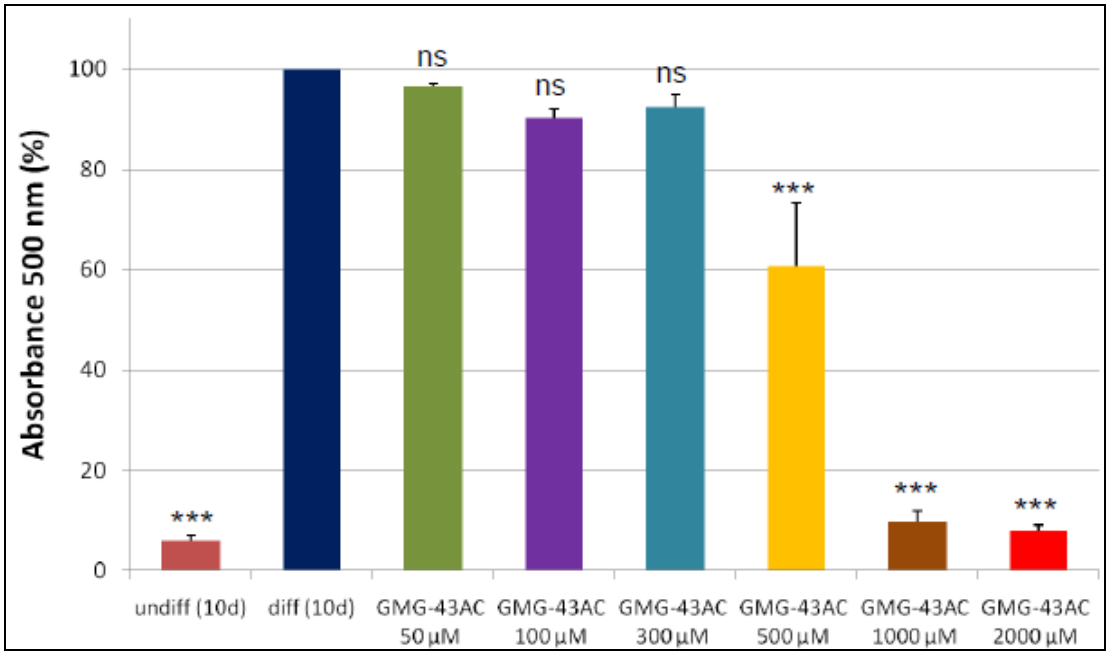

Fig. 18 Levels of accumulated triglycerides (labelled with Oil Red O) in 3T3-L1 undifferentiated cells and adipocytes as evidenced by quantitative absorbance at 500 nm wavelength (scheme 1 of treatment). Each experimental condition was assayed in triplicate and the graph is referred to the means of four independent experiments. Values are mean ± SEM. Significantly different from DIFF, *P<0.05, **P<0.01, ***P<0.001.

5.2.2. Effects of GMG-43AC on protein expression

To examine the effect of GMG-43AC on expression of factors involved in adipogenesis regulation during the differentiation period, preadipocytes were induced to differentiated in induction medium with different doses of drug and harvested at indicated time (12 hours, 48 hours, 4 days and 10 days). Western blotting was performed to analyze the expression of adipocyte marker proteins such as C/EBPβ *(CCAAT/enhancer binding protein* β*)*, C/EBPα, PPARγ *(peroxisome proliferator-activated receptor* and FABP-4 *(fatty acid binding protein-4)*. The changes of protein expression during differentiation were shown in figure 19. As expected, differentiation towards adipocytes first affected C/EBPβ. The C/EBPβ level was abundantly increased at 12 hours of adipogenesis stimulated *in vitro* by 3-isobutyl-1-methylxanthine (IBMX) and at 48 hours its expression began to decrease. Treatment with the doses 300 µM and 500 µM of GMG-43AC slowed the degradation of C/EBPβ at 48 hours. On the contrary, the dosage 1000 µM reduced the levels of this protein starting from 48 hours of differentiation.

Western blotting was also performed to evaluate the protein expression of markers specific for terminal differentiation phase, such as PPARγ and C/EBPα. As required, during the adipogenesis the levels of both of them increased and were maximal at day 10 of differentiation. It was noticeable that the drug dose of 300 µM does not modified significantly expression of PPARγ and C/EBPα. While the expression of both of them was significantly counteracted by GMG-43AC at the higher dosages (Fig. 19).

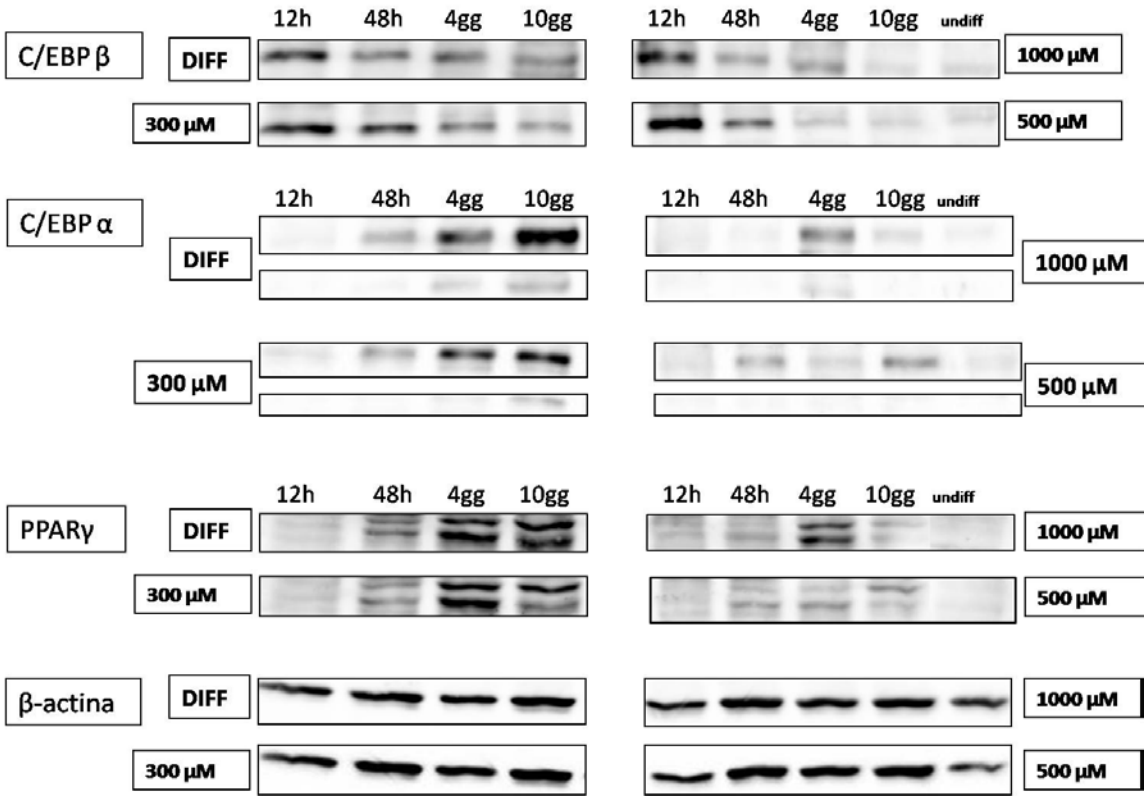

Fig. 19 **Western blotting analysis of molecular factors involved in adipogenesis.** At the indicated time cells were lysed with RIPA buffer. Sixty micrograms of total protein extracts were separated in denaturing SDS-PAGE and transferred onto nitrocellulose membrane. Specific antibodies were used to study the expression of proteins involved in adipogenesis. The experiment was repeated three time with similar results.

In this study, the levels of FABP-4 protein expression were also investigated. FAPB-4 is a characteristic protein of mature adipocytes. As figure 20 clearly shows, after treatment with GMG-43AC for 10 days the levels of FABP-4 were decreased in a dose-dependent manner.

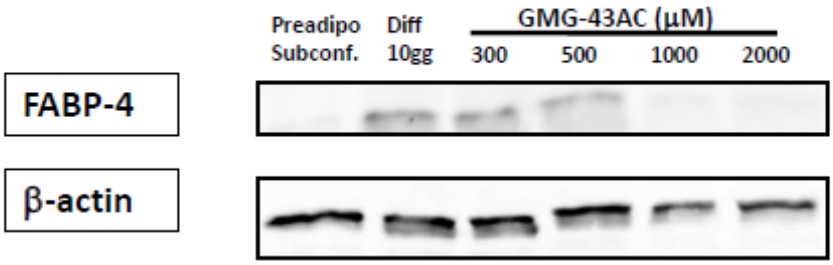

Fig. 20 **Western blotting analysis of FABP-4).** At the end the incubation period cells were lysed with RIPA buffer. Sixty micrograms of total protein extracts were separated in denaturing SDS-PAGE and transferred to a nitrocellulose membrane. FABP-4 antibody was used to study the expression of proteins involved in adipogenesis. The experiment was repeated three time with similar results.

Therefore, the phosphorylation of PPARγ in the presence of GMG-43AC was investigated. The results shows that pPPARγ levels decreased as well as PPARγ. This result suggests that GMG-43AC was not involved in the phosphorylation of PPARγ (Fig. 21).

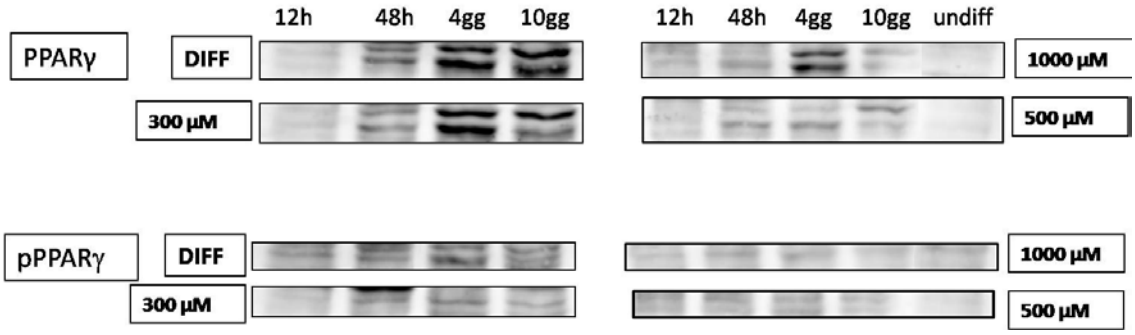

Fig. 21 **Western blotting analysis of molecular factors involved in adipogenesis**. At the indicated time cells were lysed with RIPA buffer. Sixty micrograms of total protein extracts were separated in denaturing SDS-PAGE and transferred onto nitrocellulose membrane. Phospho-PPARγ and PPARγ antibodies were used to study the expression of proteins involved in adipogenesis. The experiment was repeated three time with similar results.

The expression and localization of PPARγ and FABP-4 proteins were investigated by means of immunofluorescence experiments (Fig. 22 and 24). By using the same technique we also investigated the expression of other master proteins strictly related to adipogenesis such as C/EBPα and leptin (Fig. 23 and 25).

Briefly, 3T3-L1 were differentiated in the presence of two the most active dosages of GMG-43AC: 1000 μM and 2000 μM for 10 days as described before. As previously reported by other authors, in adipogenesis the expression of these proteins is increased during adipogenesis (Rosen B et al., 2006). Our results show that the levels of these proteins was up-regulated in our experimental condition. The exposure to GMG-43AC during the experimental period markedly reduced PPARγ and C/EBPα. (Fig. 22 and 23). As a consequence of these, the drug treatment also down-regulated FABP-4 and leptin expression (Fig. 24 and 25). Regarding leptin, it was noticeable that the dose of 1000 μM of experimental drug did not reduce the number of positive cells but changed the intracellular distribution of the protein (Fig. 25).

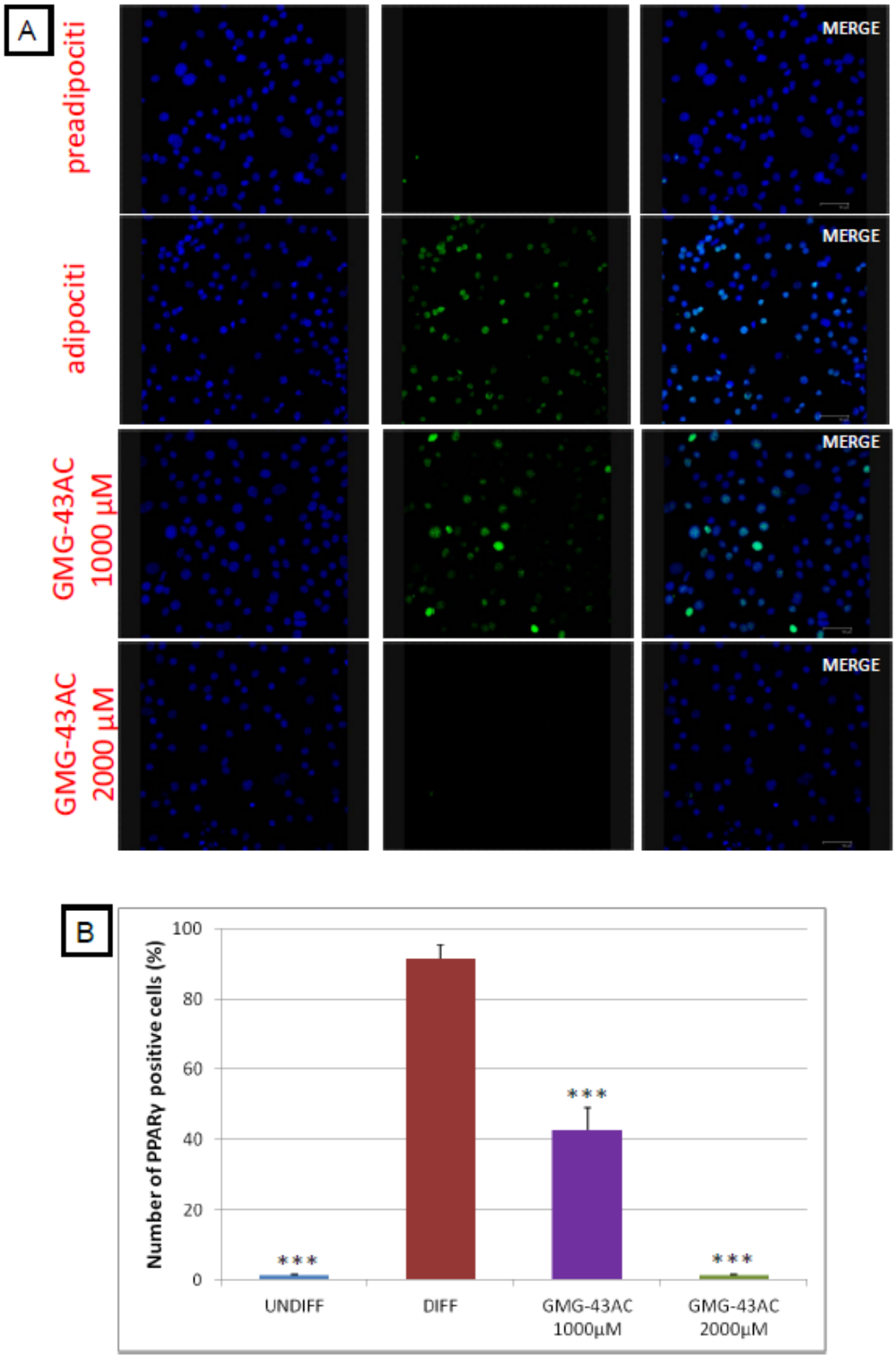

***Fig. 22* Immunofluorescence analysis of PPARγ.** (A) preadipocytes; adipocytes; adipocytes treated with 1000 µM and 2000 µM GMG-43AC for 10 days. (B) Quantification (%) of cells expressing PPARγ in different experimental conditions. Higher doses of GMG-43AC abolished the expression of PPARγ. Reported values (mean ± SEM) are the result of three independent experiments and for each experiment at least 5 fields were considered for each condition. Significantly different from DIFF, *P<0.05, **P<0.01, ***P<0.001.

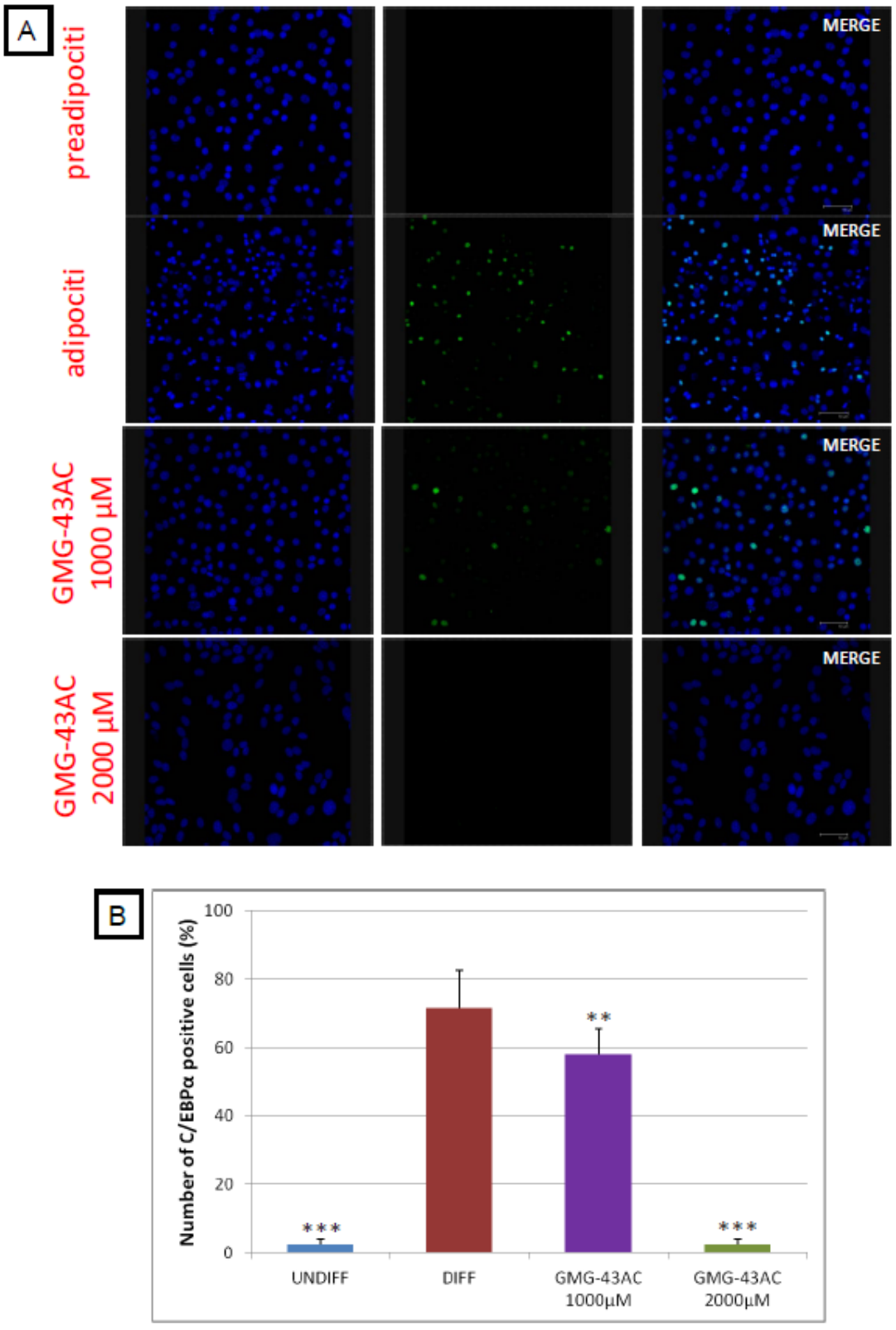

Fig. 23 **Immunofluorescence analysis of C/EBPα.** (A) preadipocytes; adipocytes; adipocytes treated with 1000 µM and 2000 µM GMG-43AC for 10 days. (B) Quantification (%) of cells expressing C/EBPα in different experimental conditions. Higher doses of GMG-43AC abolished the expression of C/EBPα. Reported values (mean ± SEM) are the result of three independent experiments and for each experiment at least 5 fields were considered for each condition. Significantly different from DIFF, *P<0.05, **P<0.01, ***P<0.001.

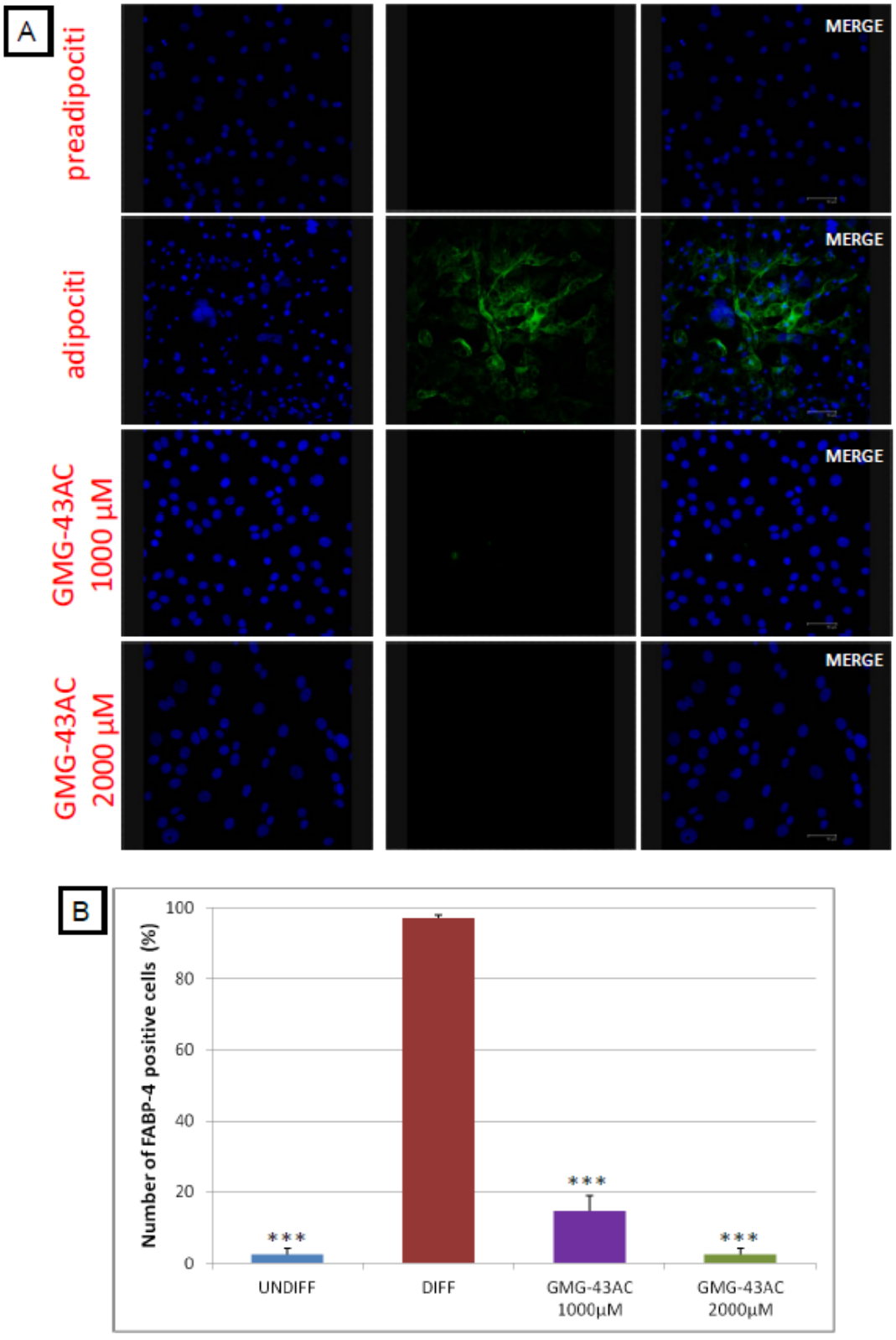

Fig. 24 **Immunofluorescence analysis of FABP-4.** (A) preadipocytes; adipocytes; adipocytes treated with 1000 µM and 2000 µM GMG-43AC for 10 days. (B) Quantification (%) of cells expressing FABP-4 in different experimental conditions. Higher doses of GMG-43AC abolished the expression of FABP-4. Reported values (mean ± SEM) are the result of three independent experiments and for each experiment at least 5 fields were considered for each condition. Significantly different from DIFF, *P<0.05, **P<0.01, ***P<0.001.

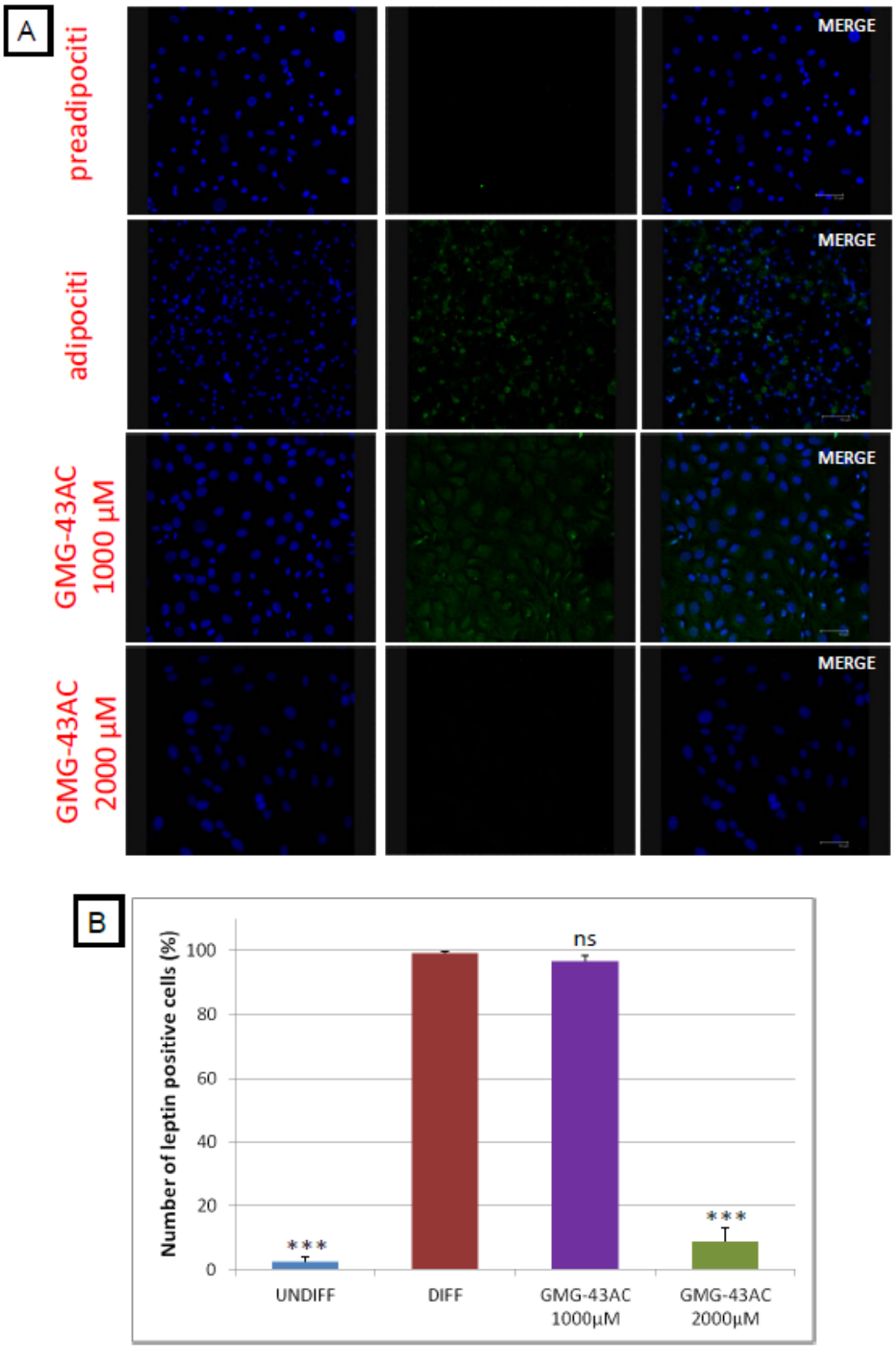

Fig. 25 **Immunofluorescence analysis of leptin.** (A) preadipocytes; adipocytes; adipocytes treated with 1000 µM and 2000 µM GMG-43AC for 10 days. (B) Quantification (%) of cells expressing leptin in different experimental conditions. Higher doses of GMG-43AC abolished the expression of leptin. Reported values (mean ± SEM) are the result of three independent experiments and for each experiment at least 5 fields were considered for each condition. Significantly different from DIFF, *P<0.05, **P<0.01, ***P<0.001.

To examine whether GMG-43AC changes expression of C/EBPβ and C/EBPδ, we differentiated 3T3-L1 cells in the presence of the drug (300, 500, 1000 and 2000 µM) for the initial 48 hours. The isoforms C/EBPβ and C/EBPδ are two critical markers for the early phase of differentiation and are dramatically up-regulated within the first hours after induction of adipogenesis by IBMX and DEX respectively (see part 1.3.1). They are known to have crucial role in the regulation of PPARγ and C/EBPα expression (Kawaji A et al., 2010). The expression of C/EBPβ and C/EBPδ proteins after exposure to GMG-43AC was investigated by means of immunofluorescence.

Our results show that the expression of these proteins was increased in our experimental condition (Fig. 26 and 28). The exposure to GMG-43AC during the initial 48 hours of adipogenesis markedly reduced C/EBPβ levels in a dose-dependent manner with the exception of the dose 300 µM (Fig. 26 and 27). Interestingly, this dosage slowed down the degradation of C/EBPβ at 48 hours of differentiation. Data is comparable to that obtained by using western blotting technique (Fig. 19).

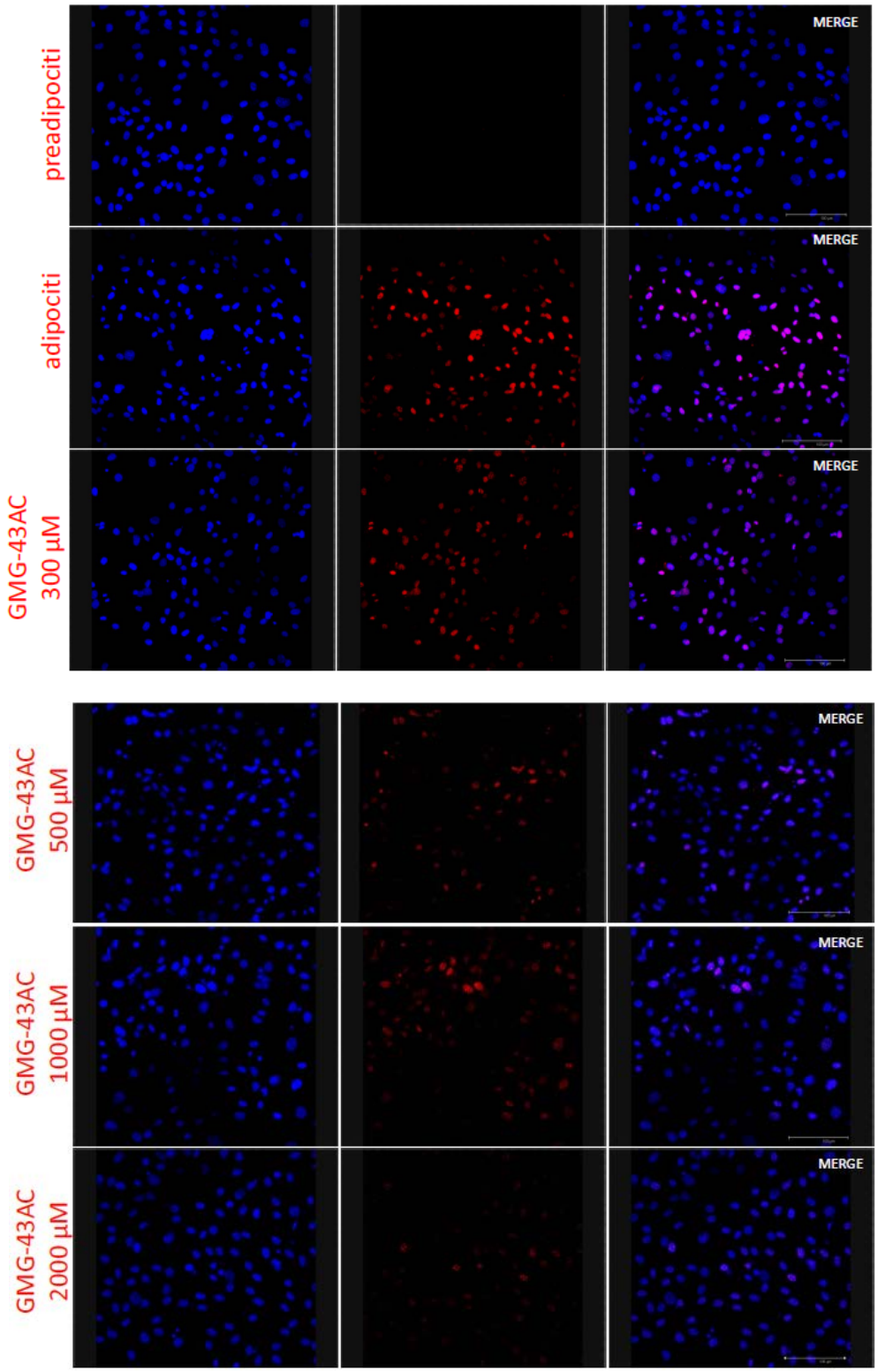

Fig. 26 **Immunofluorescence analysis of C/EBPβ.** Preadipocytes; adipocytes; adipocytes treated with 300, 500, 1000 and 2000 µM GMG-43AC for the initial 48 hours of differentiation.

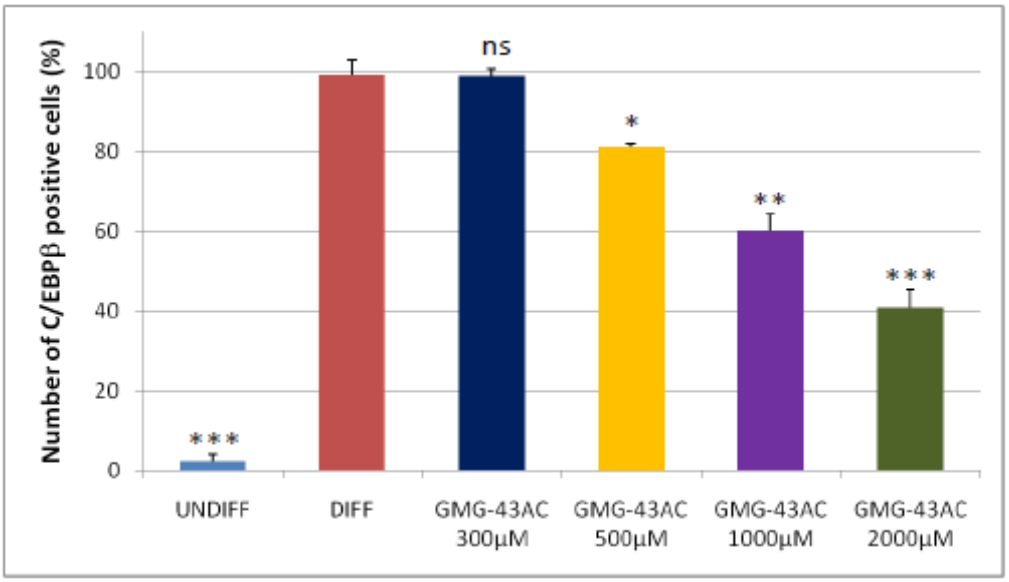

Fig. 27 **Immunofluorescence analysis of C/EBPβ.** Quantification (%) of cells expressing C/EBPβ in different experimental conditions. Reported values (mean ± SEM) are the result of three independent experiments and for each experiment at least 5 fields were considered for each condition. Significantly different from DIFF, *P<0.05, **P<0.01, ***P < 0.001.

We also evaluated the effects of GMG-43AC on the expression of C/EBPδ. Our results show that exposure to GMG-43AC markedly reduced the levels of this protein at the lower dose of 300 μM. Contrastingly, further doses did not influence the number of C/EBPδ - positive cells after 48 hours of treatment (Fig. 28 and 29).

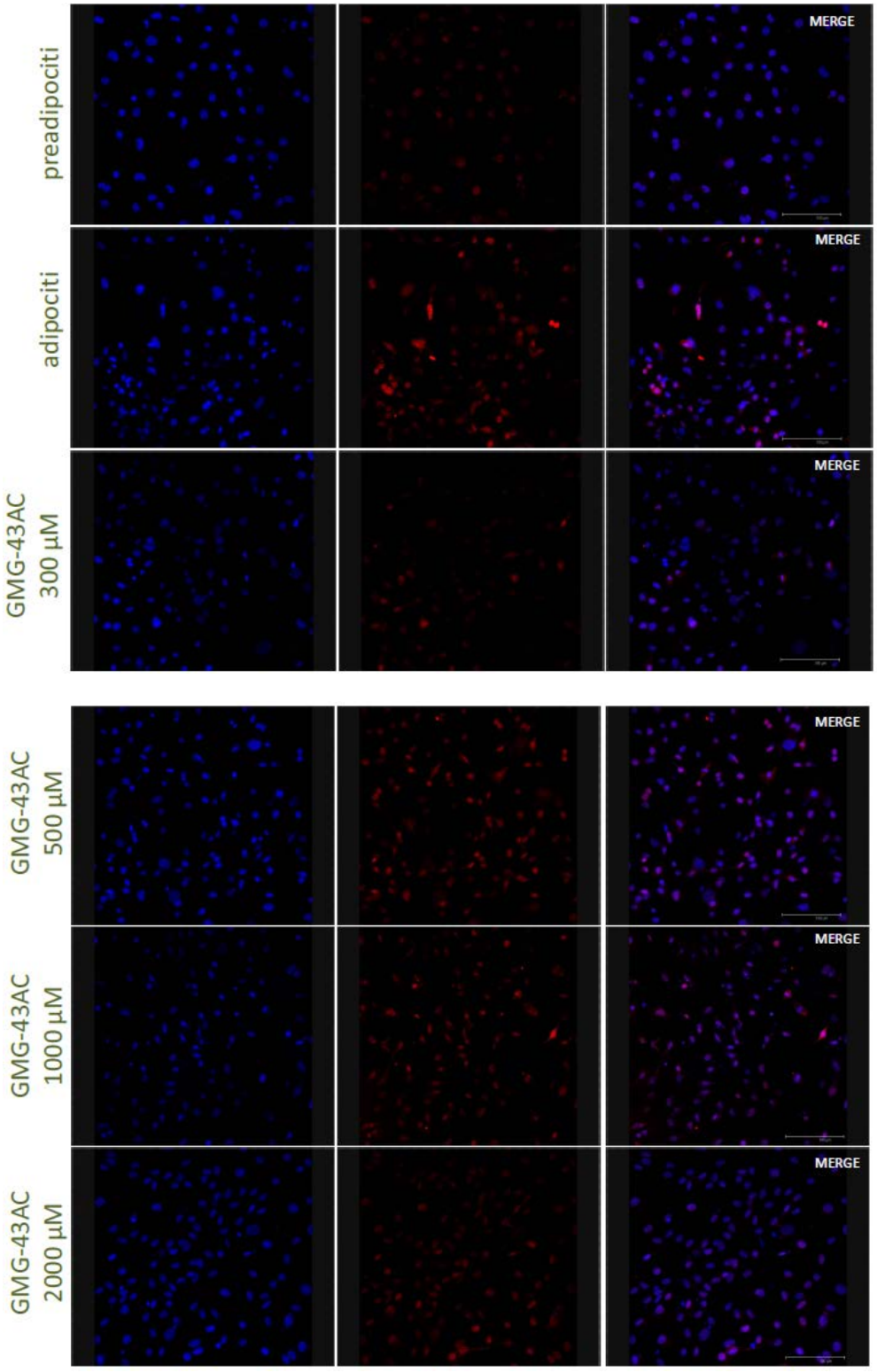

Fig. 28 **Immunofluorescence analysis of C/EBPδ.** Preadipocytes; adipocytes; adipocytes treated with 300, 500, 1000 and 2000 µM GMG-43AC for the initial 48 hours of differentiation.

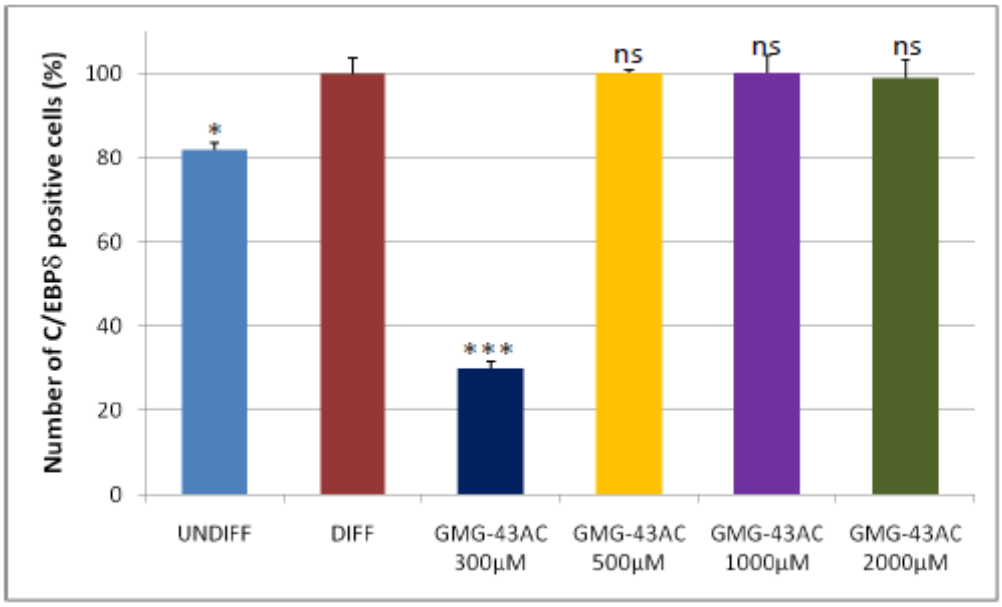

***Fig. 29* Immunofluorescence analysis of C/EBPδ.** Quantification (%) of cells expressing C/EBPδ in different experimental conditions. Reported values (mean ± SEM) are the result of three independent experiments and for each experiment at least 5 fields were considered for each condition. Significantly different from DIFF, *P<0.05, **P<0.01, ***P<0.001.

5.2.3. Effects of GMG-43AC on adipogenic transcription factors

The effect of GMG-43AC on the expression of preadipocyte and adipogenic transcription factors was also performed by means of real time RT-PCR. In particular, mRNA levels were quantified in several time points of adipogenesis: 12 hours, 48 hours, 4 days and 10 days. To this purpose, quantitative real time RT-PCR was performed in duplicate and a negative control was also included in each 96-well plate. Results obtained were quantified with comparative Ct method, using 18S ribosomal RNA as reference and the data were expressed as n-fold the calibrator by using the $2^{-\Delta\Delta Ct}$ (undifferentiated cells for Pref-1 mRNA; differentiated cells for the other mRNA).

First, we analyzed mRNA levels of C/EBPβ and C/EBPδ. Our results show that exposure to GMG-43AC significantly reduced mRNA levels of C/EBPβ by the drug at the dosages beginning from 500 µM at 12 hours of adipogenesis. However, the expression of C/EBPβ was not significantly affected at the lower dose of 300 µM (Fig. 30, panel A). Differently, at 48 hours of adipose differentiation, the drug dose of

300 µM reduced mRNA levels of C/EBPβ (P<0.001) and further doses were no longer as effective in the reduction of mRNA levels of C/EBPβ as at 12 hours (Fig. 30, panel B). We suppose that the lower dosages of GMG-43AC need more time to become effective in lowering the mRNA levels of C/EBPβ. In contrast, the higher doses faster reduce the levels of mRNA but their efficiency is short-lived. We think that it could be a saturation phenomenon or compensatory effect.

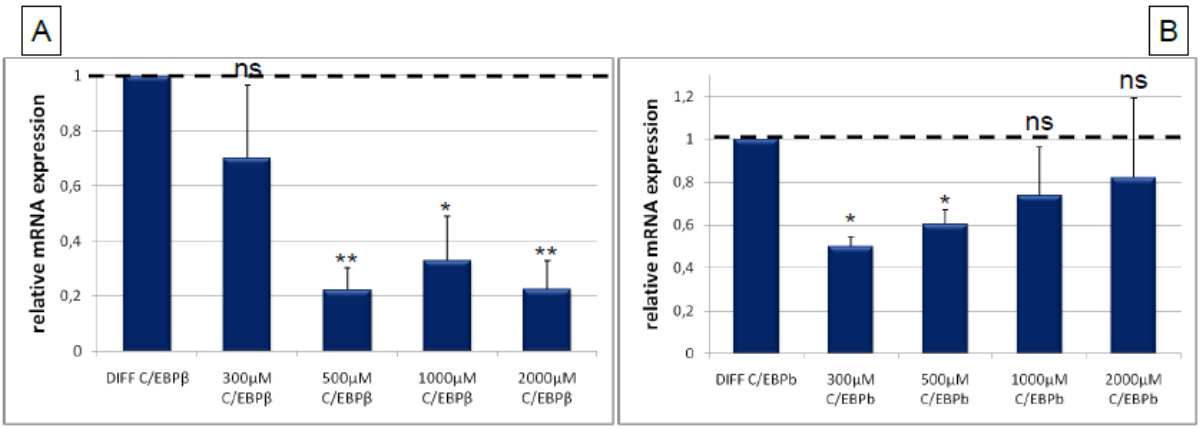

***Fig. 30* Effects of GMG-43AC on the expression of C/EBPβ during adipocyte differentiation.** 3T3-L1 cells were treated with GMG-43AC (300, 500, 1000, 2000 µM) for the initial (A) 12 hours or (B) 48 hours of adipogenesis. Data are the mean ± SEM of at least four determinations for each time point. Significantly different from DIFF C/EBPβ, *P<0.05, **P<0.01, ***P<0.001.

We further examined the effect of GMG-43AC on the expression of C/EBPδ mRNA. Our results show that after 12 hours of treatment with GMG-43AC there was no significant changes in the expression of C/EBPδ (Fig. 31, panel A). Differently, at 48 hours the dose of 300 µM slightly reduced expression of C/EBPδ (P<0.05), but interestingly, the dosage of 1000 µM significantly raised mRNA levels (P<0.01) (Fig. 31, panel B). Further doses had no significant effects on the expression of mRNA levels of C/EBPδ (Fig. 31, panel B). Together, these results suggest that the dose of 300 µM of GMG-43AC may need more time to decrease the expression of C/EBPδ. Differently, we suspect that it could be some compensatory or saturation phenomenon in case of the dosage 1000 µM of the drug.

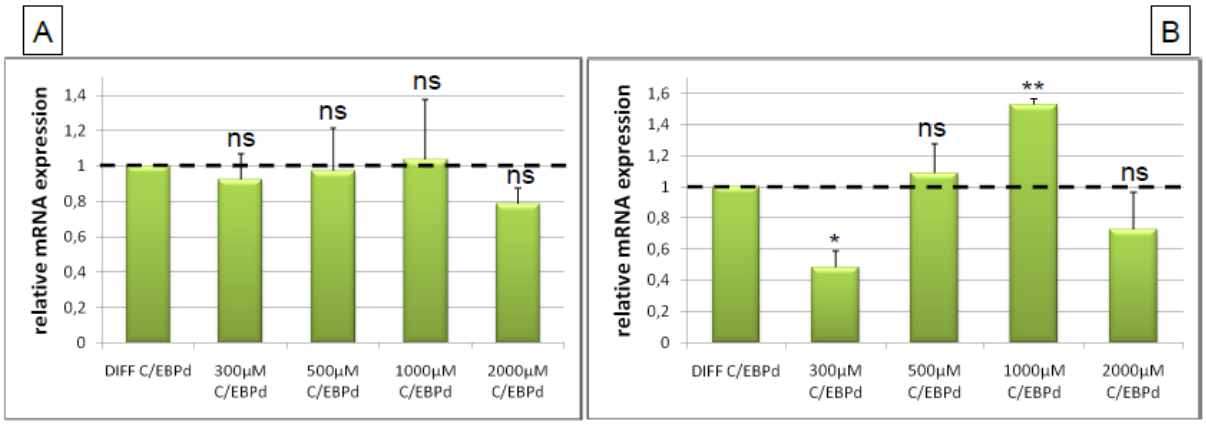

Fig. 31 **Effects of GMG-43AC on the expression of C/EBPδ during adipocyte differentiation.** 3T3-L1 cells were treated with GMG-43AC (300, 500, 1000, 2000 µM) for the initial (A) 12 hours or (B) 48 hours of adipogenesis. Data are the mean ± SEM of at least four determinations for each time point. Significantly different from DIFF C/EBPδ, *P<0.05, **P<0.01, ***<0.001.

We then examined the expression of PPARγ and C/EBPα, late adipogenic markers, which are crucial for adipocyte differentiation (Kim KJ et al., 2010).

Our results show that exposure to GMG-43AC markedly reduced mRNA levels of PPARγ at the dose of 2000 µM at 48 hours of differentiation process and this effect was maintained until the end of the adipogenesis (Fig. 32, panels A-C). GMG-43AC at 1000 µM decreased the mRNA levels starting from 4th day of differentiation. Interestingly, after 4 days of experiment the dose 500 µM significantly abolished (P<0.001) the expression of PPARγ, however, this effect was not maintained at the end of adipocyte differentiation (Fig. 32, panels B and C).

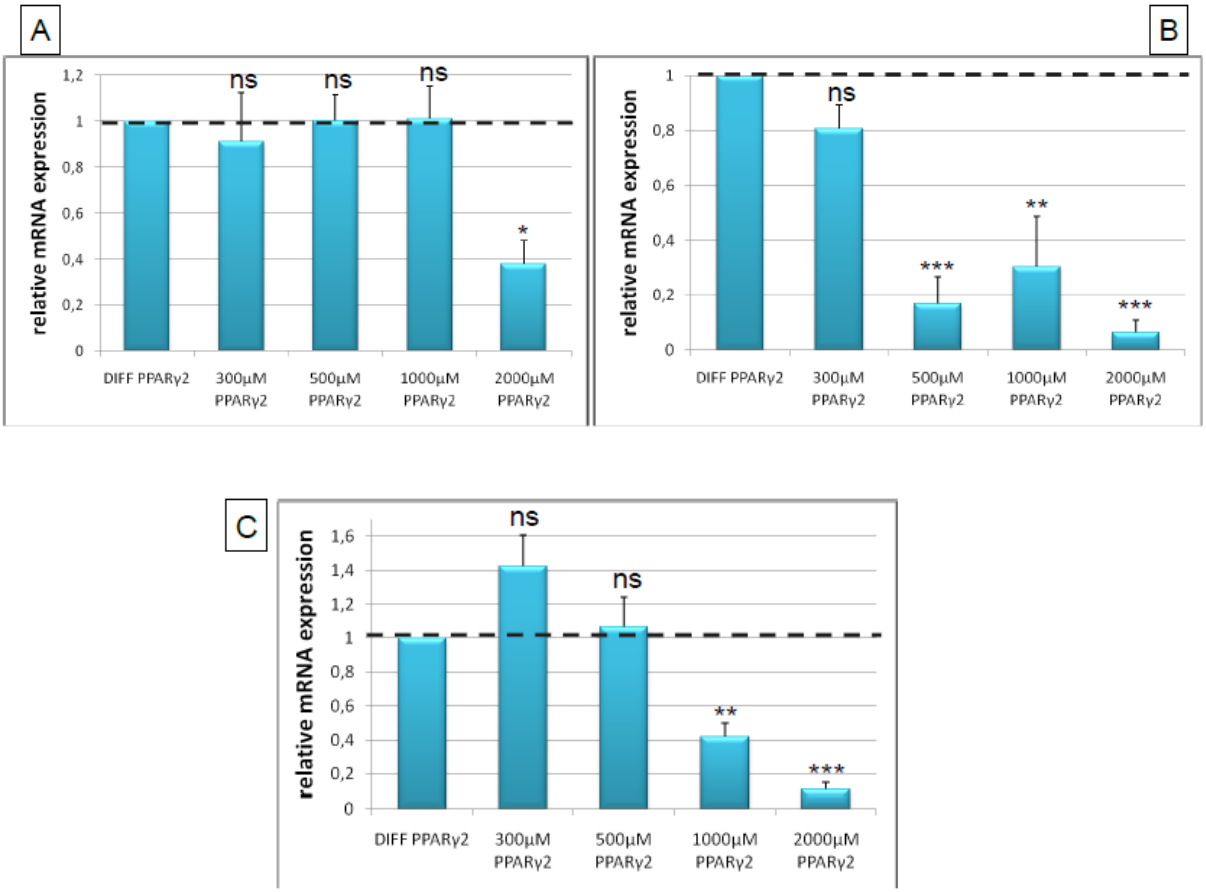

***Fig. 32* Effects of GMG-43AC on the expression of PPARγ during adipocyte differentiation.** 3T3-L1 cells were treated with GMG-43AC (300, 500, 1000, 2000 µM) for (A) 48 hours, (B) 4 days or (C) 10 days of adipogenesis. Data are the mean ± SEM of at least four determinations for each time point. Significantly different from DIFF PPARγ2 , *P<0.05, **P<0.01, ***P<0.001.

Therefore we evaluated the effects of GMG-43AC on the mRNA levels of C/EBPα from 48 hours to 10 days of differentiation. As shown in Figure 33, the experimental drug markedly inhibited the expression of this gene at the dosages 1000 µM and 2000 µM. This effect was maintained until day 10 of the adipogenesis. As in the case of PPARγ, after 4 days of experiment the dose 500 µM significantly abolished (P<0.001) the mRNA levels of C/EBPα, however, this effect was not sustained at the end of adipocyte differentiation (Fig. 33, panels B and C). Interestingly, the dosage of 300 µM significantly raised mRNA levels at 10 day (Fig 33, panel C).

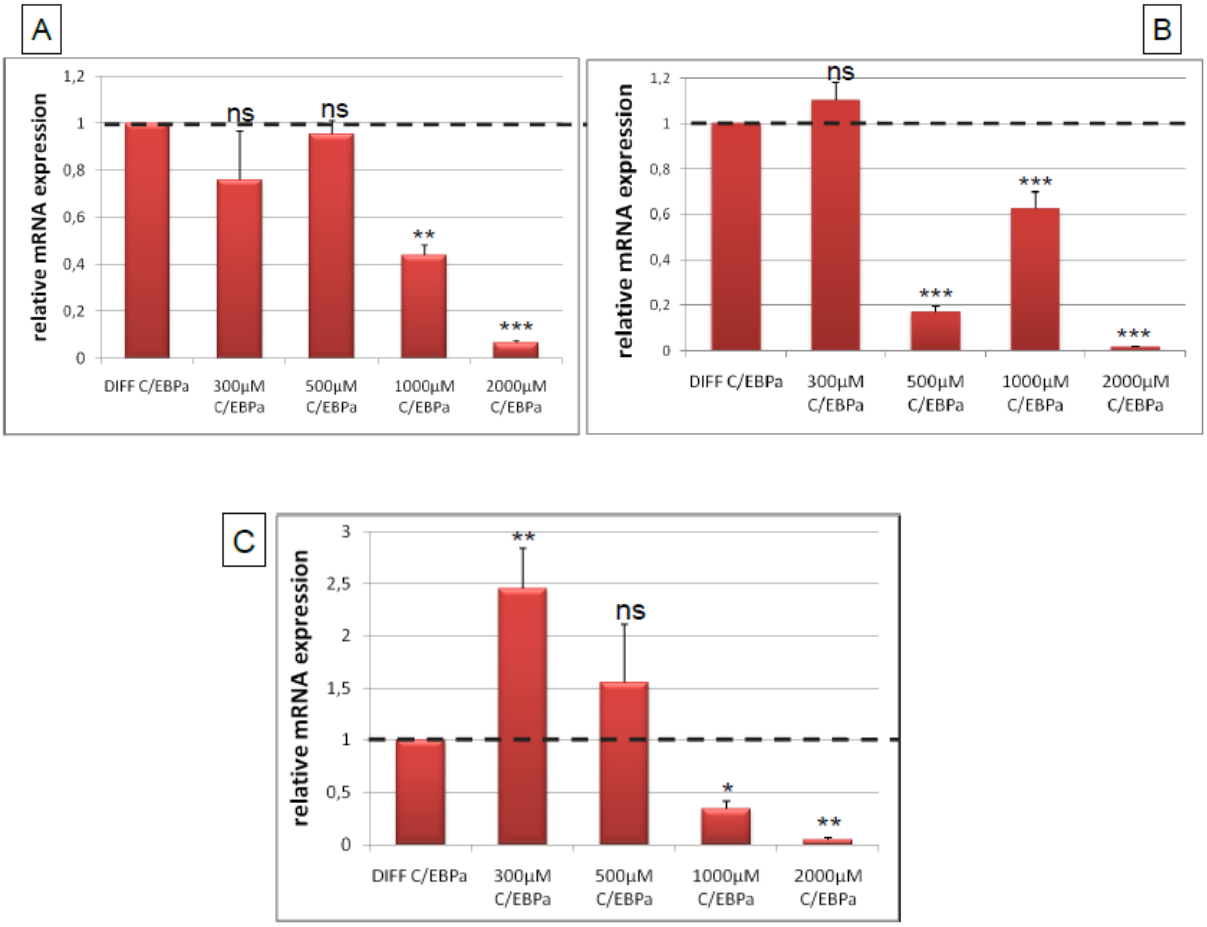

***Fig. 33* Effects of GMG-43AC on the expression of C/EBPα during adipocyte differentiation.** 3T3-L1 cells were treated with GMG-43AC (300, 500, 1000, 2000 µM) for (A) 48 hours, (B) 4 days or (C) 10 days of adipogenesis. Data are the mean ± SEM of at least four determinations for each time point. Significantly different from DIFF C/EBPα, *P<0.05, **P<0.01, ***P<0.001.

At days 4 and 10 of adipogenesis RT-PCR was performed to analyze the mRNA levels of FABP-4 and leptin that were known to be expressed in mature adipocytes (Xing Y et al., 2010). As might be expected, the genes encoding these proteins were expressed in the terminal phase of adipogenesis. FABP-4 and leptin were not critical to the differentiation process, but occurred as a result of adipocyte differentiation (Cowhed RM et al., 1999).

In our experimental conditions the mRNA levels of FABP-4 and leptin were down-regulated in a dose-dependent manner with all tested doses of GMG-43AC (Fig. 34 and 35). Data is comparable to that of immunofluorescence (Fig. 23 and 24).

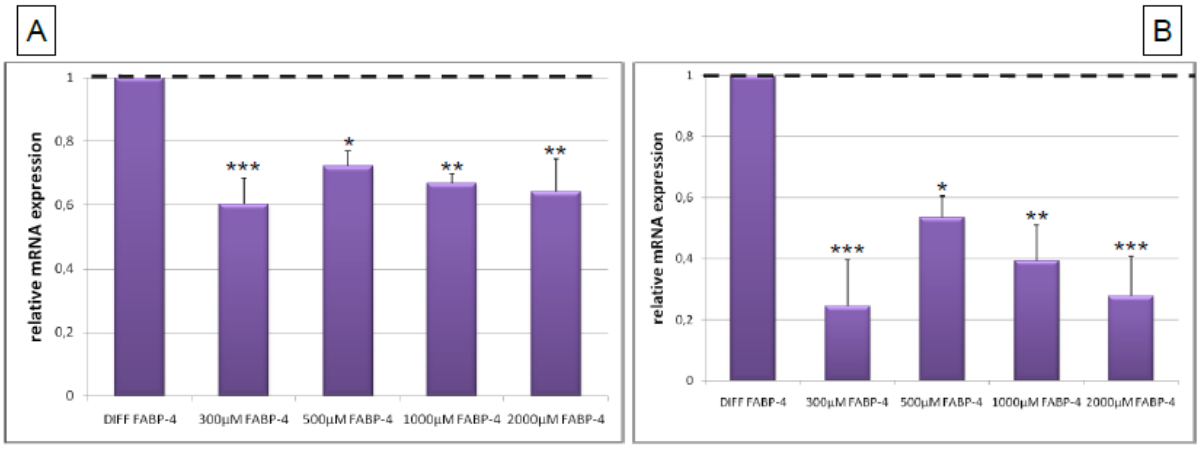

***Fig. 34* Effects of GMG-43AC on the expression of FABP-4 during adipocyte differentiation.** 3T3-L1 cells were treated with GMG-43AC (300, 500, 1000, 2000 µM) for (A) 4 days or (B) 10 days of adipogenesis. Data are the mean ± SEM of at least four determinations for each time point. Significantly different from DIFF FABP-4, *P<0.05, **P<0.01, ***P<0.001.

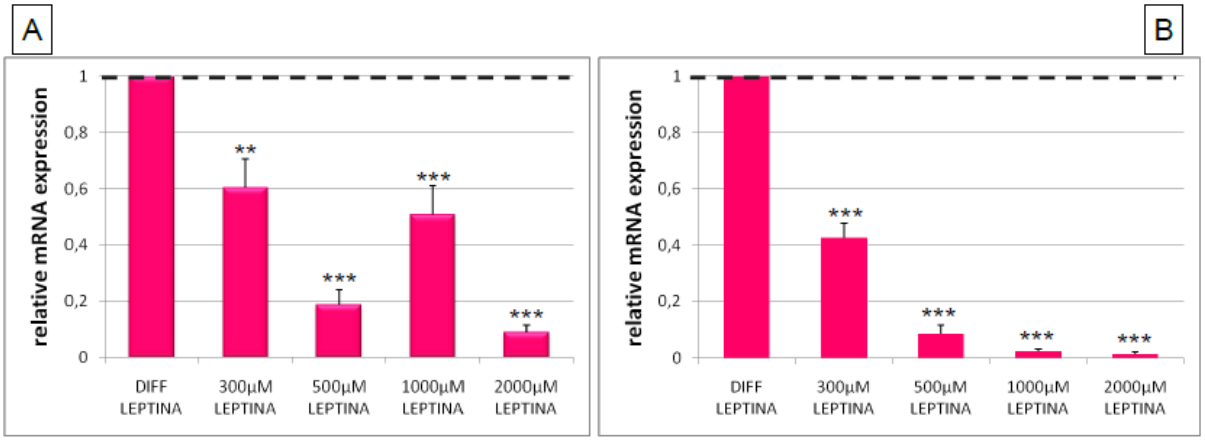

***Fig. 35* Effects of GMG-43AC on the expression of leptin during adipocyte differentiation.** 3T3-L1 cells were treated with GMG-43AC (300, 500, 1000, 2000 µM) for (A) 4 days or (B) 10 days of adipogenesis. Data are the mean ± SEM of at least four determinations. Significantly different from DIFF leptin, *P<0.05, **P<0.01, ***P<0.001.

To further investigate the effects of GMG-43AC on the initial phase of adipogenic differentiation, the expression of mRNA levels of Pref-1 was examined. Pref-1 is abundantly expressed in preadipocytes and disappears in adipocytes. Moreover, it is an inhibitor of adipocyte differentiation (Gao Y et al., 2008). As was shown by Sul, dexamethasone inhibits the transcription of protein Pref-1 (Sul HS, 2009).

As figure 36 made clear, the expression of Pref-1 was significantly reduced during the period of adipogenesis. At 12 hours of differentiation all doses of GMG-43AC appeared to potentiate the down-regulation effect of dexamethasone (Fig. 36, panel A). After the initial 48 hours, the dosage of 2000 µM started to be significant in increasing the mRNA levels of this gene (Fig. 36, panels B-D).

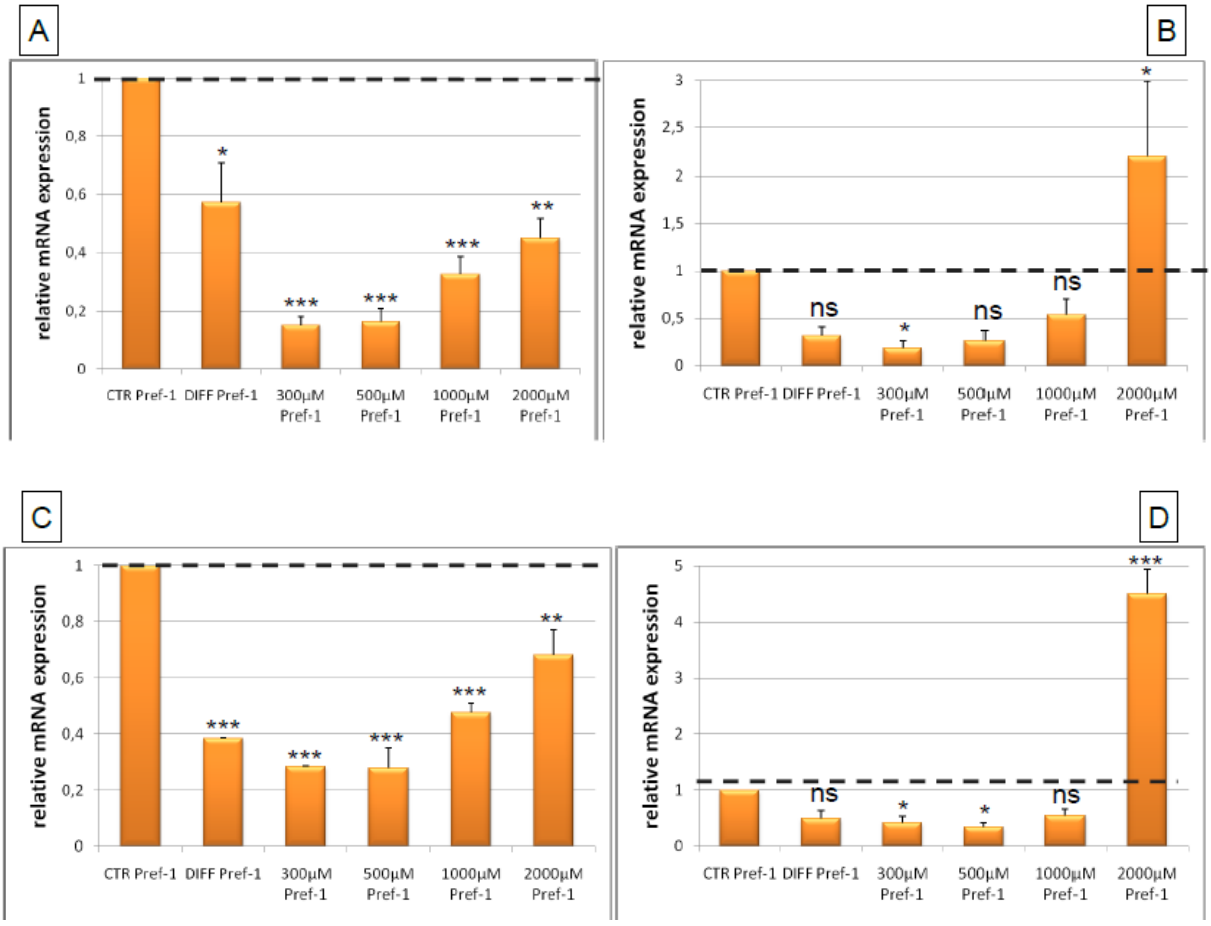

Fig. 36 Effects of GMG-43AC on the expression of Pref-1 during adipocyte differentiation. 3T3-L1 cells were treated with GMG-43AC (300, 500, 1000, 2000 µM) for (A) 12 hours, (B) 48 hours, (C) 4 days or (D) 10 days of adipogenesis. Data are the mean ± SEM of at least four determinations for each time point. Significantly different from CTR Pref-1, *P<0.05, **P<0.01, ***P<0.001.

5.2.4. Effect of GMG-43AC on actin cytoskeleton reorganization in 3T3-L1 adipocytes

We also studied the effect of GMG-43AC on actin cytoskeleton reorganization in the 3T3-L1 cells by means of immunofluorescence. The actin cytoskeleton is composed of actin filaments and many specialized actin-binding proteins (Takai Y et al., 2001).

For this experiment cells were differentiated in adipocytes for 3 and 6 days in the presence of the drug and analyzed for actin cytoskeleton organization after the staining with fluorescent phallotoxin. The phallotoxin was isolated from the deadly *Amanita phalloides* which binds specifically at the interface between F-actin subunits (see Materials and methods).

Our results show that that differentiating 3T3-L1 cells treated for 3 days with the doses 300 µM and 500 µM of GMG-43AC did not have any strong differences in actin filament rearrangement in relation to non treated adipocytes (Fig. 37, panels B-D). However, the dosages 1000 µM and 2000 µM of drug made redistribution of actin filaments to the terminal point of the cells (Fig. 37, panels E-F).

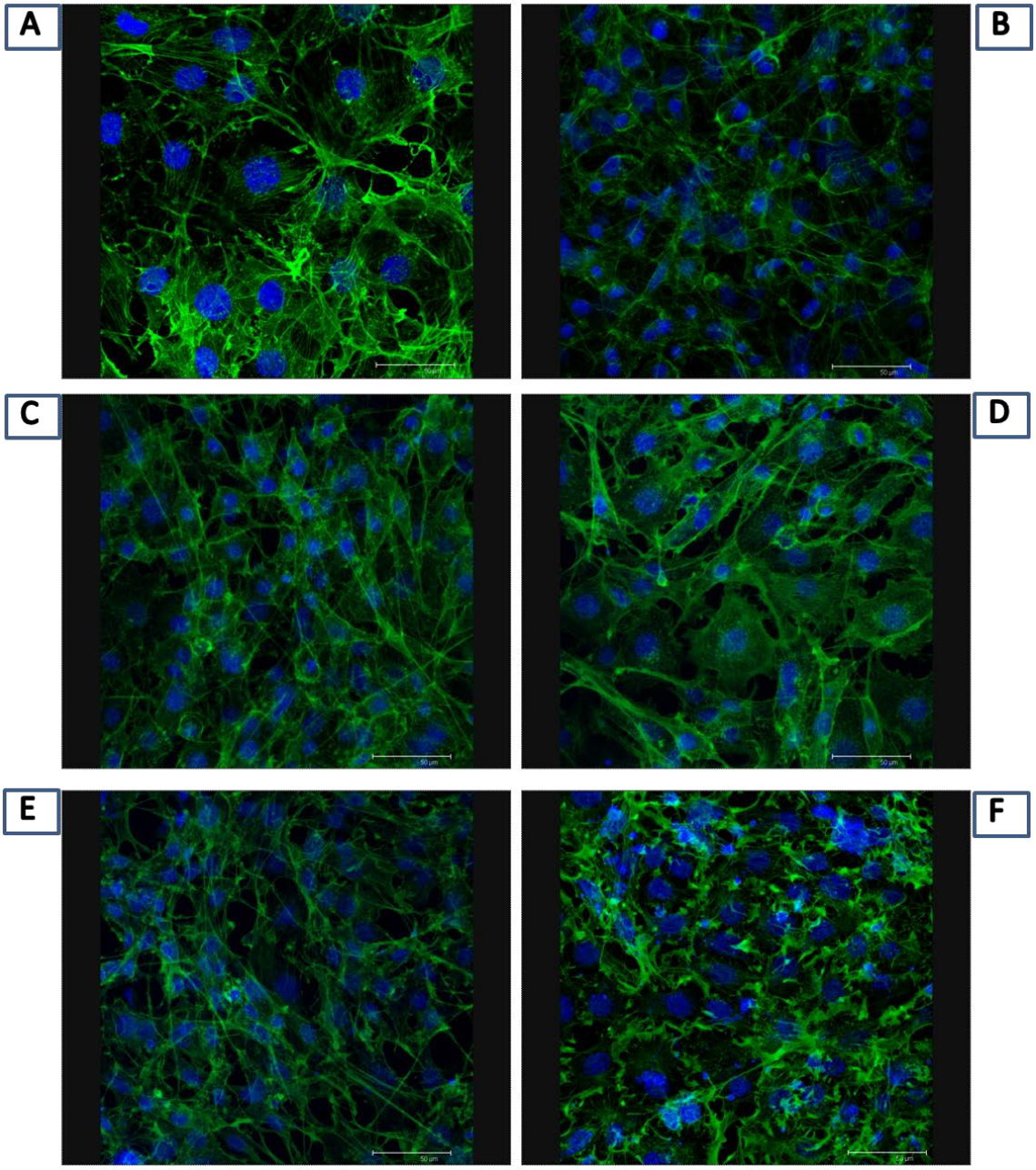

***Fig. 37* Immunofluorescence images of actin localization in 3T3-L1 cells differentiated in adipocytes for 3 days in the presence of GMG-43AC.** (A) preadipocytes; (B) adipocytes; (C) adipocytes 3T3-L1 cells treated with 300 µM GMG-43AC; (D) adipocytes 3T3-L1 cells treated with 500 µM GMG-43AC; (E) adipocytes 3T3-L1 cells treated with 1000 µM GMG-43AC; (F) adipocytes 3T3-L1 cells treated with 2000 µM GMG-43AC.

On the other hand, 3T3-L1 cells differentiated in the presence of GMG-43AC for 6 days show actin membrane ruffling starting from the dose of 500 µM (Fig. 38, panels B-F).

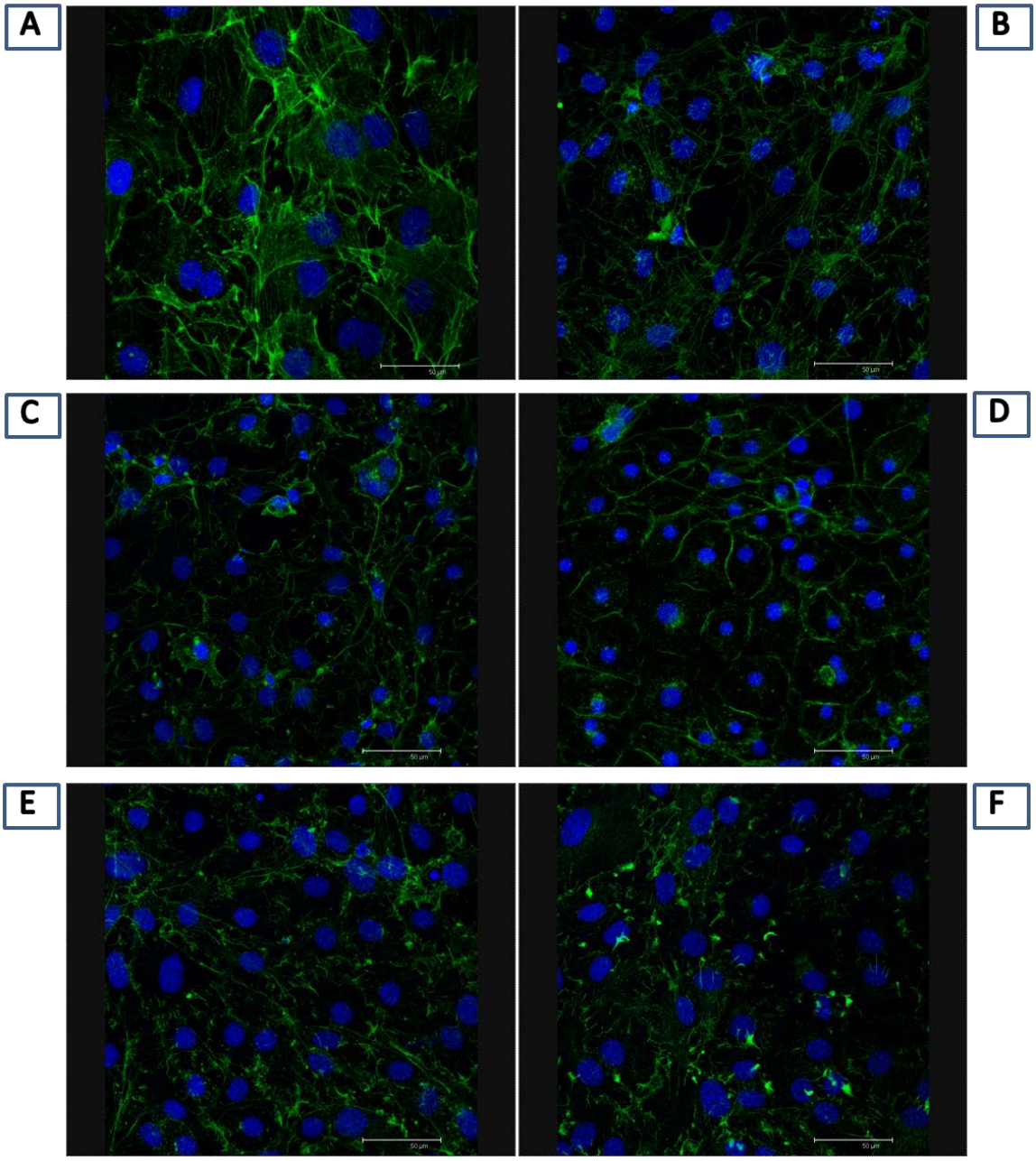

Fig. 38 **Immunofluorescence images of actin localization in 3T3-L1 cells differentiated in adipocytes for 6 days in the presence of GMG-43AC.** (A) preadipocytes; (B) adipocytes; (C) adipocytes 3T3-L1 cells treated with 300 µM GMG-43AC; (D) adipocytes 3T3-L1 cells treated with 500 µM GMG-43AC; (E) adipocytes 3T3-L1 cells treated with 1000 µM GMG-43AC; (F) adipocytes 3T3-L1 cells treated with 2000 µM GMG-43AC.

The effect of GMG-43AC on actin cytoskeleton reorganization in 3T3-L1 cells showed above was also investigated evaluating the expression of Small GTP binding protein RhoA by means of western blotting. Cells were differentiated in adipocytes for 7 days in the presence of investigated dosages of the drug and analyzed for presence of RhoA protein. RhoA is a master regulator of various cellular processes such as cell migration,

adhesion, cytokinesis, cell cycle progression, vesicular trafficking, and cytoskeletal regulation. RhoA works as a molecular switch, shuttling between the GDP-bound inactive form and the GTP-bound active form (Nakayama Y. et al,. 2009).

Our results suggest that after 7 days of differentiation RhoA was expressed at high levels in 3T3-L1 cells. Its levels were drastically reduced in a dose-dependent manner after the treatment with GMG-43AC (Fig. 39).

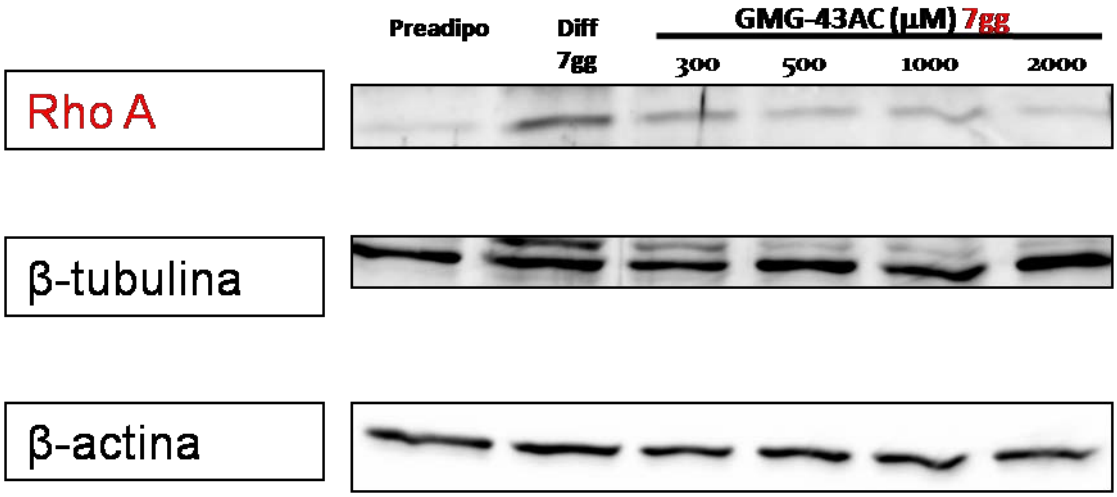

Fig. 39 **Western blotting analysis of RhoA in 3T3-L1 cells after 7 days of differentiation.** At the indicated time cells were lysed with RIPA buffer. Sixty micrograms of total protein extracts were separated in denaturing SDS-PAGE and transferred onto nitrocellulose membrane. RhoA antibody was used to this study.

5.2.5. GMG-43AC induced lipolysis of triglycerides in 3T3-L1 cells

In this experiments the effect of GMG-43AC on lipolysis was investigated. Lipolysis was assessed by the amount of glycerol released into media in 3T3-L1 cells treated for 2 (Fig. 40, green columns), 4 (Fig. 40, orange columns) or 7 (Fig. 40, blue columns) days with the drug (scheme 1) after the activation of HSL (see Materials and methods).

Our data shows that the amount of glycerol released into media was significantly increased during the adipocyte differentiation as expected. These results suggest that the activity of hormone-sensitive lipase (HSL) was raised for the duration of adipogenesis (Fig. 40). Moreover, as shown in this figure (green columns), exposure to GMG-43AC (doses 300-1000 μM) for the initial 2 days of differentiation, significantly increased the levels of glycerol released into the media by the 3T3-L1 cells. Contrastively, during the treatment with the dose 2000 μM we were not able to find any increase of glycerol release. Probably because of the fact that this dosage markedly abolished the differentiation of 3T3-L1 cells and synthesis of triglycerides. As a consequence, there was no substratum for activity of HSL (Fig. 40, green columns).

Then we evaluated the levels of glycerol on 4^{th} day of differentiation in the presence of the drug. Our results indicated that the amount of glycerol released into the media was down-regulated in dose-dependent manner (Fig. 40, orange columns). It might be an effect caused by insulin which was in the culture medium on the 4^{th} day of differentiation. It has been reported that insulin inhibits lipolysis via phosphorylation and activation of phosphodiesterase 3B, which in turn lowers cAMP levels (see Materials and Methods) (Kershaw EE et al., 2006). We suppose that GMG-43AC potentiated the inhibitory effect of insulin.

Thus, the significant increase of glycerol released into media was observed after 7 days treatment with 300 μM of GMG-43AC. However, dosages of 1000 and 2000 μM of drug markedly abolished the activity of HSL probably because of the fact that these dosages almost completely inhibited the differentiation process and as a consequence there was no substratum for activity of HSL (Fig. 40, blue columns).

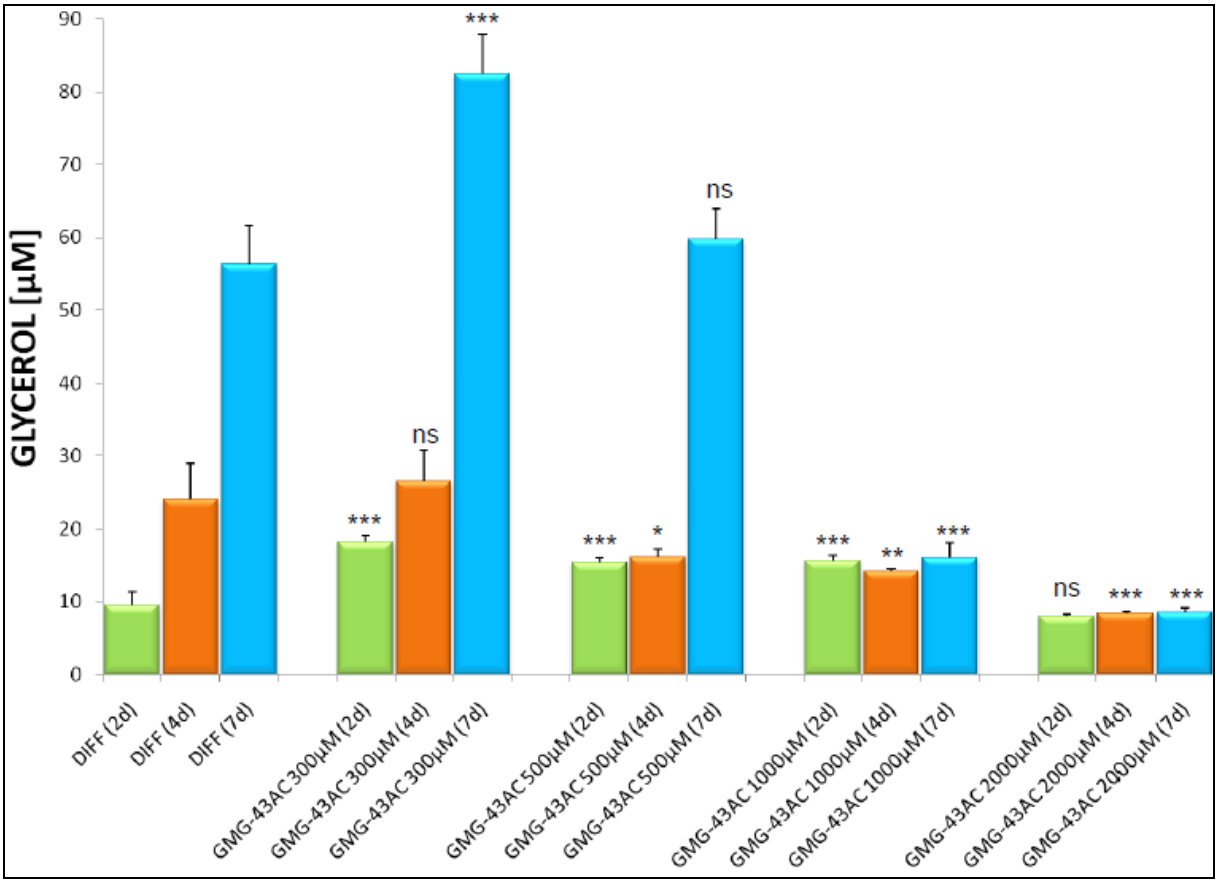

***Fig. 40* GMG-43AC stimulates lipolysis in 3T3-L1 cells.** 3T3-L1 preadipocytes were differentiated in presence of GMG-43AC (300-2000 µM) for 2(green), 4 (orange) and 7 (blue) days. Lipolysis was assessed by the amount of glycerol released into media. Data are expressed as mean ± S.E.M of 3 experiments. Significantly different from DIFF (2d), DIFF (4d) and DIFF (7d) respectively, *P<0.05, **P<0.01, ***P<0.001.

The effect of GMG-43AC on lipolysis was also investigated by means of real time RT-PCR. Our results show that exposure to GMG-43AC significantly reduced mRNA levels of HSL. This inhibitory action was evident starting from the dosage 1000 µM. Interestingly, the dosage of 300 µM raised mRNA levels (Fig. 41). Data was comparable to that of lipolysis measurement (Fig. 40).

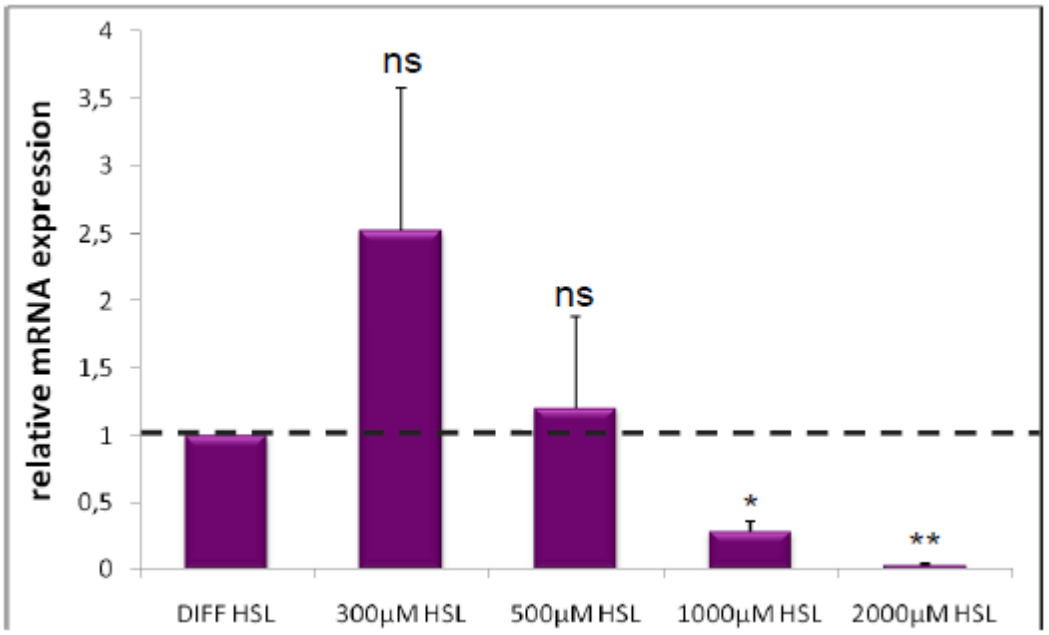

***Fig. 41* Analysis of HSL mRNA levels by Real-Time PCR after GMG-43AC treatment.** Levels of HSL mRNA were assessed in mature 3T3-L1 adipocytes after 10 days of treatment. Data are expressed as mean ± S.E.M of 3 experiments. Significantly different from DIFF HSL, *P<0.05, **P<0.01, ***<0.001.

5.2.6. Permanent inhibitory effect of GMG-43AC on adipocyte differentiation in 3T3-L1 cells

To examine whether GMG-43AC inhibitory effect on adipocyte differentiation was stable, the 3T3-L1 cells were differentiated in the presence of drug for 10 days (scheme 1) then the drug was removed and cells were maintained in the maintenance medium for the following 14 days without the drug. As shows in figure 42, the accumulation of triglycerides in two experiments was similar. Moreover, there were no any significant differences between 10-days treatment (Fig. 42, green columns) and 10-days treatment with following 14-days incubation (Fig. 42, red columns) (P<0.05). Collectively, 3T3-L1 cells differentiated in adipocytes in the presence of GMG-43AC and subsequently incubated in the maintenance medium for 14 days, did not restart to synthesize and accumulate triglycerides. Furthermore, the results suggested that GMG-43AC inhibition of triglycerides synthesis was permanent and achieved the significant effects at the maximal tested concentrations of 1000 µM and 2000 µM (P<0.001) (Fig. 42).

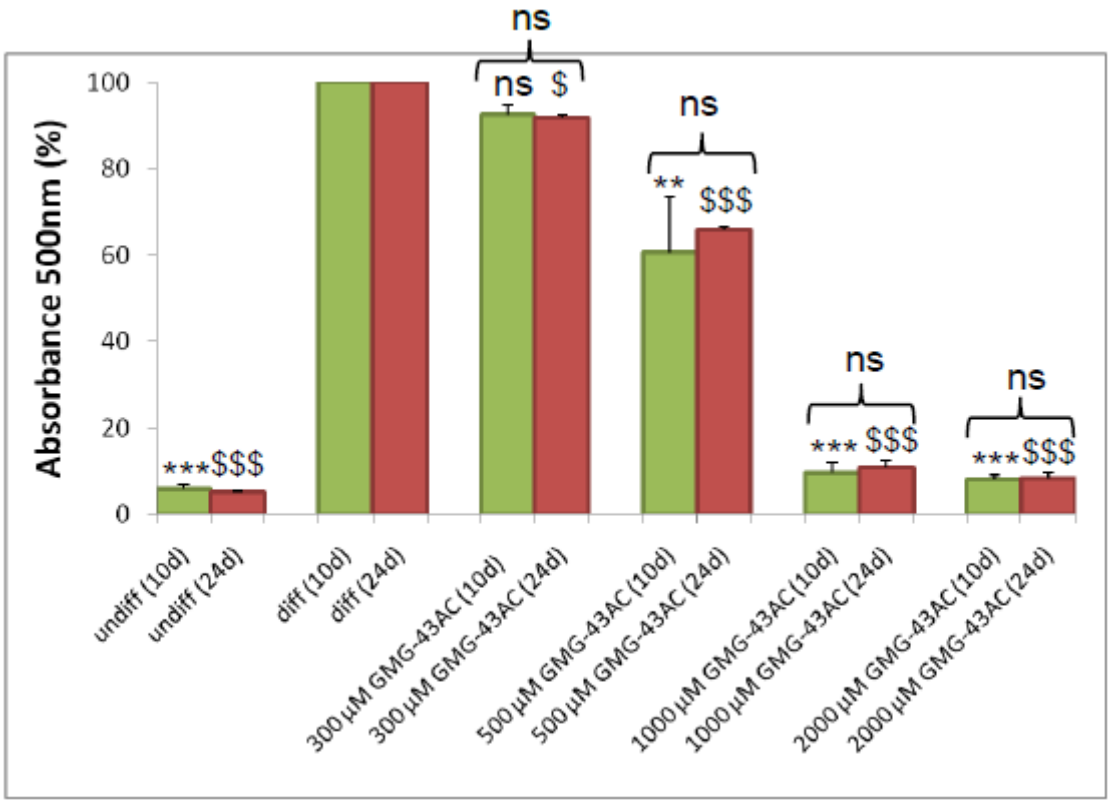

***Fig. 42* GMG-43AC permanently inhibits adipocyte differentiation in 3T3-L1 cells.** 3T3-L1 preadipocytes were differentiated in presence of GMG-43AC (300-2000 µM) for 10 days (green columns) and then cells were incubated in the maintenance medium for the following 14 days without the drug (red columns). Levels of accumulated triglycerides (labelled with Oil Red O) were quantified as evidenced by absorbance at 500 nm wavelength. Each experimental condition was assayed in triplicate and the graph is referred to the means of three independent experiments. Data are expressed as mean ± S.E.M of 3 experiments. Significantly different from DIFF (10d), *P<0.05, **P<0.01, ***P<0.001; Significantly different from DIFF (24d), $P<0.05, $$<P<0.01, $$$P<0.001.

The effect of GMG-43AC on adipocyte differentiation was also investigated after 5 weeks of drug treatment. Briefly, 3T3-L1 cells were differentiated as described before (see Materials and Methods) in the presence of GMG-43AC. The treatment was prolonged until 5 weeks to evaluate whether the doses 300 µM and 500 µM of the drug will become more effective in the inhibition of adipocyte differentiation.

Our results show that the dose of 500 µM of GMG-43AC left in the culture medium for 5 weeks became more effective in the inhibition of differentiation in respect to the treatment for 10 days (Fig. 43).

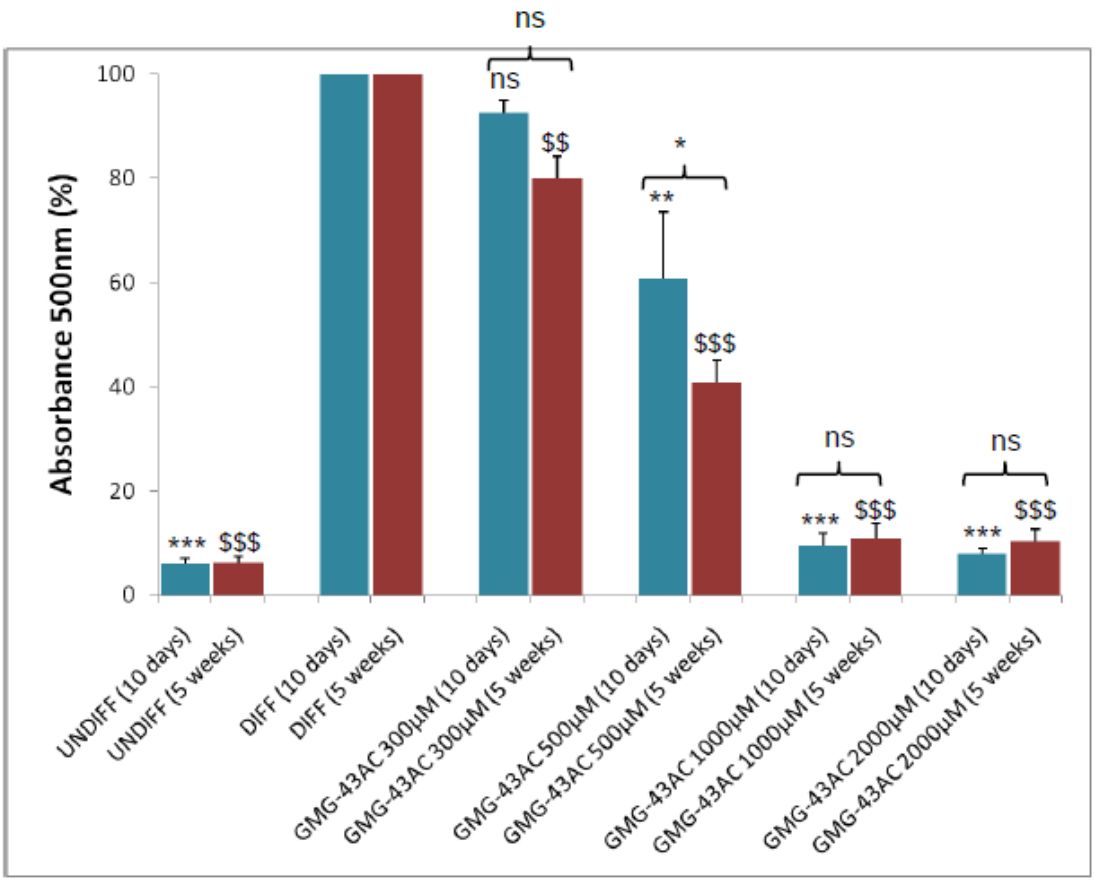

***Fig. 43* Treatment with GMG-43AC of 3T3-L1 cells for 5 weeks.** 3T3-L1 preadipocytes were differentiated in presence of GMG-43AC (300-2000 µM) for 10 days (blue columns) or 5 weeks (red columns). Levels of accumulated triglycerides (labelled with Oil Red O) were quantified as evidenced by absorbance at 500 nm wavelength. Each experimental condition was assayed in triplicate and the graph is referred to the means of three independent experiments. Data are expressed as mean ± S.E.M of 3 experiments. Significantly different from DIFF (10d), *P<0.05, **P<0.01, ***P<0.001; Significantly different from DIFF (24d), $P<0.05, $$<P<0.01, $$$P<0.001.

5.3. GMG-43AC inhibition of lipids accumulation during 3T3-L1 differentiation in adipocyte promoting medium: results of scheme 2

GMG-43AC was applied during the first 2 days of differentiation process, that is defined as the inductive period. In this condition the only effective dose was 2000 µM that caused an inhibition of 60%. The doses lower than 1000 µM had no effect (Fig. 44 and 45).

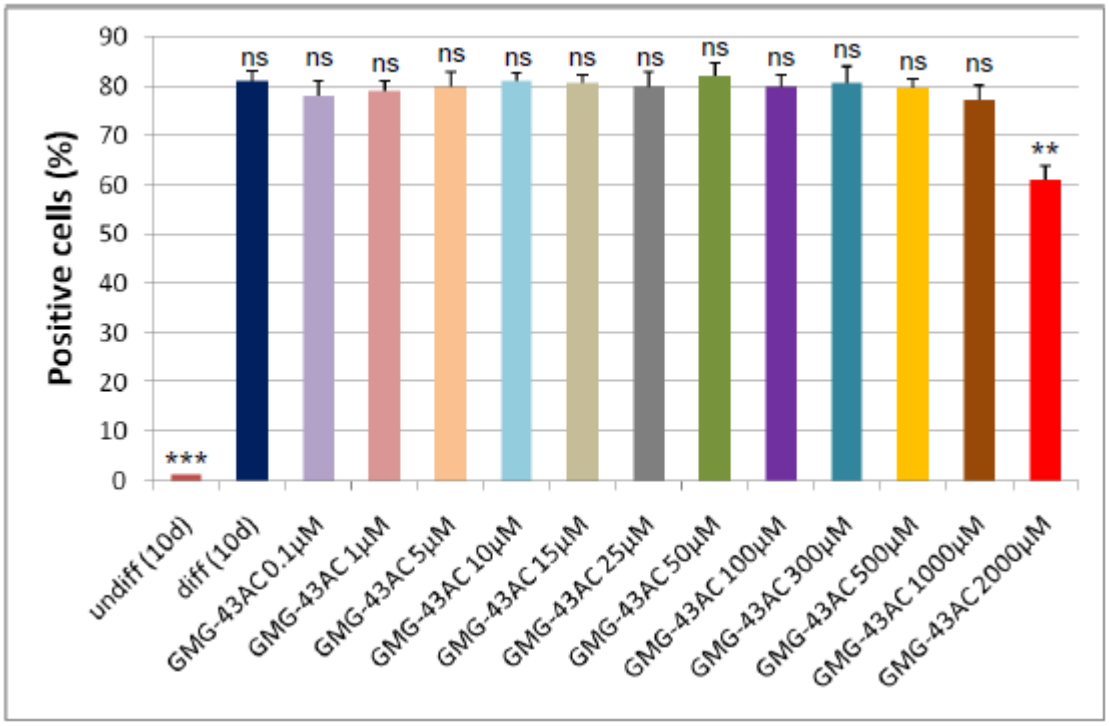

***Fig. 44* Oil Red O staining of undifferentiated 3T3-L1 cells and adipocytes.** Percentage of positive cells in reference to total cell population. Reported values (mean ± SEM) are the result of two independent experiments and for each experiment 5 fields were considered for each condition. Significantly different from DIFF (10d), *P<0.05, **P<0.01, ***P < 0.001.

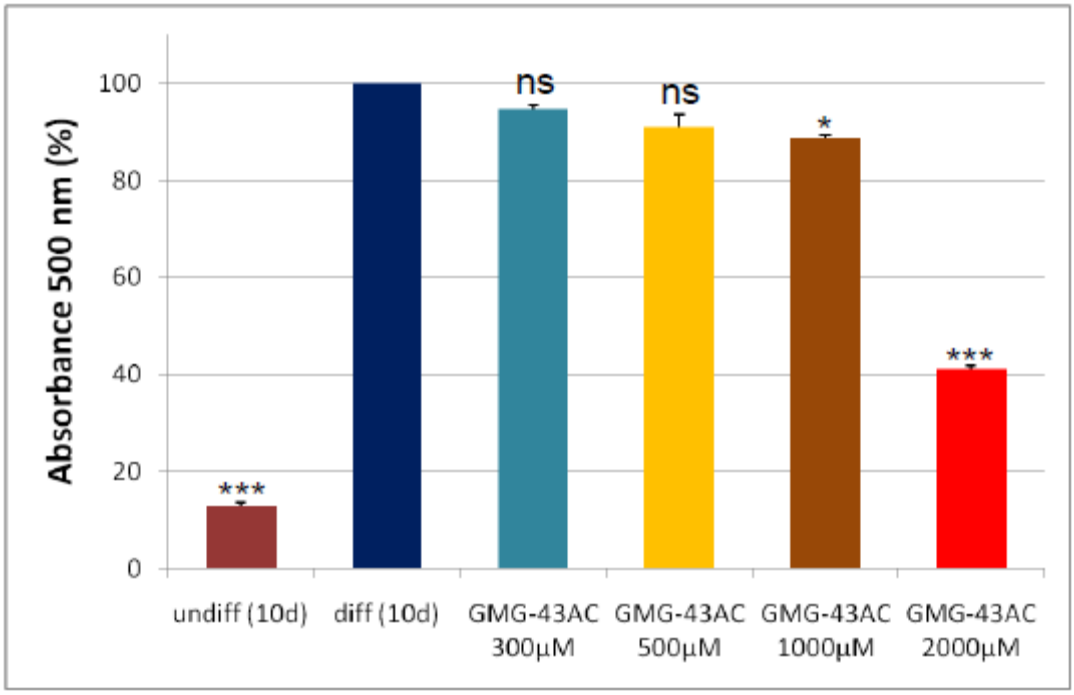

Fig. 45 Levels of accumulated triglycerides (labeled with Oil Red O) in 3T3-L1 undifferentiated cells and adipocytes as evidenced by quantitative absorbance at 500 nm wavelength. Each experimental condition was assayed in triplicate and the graph is referred to the means of one experiment. Values are mean ± SEM. Significantly different from DIFF (10d), *P<0.05, **P<0.01, ***P<0.001.

5.4. GMG-43AC inhibition of lipids accumulation during 3T3-L1 differentiation in adipocyte promoting medium: results of scheme 3

GMG-43AC was added to the culture medium after the first 48 hours of the induction and maintained for the following 48 hours. We observed an inhibition both adipogenesis and lipid accumulation. Figure 46 shows an Oil Red O staining of lipid accumulation in differentiated adipocytes (Fig. 46, panel A), this was previously reduced with increasing dosages (Fig. 46, panel B-D). The lowest effective dose was 300 µM (Fig. 47 and 48).

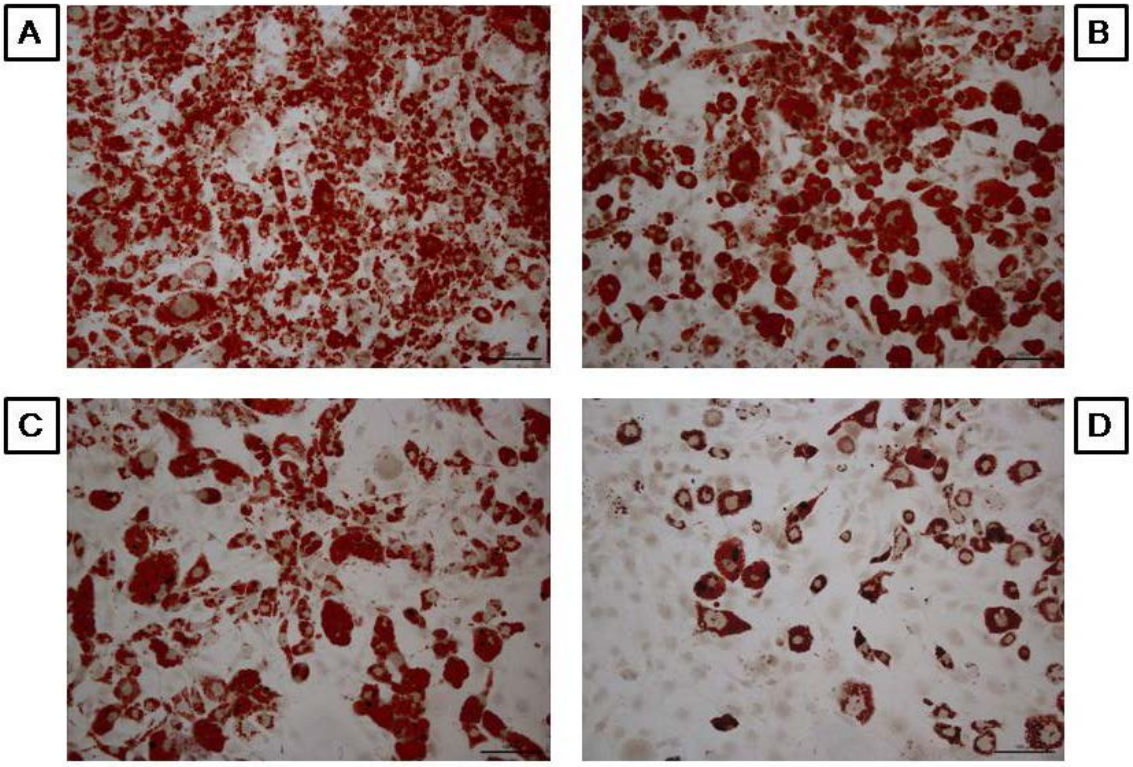

***Fig. 46* Oil Red O staining of 3T3-L1 cells with drug regimen type 3**. (A) adipocytes in no drug medium; (B) adipocytes grown in medium containing 500 µM GMG-43AC ; (C) adipocytes grown in medium containing 1000 µM GMG-43AC; (D) adipocytes grown in medium containing 2000 µM GMG-43AC.

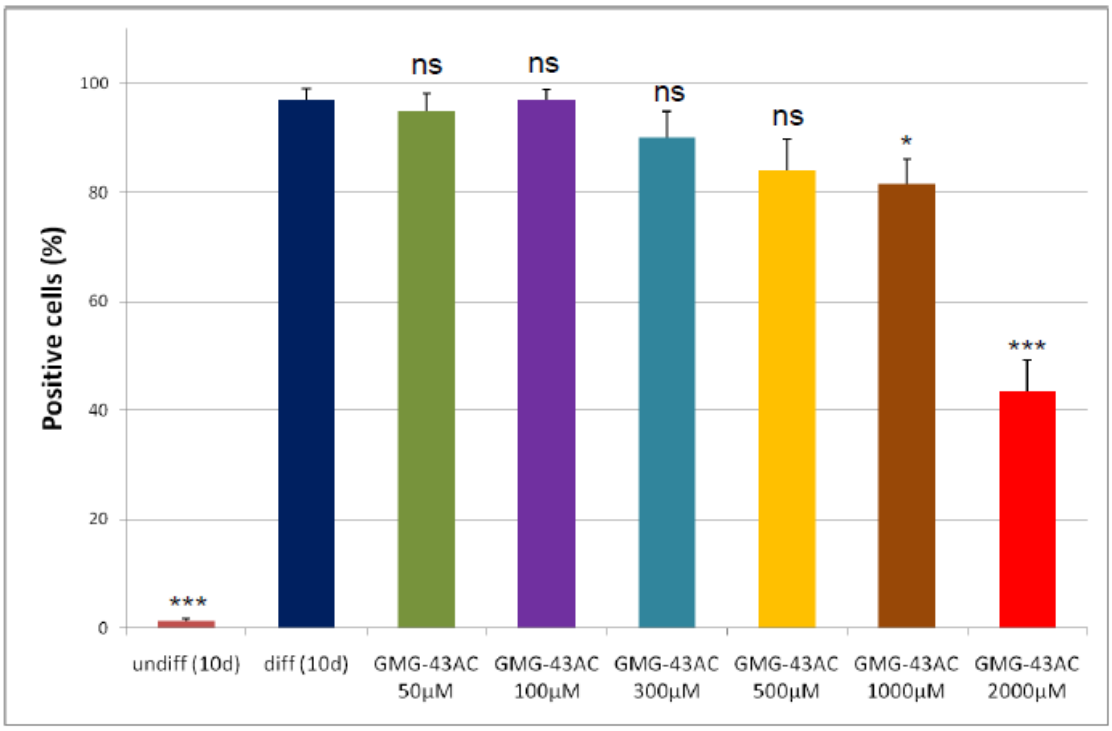

Fig. 47 Oil **Red O staining of undifferentiated 3T3-L1 cells and adipocytes.** Percentage of positive cells in reference to total cell population. Reported values (mean ± SEM) are the result of two independent experiments and for each experiment 5 fields were considered for each condition. Significantly different from DIFF (10d), *P<0.05, **P<0.01, ***P<0.001.

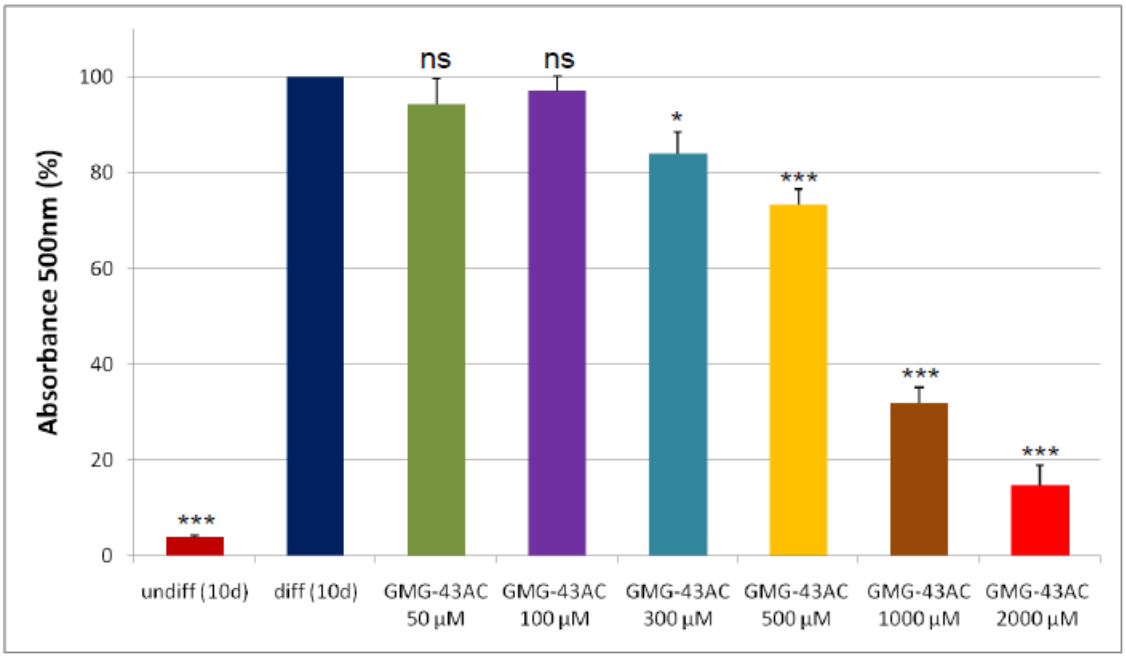

Fig. 48 Levels of accumulated triglycerides (labeled with Oil Red O) in 3T3-L1 undifferentiated cells and adipocytes as evidenced by quantitative absorbance at 500 nm wavelength. Each experimental condition was assayed in triplicate and the graph is referred to the means of three independent experiments. Values are mean ± SEM. Significantly different from DIFF (10d), *P<0.05, **P<0.01, ***P<0.001.

5.5. GMG-43AC inhibition of lipids accumulation during 3T3-L1 differentiation in adipocyte promoting medium: results of scheme 4

GMG-43AC treatment of 3T3-L1 cells through the differentiation period with the incubation starting immediately after the induction period (after the first 48 hours) inhibited adipocyte differentiation and lipid accumulation in a dose-dependent fashion (Fig. 49).

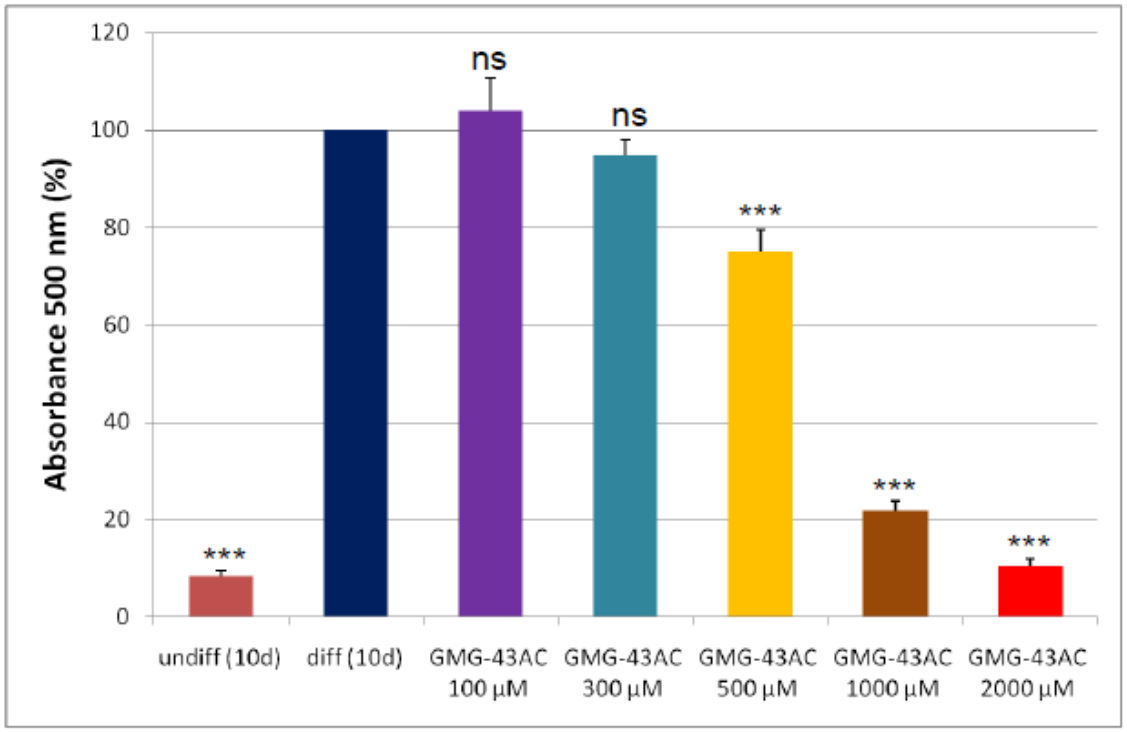

Fig. 49 Levels of accumulated triglycerides (labeled with Oil Red O) in 3T3-L1 undifferentiated cells and adipocytes as evidenced by quantitative absorbance at 500 nm wavelength. Each experimental condition was assayed in triplicate and the graph is referred to the means of three independent experiments. Values are mean ± SEM. Significantly different from DIFF (10d), *P<0.05, **P<0.01, ***P<0.001.

5.6. Reversion of adipogenesis process by GMG-43AC

GMG-43AC was capable of promoting the loss of accumulated triglycerides when fully differentiated 3T3-L1 cells were treated with the drug for 7 days (scheme 5). The effect was dose-dependent and significant with dose starting from 500 µM (Fig. 50, panels B-D; Fig. 51 and Fig. 52).

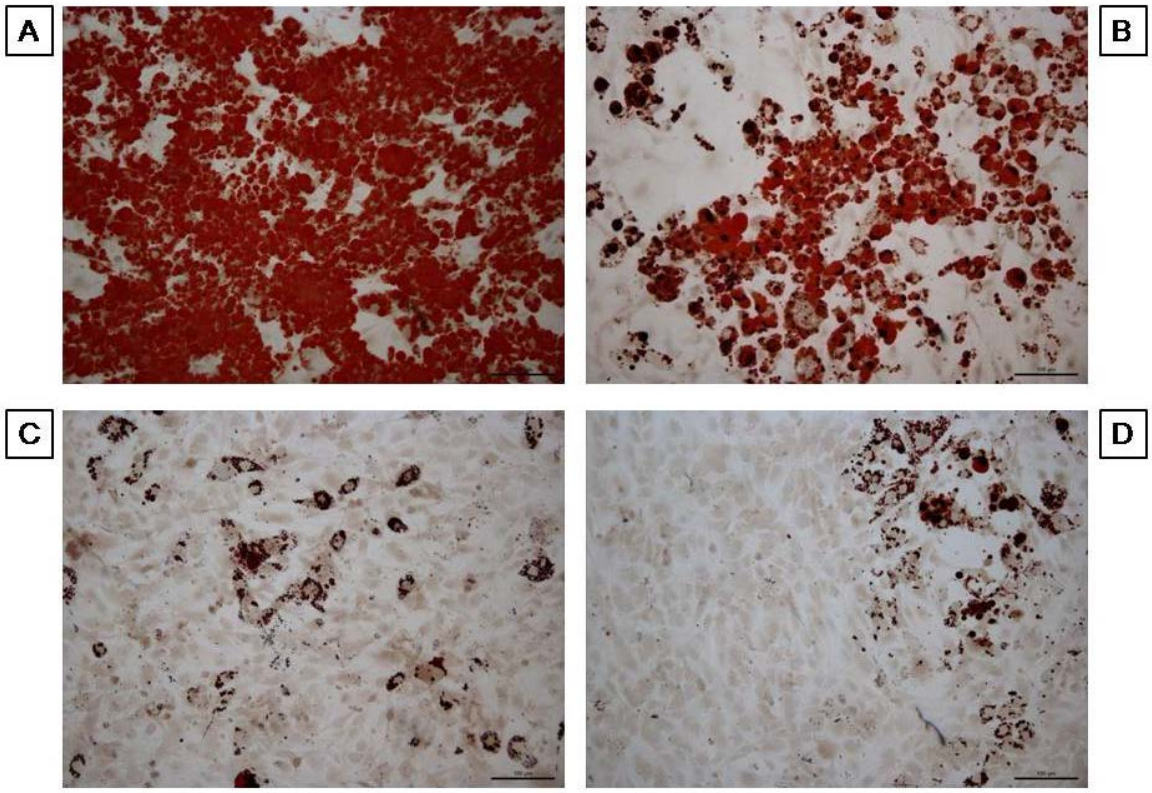

Fig. 50 *(A)* Oil Red O staining of adipocytes (differentiated for 15 days) ; (B) Loss of accumulated fat with GMG-43AC treatment (500 µM); (C) Loss of accumulated fat with GMG-43AC treatment (1000 µM); (D) Loss of accumulated fat with GMG-43AC treatment (2000 µM).

The quantification of the effects of GMG-43AC on the decrease of fat cell number and total fat was shown in figures 51 and 52. The reverting effect of GMG-43AC treatment can be observed from concentration of 500 µM and further.

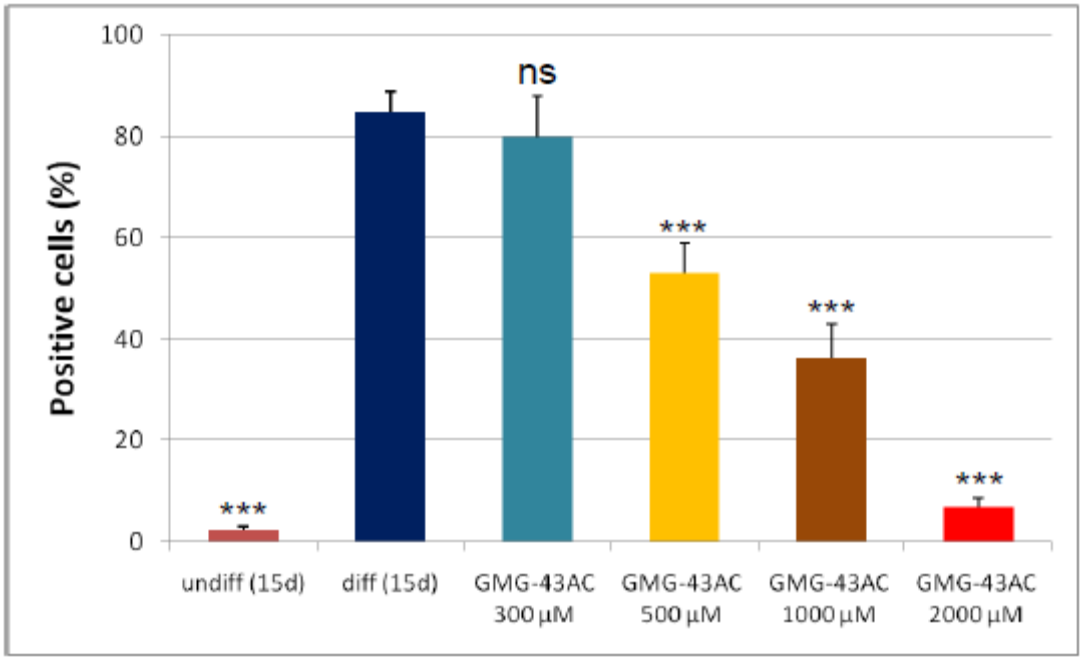

***Fig. 51* 7 days reversion with GMG-43AC.** Oil Red O staining of undifferentiated 3T3-L1 cells and adipocytes**.** Percentage of positive cells in reference to total cell population. Reported values (mean ± SEM) are the result of two independent experiments and for each experiment 5 fields were considered for each condition. Significantly different from DIFF (15d), *P<0.05, **P<0.01, ***P<0.001.

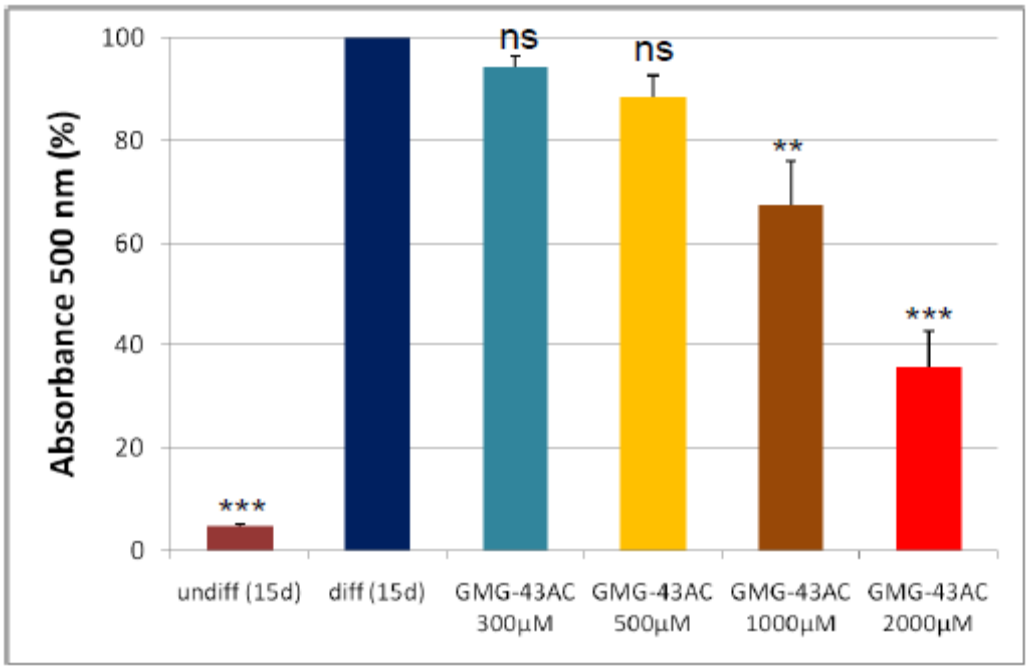

***Fig. 52* 7 days reversion with GMG-43AC.** Levels of accumulated triglycerides (labeled with Oil Red O) in 3T3-L1 undifferentiated cells and adipocytes after 7 days reversion with GMG-43AC as evidenced by quantitative absorbance at 500 nm wavelength. Each experimental condition was assayed in triplicate and the graph is referred to the means of two independent experiments. Values are mean ± SEM. Significantly different from DIFF (15d), *P<0.05, **P<0.01, ***P<0.001.

The ability of GMG-43AC to revert the adipocyte phenotype has also been confirmed at the molecular level. By means of western blotting analyses we assayed the expression of PPARγ and its phosphorylated form. The results show that after treating the differentiated 3T3-L1 cells with GMG-43AC the expression of PPARγ and its phosphorylated form decreased significantly. In all experimental sets the amount of proteins was normalized with the expression of β-actin (Fig. 53).

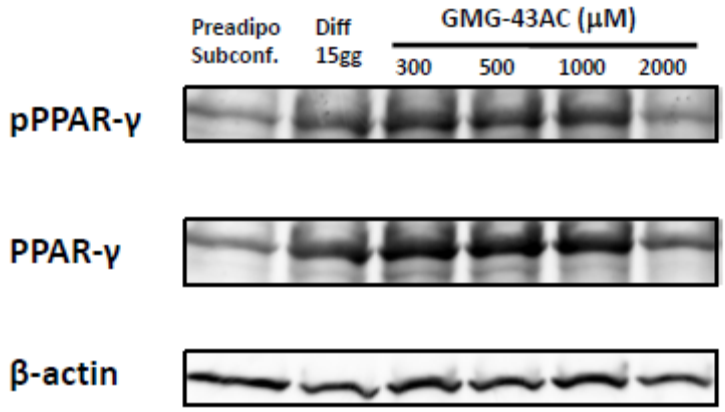

Fig. 53 **Western blotting analysis of molecular factors involved in adipogenesis.** At the end the incubation period cells were lysed with RIPA buffer. Sixty micrograms of total protein extracts were separated in denaturing SDS-PAGE and transferred to a nitrocellulose membrane. Specific antibodies were used to study the expression of proteins involved in the reversion of adipogenesis.

To examine if the reversal effect of GMG-43AC was stable, we differentiated the 3T3-L1 cells in adipocytes and then we treated the adipocytes with the drug according to scheme 5. Next, the drug was removed from the culture medium and the cells were incubated in the maintenance medium for the following 7 days. As figure 54 clearly shows, the effect of GMG43AG resulted to be reversible and the cells began again to produce and accumulate the drops of triglycerides.

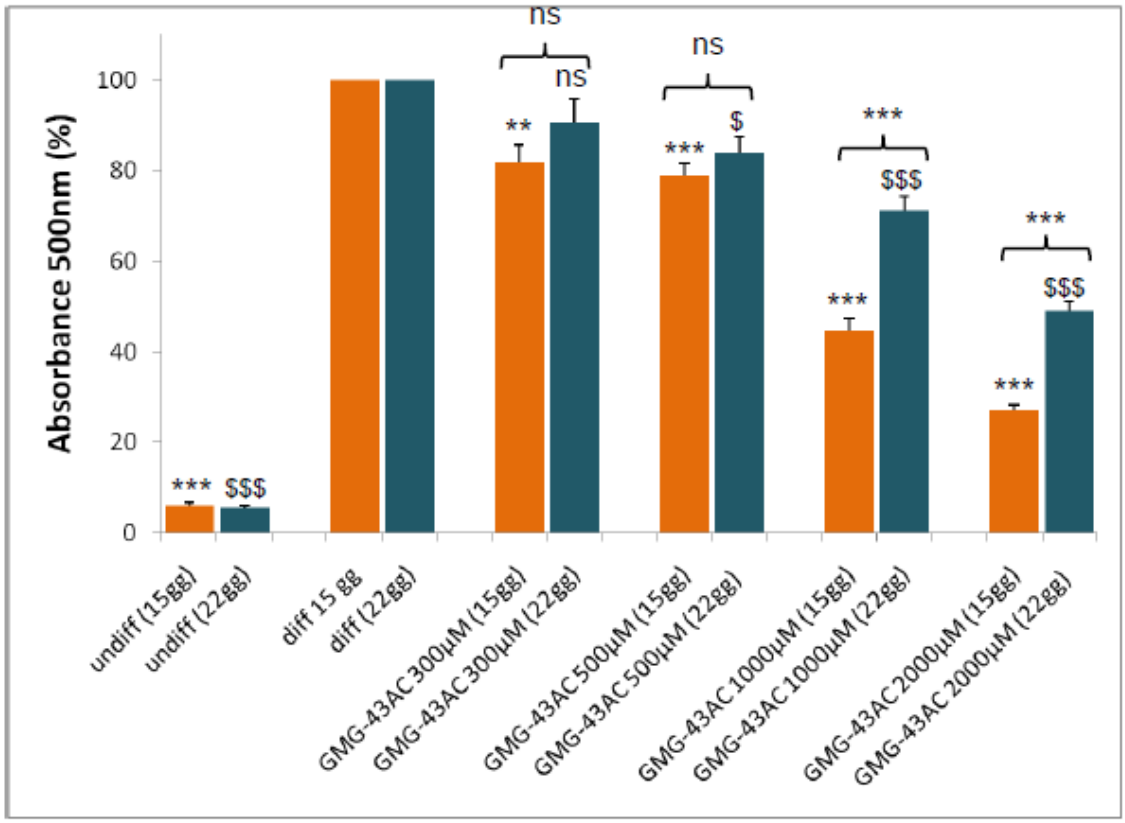

***Fig. 54* Comparison between 7 days reversion with GMG-43AC (scheme 5) and 7 days reversion with successive 7 days incubation in the maintenance medium.** Measurement of accumulated triglycerides. Orange columns: 7 days reversion; blue columns: 7 days reversion with successive 7 days incubation in the maintenance medium. Each experimental condition was assayed in triplicate and the graph is referred to the means of two experiments. Values are mean ± SEM. Significantly different from DIFF (15d), *P<0.05, **P<0.01, ***P<0.001. Significantly different from DIFF (22d), $P<0.05, $$<P<0.01, $$$P<0.001.

The effect of GMG-43AC on the reversion of the adipocyte phenotype has also been investigated after 14 days of treatment (as presented in scheme 6, materials and methods). Our results show that the drug administration to 3T3-L1 cells from day 8 of adipogenesis for successive 14 days reverted differentiation and lipid accumulation beginning from 300 µM (Fig. 54).

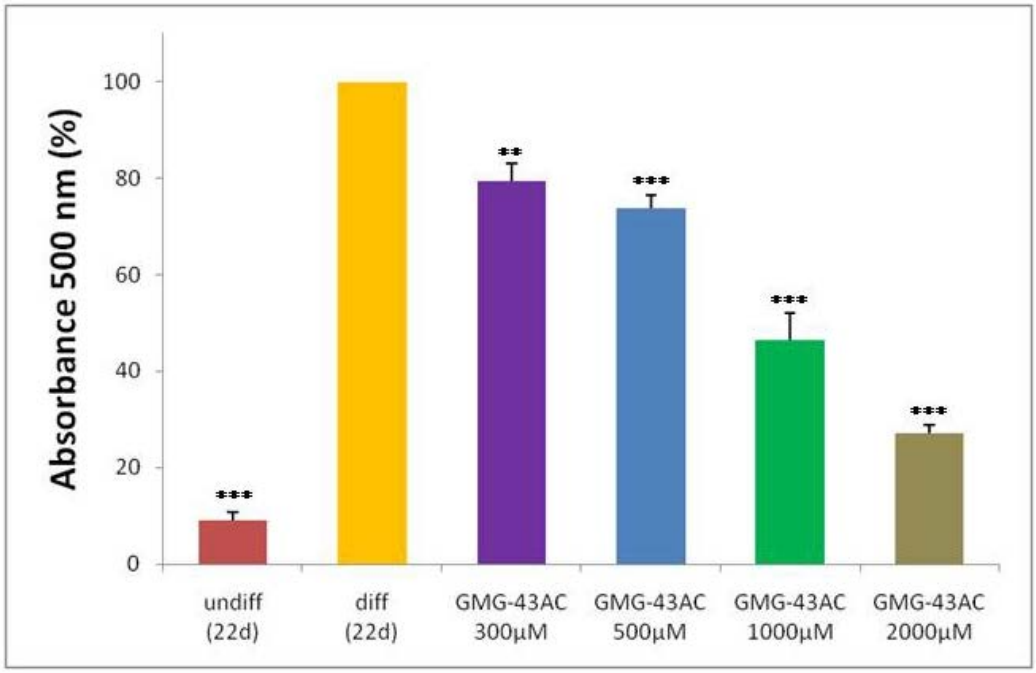

***Fig. 54* 14 days reversion with GMG-43AC.** Levels of accumulated triglycerides (labeled with Oil Red O) in 3T3-L1 undifferentiated cells and adipocytes after 14 days reversion with GMG-43AC as evidenced by quantitative absorbance at 500 nm wavelength. Each experimental condition was assayed in triplicate and the graph is referred to the means of two independent experiments. Values are mean ± SEM. Significantly different from DIFF (15d), *P<0.05, **P<0.01, ***P<0.001.

Comparison between two schemes of reversion

The following results show that GMG-43AC administration to 3T3-L1 cells for longer periods (14 days) reverted differentiation and lipid accumulation with a better efficiency and moreover, these results were observed by using lower doses (Fig. 55).

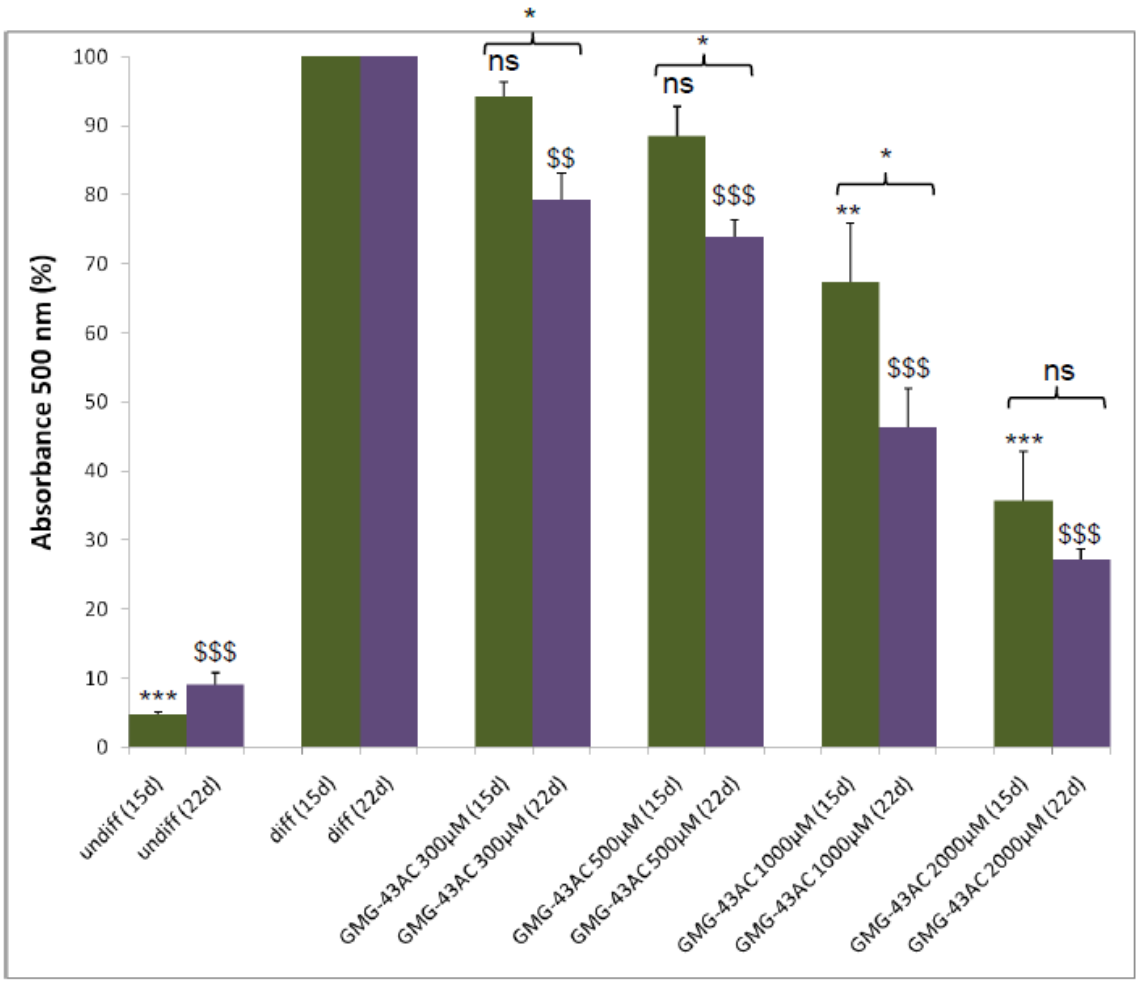

***Fig. 55* Comparison between two reversion of adipocyte differentiation with GMG-43AC.** Measurement of accumulated triglycerides. Green columns: 7 days reversion; violet columns: 14 days reversion. Each experimental condition was assayed in triplicate and the graph is referred to the means of two experiments. Values are mean ± SEM. Significantly different from DIFF (15d), *P<0.05, **P<0.01, ***P<0.001. Significantly different from DIFF (22d), $P<0.05, $$P<0.01, $$$P<0.001.

During the longer reversion period (as presented in scheme 6, materials and methods) we also investigated an effect of GMG-43AC on apoptosis. Apoptosis was studied by means of TUNEL assay and the results showed that the number of TUNEL positive cells was similar to that of adipocytes. The number of apoptotic cells was very low and reached a maximum percentage of 2% (Fig. 56).

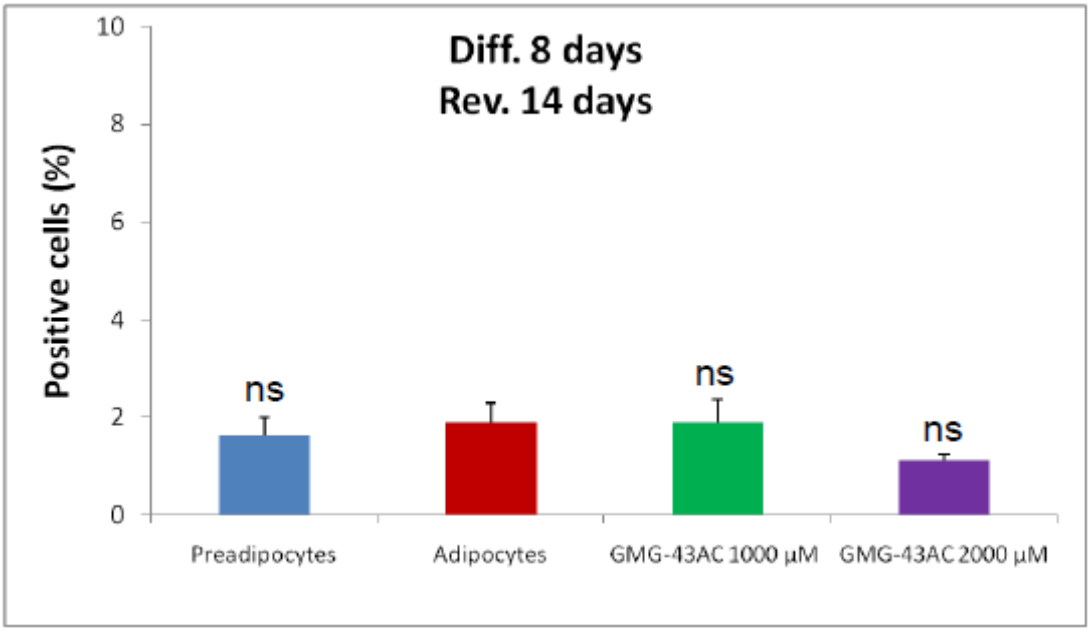

Fig. 56 **TUNEL assay after 14 days reversion with GMG-43AC.** Percentage of positive cells in reference to total cell population. Reported values (mean ± SEM) are the result of two independent experiments and for each experiment 8 fields were considered for each condition. Significantly different from ADIPOCYTES, *P<0.05, **P<0.01, ***P<0.001.

5.7. GMG-43AC inhibits lipid accumulation and promotes the loss of accumulated triglycerides in the differentiation induced by troglitazone: results of schemes 7 and 8

In these sets of experiments troglitazone (TZD; 10 µM), a potent inducer of adipocyte differentiation, was added to culture medium in presence of insulin (10 µg/ml), and the adipocyte differentiation was studied at day 10 (Han KL et al., 2006). GMG-43AC at a different concentration was added to the culture medium (in presence of TZD and insulin) at *day 0* and maintained until the end of the differentiation. Our results show that GMC-43AC was able to counteract synthesis and accumulation of triglycerides induced by TZD (Fig. 57 and 58). This inhibitory action was evident starting from the dosage 500 µM.

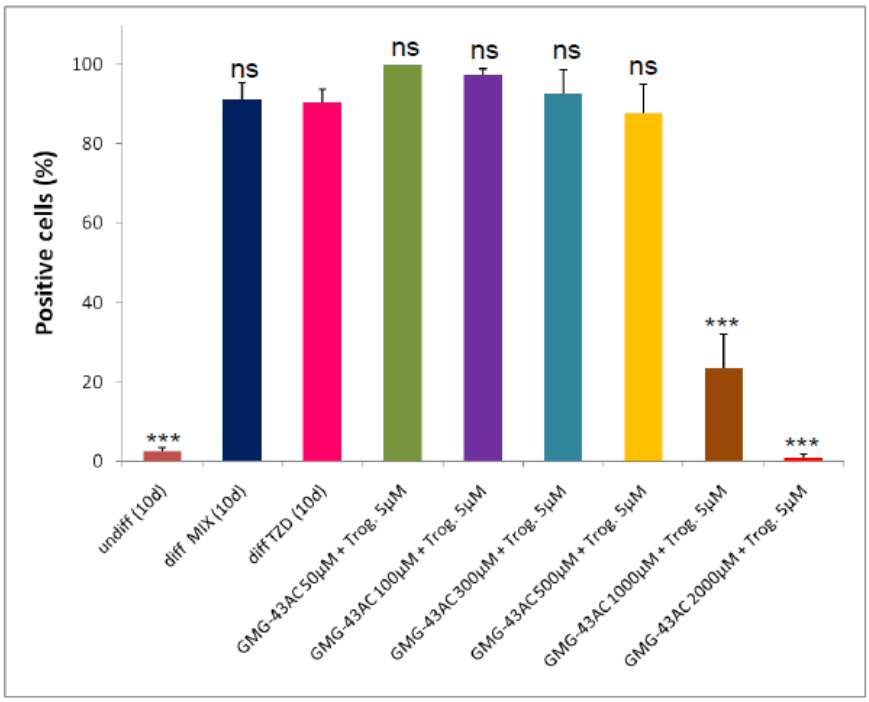

***Fig. 57* Oil Red O staining of differentiated 3T3-L1 adipocyte-like cells**. Quantification of positive cells in presence of troglitazone with or without GMG-43AC treatment. Reported values (mean ± SEM) are the result of three experiments. 8 fields were considered for each condition. Significantly different from DIFF TZD, *P<0.05, **P<0.01, ***P<0.001.

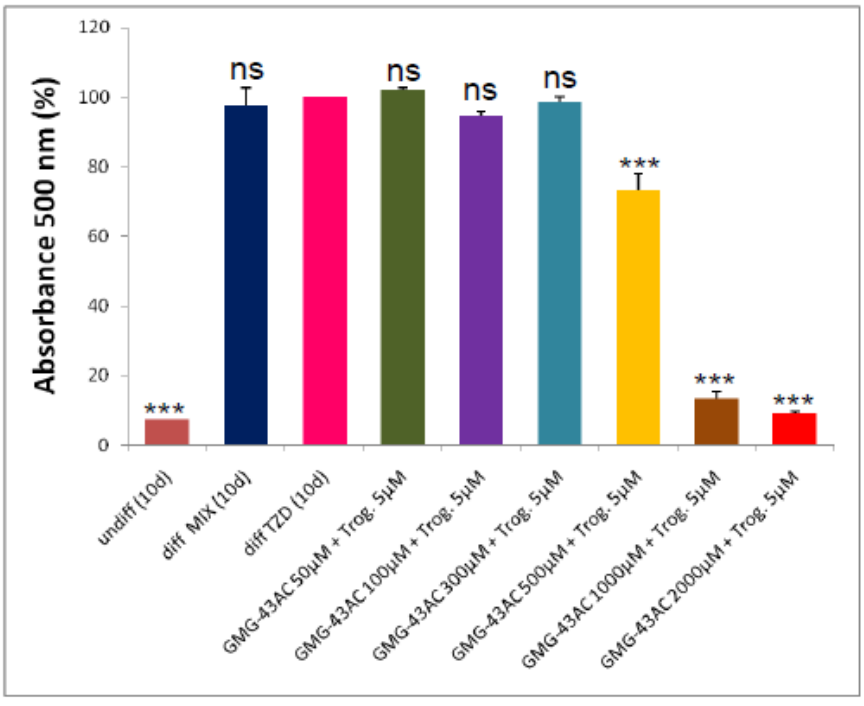

***Fig. 58* Oil Red O staining of differentiated 3T3-L1 adipose-like cells**. Measurement of accumulated triglycerides. Each experimental condition was assayed in triplicate and the graph is referred to the means of three experiments. Value are mean ± SEM. Significantly different from DIFF TZD, *P<0.05, **P<0.01, ***P<0.001.

The effect of GMG-43AC on TZD-promote adipocyte-like differentiation of 3T3-L1 cells was studied also in the reversion approach (see scheme 8, materials and methods). We observed previously that TZD used at two different concentrations (5 and 10 μM) was able to induce a 3T3-L1 cell differentiation with very similar efficiency. To investigate the GMG-43AC reversion capability of 3T3-L1 lipids accumulation the differentiation was induced with 5 μM TZD for 9 days, the investigated drug was added at different concentrations (see fig. 59) and maintained for 8 days. GMG-43AC treatment reverted the lipid accumulation in a dose-dependent fashion (Fig. 59).

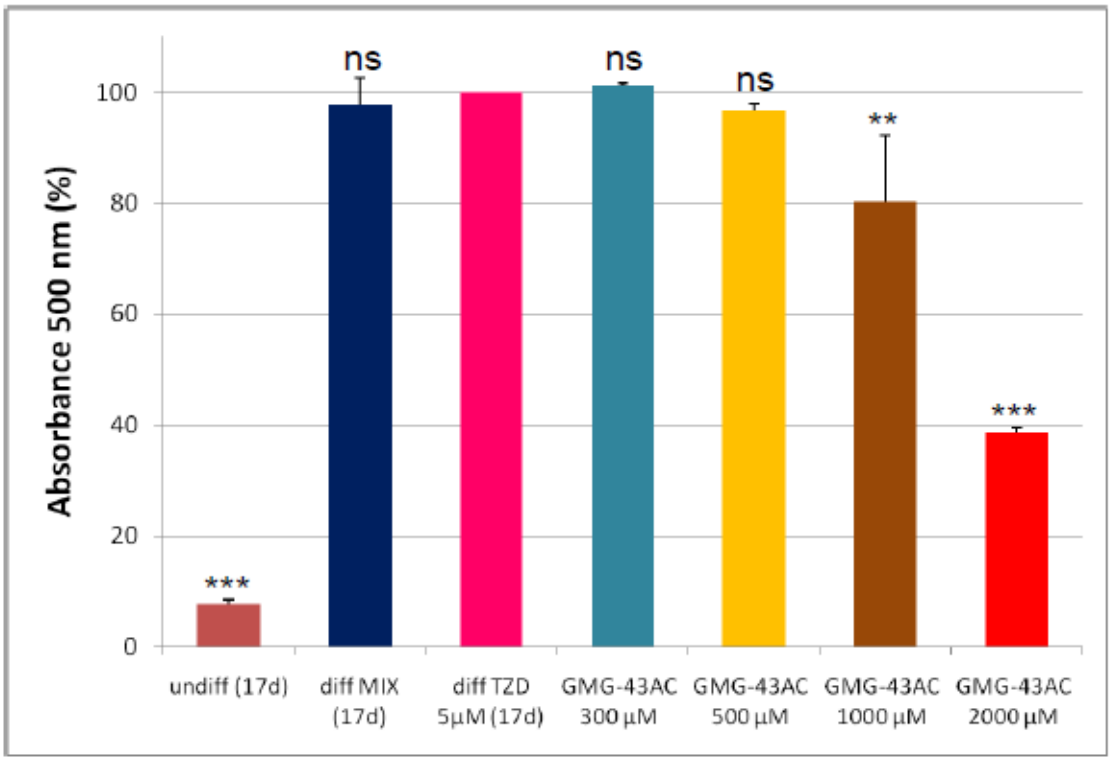

***Fig. 59* Oil Red O staining of differentiated 3T3-L1 adipose-like cells.** Measurement of accumulated triglycerides. Each experimental condition was assayed in triplicate and the graph is referred to the means of three experiments. Value are mean ± SEM. Value are mean ± SEM. Significantly different from DIFF TZD 5μM, *P<0.05, **P<0.01, ***P<0.001.

5.8. Comparison between the action of GMG-43AC, GMG-43AC raceme mixture, caffeine, L-Thyroxine and Eutirox® (50 µg)

The effect of GMG-43AC, its raceme mixture, caffeine, L-Thyroxine and Eutirox® on adipogenesis was investigated. The drugs were added in cultured medium at *day 0* and were maintained until *day 10 (*see scheme 9).

The results show that the GMG-43AC raceme mixture was as effective as GMG-43AC in inhibiting 3T3-L1 differentiation toward adipocyte phenotype (Fig. 35; green bar).

As reported earlier by other authors *(Nakabayashi H. et al., 2008),* caffeine failed to inhibit the differentiation of 3T3-L1 preadipocytes to adipocytes. The inhibition was of the order of 20% and independent of the dosages used (Fig. 35; violet bars).

Eutirox® is a drug which consists of levothyroxine sodium salt (50 µg/capsule) and was used at 130 nM final concentration. Treatment with this drug practically did not affect lipid accumulation during 3T3-L1 differentiation into adipocytes (Fig. 35; yellow bars).

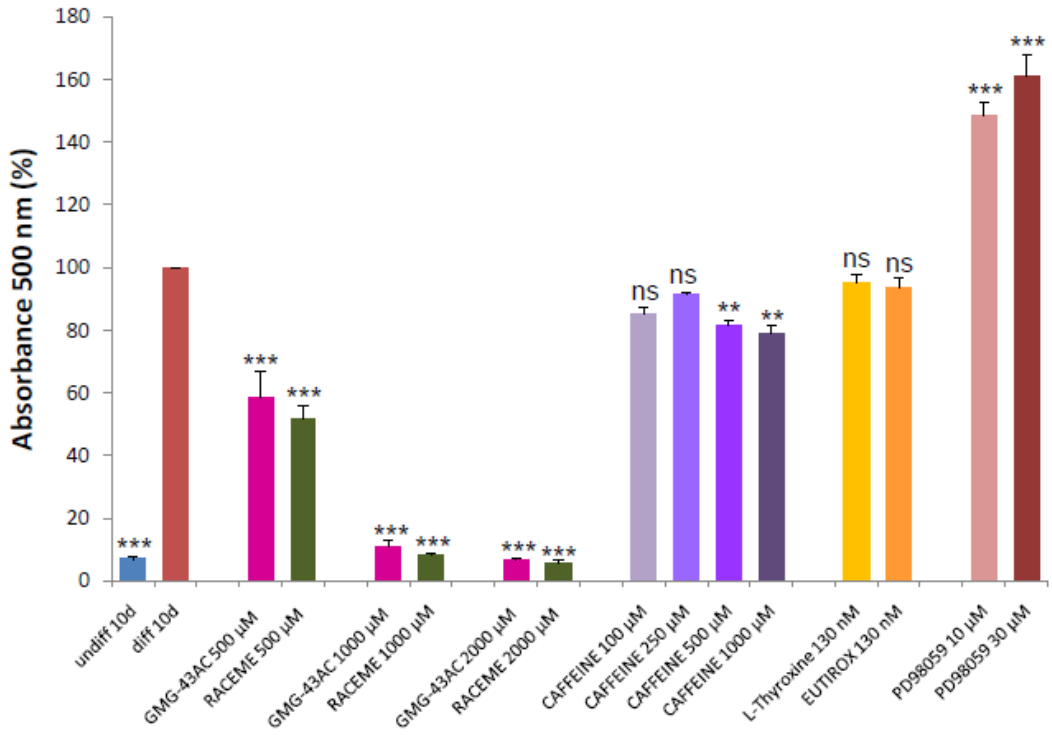

Fig. 60 Levels of accumulated triglycerides (labeled with Oil Red O) in 3T3-L1 undifferentiated cells and adipocytes as evidenced by quantitative absorbance at 500 nm wavelength. Each experimental condition was assayed in triplicate and the graph is referred to the means of three independent experiments. Values are mean ± SEM. Significantly different from DIFF 10d, *P<0.05, **P<0.01, ***P<0.001.

5.9. Comparison of the actions of GMG-43AC and PD98059 in adipogenesis

As shown above, the addition of GMG-43AC to the culture medium at *day 2* of differentiation process for the following 48 hours (see scheme 10, materials and methods), inhibited adipogenesis in a dose-dependent manner (Fig. 61 and 62). Differently, adipogenesis was enhanced when PD98059, an inhibitor of MEK1, was added to the culture medium. The results strongly suggested that the pathway MEK/ERK is likely involved in the adipogenesis process observed in 3T3-L1 cells (Fig. 61 and 62).

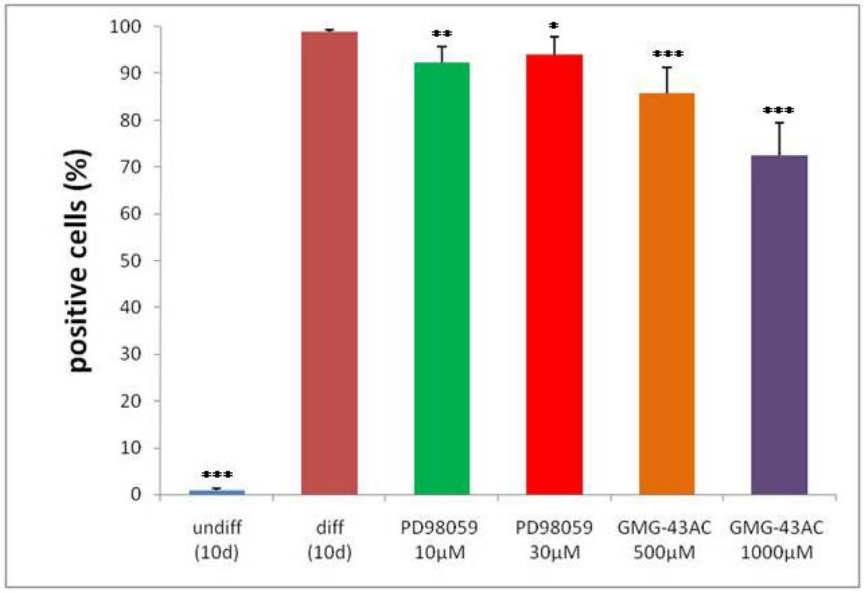

***Fig. 61* Oil Red O staining of undifferentiated 3T3-L1 cells and adipocytes.** Percentage of positive cells is refereed to total cell population. Reported values (mean ± SEM) are the result of two independent experiments and for each experiment 5 fields were considered for each condition. Significantly different from DIFF 10d, *P<0.05; **P < 0.01; ***P < 0.001.

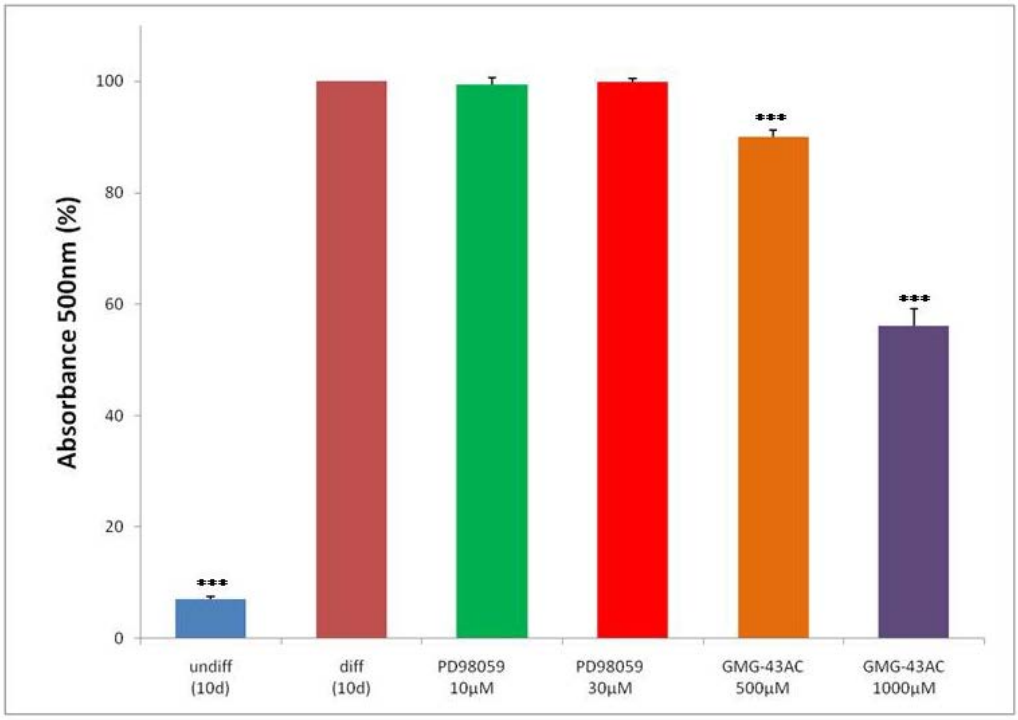

Fig. 62 Levels of accumulated triglycerides (labeled with Oil Red O) in 3T3-L1 undifferentiated cells and adipocytes as evidenced by quantitative absorbance at 500 nm wavelength. Each experimental condition was assayed in triplicate and the graph is referred to the means of three independent experiments. Values are mean ± SEM. Significantly different from DIFF 10d, *P<0.05, **P < 0.01, ***P < 0.001.

The effect of GMG-43AC and PD98059 on adipocyte differentiation was also evaluated after 4 days with PD98059 and GMG-43AC added between *days 2 and 4* (see scheme 11, materials and methods). It may be noted that the proadipogenic action of PD98059 was rapid almost doubling the lipid accumulation in 48 hours (Fig. 63).

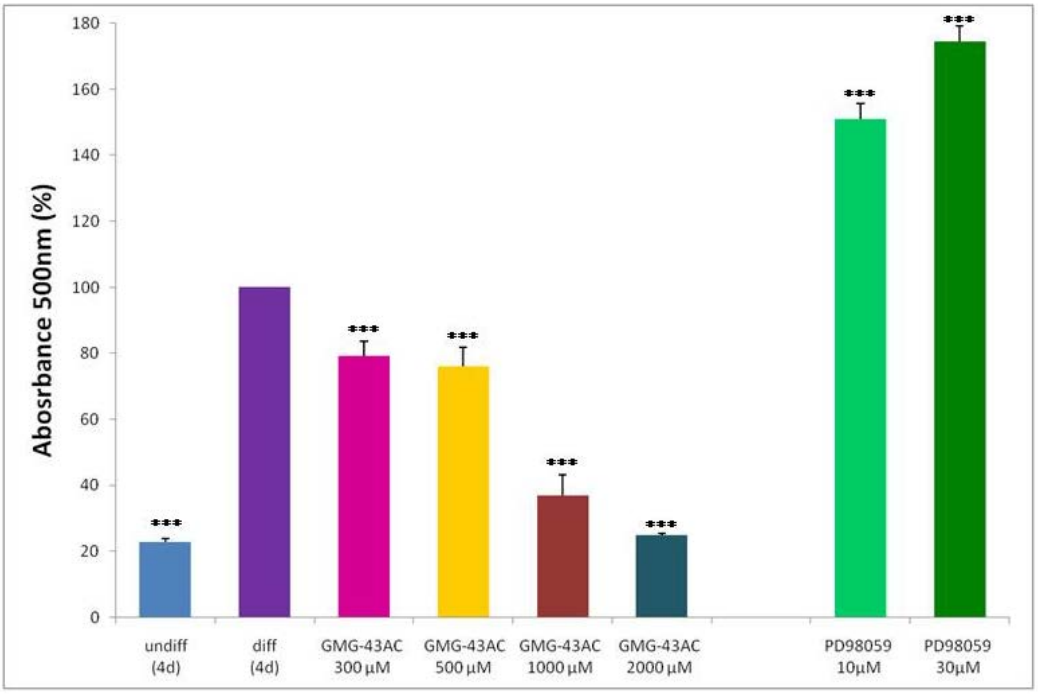

Fig. 63 Levels of accumulated triglycerides (labeled with Oil Red O) in 3T3-L1 undifferentiated cells and adipocytes as evidenced by quantitative absorbance at 500 nm wavelength. Each experimental condition was assayed in triplicate and the graph is referred to the means of three independent experiments. Values are mean ± SEM. Significantly different from DIFF 4d, *P<0.05, **P < 0.01, ***P < 0.001.

6. DISCUSSION

Obesity is one of the world's greatest public health challenges, contributing to morbidity and mortality through the increased risk for many chronic diseases, including type-2 diabetes mellitus, hypertension, dyslipidemia, coronary artery disease, stroke, osteoarthritis and certain forms of cancer (Youngson N. A. et al., 2012). The increasing prevalence of overweight and obesity has been observed worldwide, and obesity is likely to continue to be an important risk factor for the health of all populations, in particular of those in developing countries (Day F. R. et al., 2011). The main reasons of obesity are rising incomes, increasing urban populations, diets high in fats and simple sugars, and societal changes (Haidar Y. M. et al., 2011).

Obesity is defined as an excessively high amount of body fat or adipose tissue in relation to lean body mass. Obesity is characterized by the accumulation of adipose tissue, which expands due to an increase in adipocyte size (hypertrophy) and number (hyperplasia). Today several cellular models are available to study adipogenesis. The most frequently employed murine cell line is 3T3-L1. *In-vitro*-differentiated 3T3-L1 adipocytes have many characteristics of adipose cells *in vivo* (Gregoire F. M. et al., 1998).

In the present study, we evaluate the effect of GMG-43AC, the new experimental drug of Giuliani Sp. A. (Milan, Italy), on adipogenesis induced in post-confluent 3T3-L1 preadipocytes exposure to hormone stimulants (IBMX, DEX and insulin) or troglitazone, the potent activator of the peroxisome proliferator-activated receptor γ (PPARγ). In addition, we also investigate the ability of GMG-43AC to revert the adipocyte differentiation process induced by hormone mixture or troglitazone. We observed that GMG-43AC inhibited 3T3-L1 preadipocyte differentiation, and moreover it was able to revert the adipocyte phenotype into fully differentiated adipocytes.

It has been demonstrated that adipose alteration in tissue mass is related to the number of adipocytes. Thus, one strategy to reduce adiposity would be to reduce adipocyte numbers and fat content of adipocytes. Mature adipocytes are round and filled with many lipid droplets, which is distinguished from fibroblast-like preadipocytes in morphology. In the current study, GMG-43AC treatment reduced lipid accumulation in all investigated types of treatment, as shown by decreases in the percentage of lipid

area. These observations were further confirmed by by the counting of Oil Red O positive stained cells compared to all the cells indicated by hematoxylin staining.

Moreover, we showed that after the removal of the drug from 3T3-L1 cells differentiated in adipocytes in the presence of GMG-43AC, cells did not resume to synthesize and accumulate triglycerides. This result suggests that GMG-43AC inhibition of triglycerides synthesis was permanent and achieved the significant effects at the maximal tested concentration of 2000 µM. Interestingly, the drug left in the culture medium for a longer period (5 weeks) became more effective in the inhibition of differentiation with respect to the treatment for 10 days. Importantly, the results of TUNEL assay showed that the number of apoptotic cells was similar to that of non-treated adipocytes and reached a maximum percentage of 2%.

The differentiation of preadipocytes is regulated by a complex network of transcriptional factors. At the centre of this network are the nuclear receptor PPARγ and members of the C/EBP family (CCAAT/enhancer binding protein) which are important for adipogenesis. PPARγ has been shown to be sufficient and necessary for adipogenesis in 3T3-L1 preadipocytes and also is required for maintenance of the differentiated state (Gregoire F. et al., 1998; Xing Y. et al., 2010). Moreover, C/EBPα is essential for the terminal differentiation (Rosen E. D. et al., 2006). In the presence of hormonal stimulants, C/EBPβ and C/EBPδ levels increase rapidly and then synergistically stimulate the expression of PPARγ and C/EBPα, which cross-regulate each other through a positive feedback (Rosen ED et al., 2006; Xing Y et al., 2010). The present study indicated that GMG-43AC 10-day treatment inhibited the expression of PPARγ and C/EBPα both at mRNA and protein levels. Thus, GMG-43AC inhibited adipogenesis by suppressing the expression of the transcriptional factor required for the differentiation process. The downstream target genes of PPARγ and C/EBPα, such as FABP-4 and leptin, are adipocyte-specific genes involved in maintaining adipocyte phenotype. These genes are regulated by PPARγ and C/EBPα, and the inhibitory effect of GMG-43AC on FABP-4 and leptin may be mediated by inhibition of the two transcriptional factors' expression. Furthermore, the exposure to GMG-43AC during the initial 48 hours of adipocyte differentiation markedly reduced C/EBPβ levels in a dose-dependent manner with the exception of the dose of 300 µM. Interestingly, this dosage slowed down the degradation of C/EBPβ at 48 hours of differentiation. Our results show

that the experimental drug also markedly reduced protein levels of C/EBPδ at the lower dose of 300 μM. In contrast, further doses did not influence C/EBPδ expression after 48 hours of treatment.

Lipolysis plays a central role in the regulation of energy balance. The control of lipolysis is complex and involves multiple players such as lipolytic (β-adrenergic agonists, ACTH, etc.) and anti-lipolytic (insulin, adenosine, etc.) hormones, their cognate receptors and signalling pathways, lipid droplet-associated proteins, such as perilipins, and hormone-sensitive lipase (HSL), which is the rate-limiting enzyme responsible for mediating the hydrolysis of triglycerides (Greenberg A. S. et al, 2001). Our results showed that exposure to GMG-43AC significantly reduced activity and mRNA levels of HSL, and this inhibitory action was evident starting from the dosage of 1000 μM.

In summary, the data demonstrated that 10-day treatment with GMG-43AC inhibited 3T3-L1 preadipocyte differentiation via the suppression of C/EBPβ, PPARγ and C/EBPα, although the effects of GMG-43AC on adipose tissue remain to be determined *in vivo*. Inhibition of adipogenesis may regulate the amount of adipose tissue and, as a consequence, decrease the number of obese persons. Our study could provide an alternative approach for the treatment of obesity.

We also noticed that GMG-43AC was capable of promoting the loss of accumulated triglycerides when fully-differentiated 3T3-L1 cells were treated with the drug. Moreover, the reverting effect of GMG-43AC treatment can be observed from concentrations of 500 μM and greater. Unfortunately, this result was reversible and the cells were able to re-synthesize and accumulate the drops of triglycerides when they were left without the treatment. Interestingly, the drug left in the culture medium for the period of 14 days became more effective in the reversion of differentiation with respect to the treatment for 7 days. The accurate mechanisms that regulate loss of accumulated triglycerides in fully-differentiated adipocytes are still unclear. Our initial data have shown that exposure of the differentiated 3T3-L1 cells to GMG-43AC decreased the total expression of PPARγ.

In conclusion, further study is still needed to explore clearly the molecular mechanism explained by the inhibitory and reversion effects of GMG-43AC involved in the fat loss

phenomenon. However, GMG-43AC has the potential to be an innovative product for the prevention and treatment of obesity.

7. BIBLIOGRAPHY

1. Burgermeister E and Seger R. MAPK kinases as nucleo-cytoplasmic shuttles for PPARgamma. Cell Cycle, 2007, 6, 1539-1548.

2. Burgermeister E, Chuderland D, Hanoch T, Meyer M, Liscovitch M, Seger R. Interaction with MEK causes nuclear export and downregulation of peroxisome proliferator-activated receptor gamma. Mol Cell Biol., 2007, 27, 803-817.

3. Berger J and Moller DE. The mechanism of action of PPARs. Annu. Rev. Med., 2002, 53, 409-435.

4. Bost F, Aouadi M, Caron L, Binétruy B. The role of MAPKs in adipocyte differentiation and obesity. Biochimie, 2005, 87, 51-56.

5. Burns KA, Vanden Heuvel JP. Modulation of PPAR activity via phosphorylation. Biochim Biophys Acta., 2007, 1771, 952-960.

6. Cowherd RM, Lyle RE, McGehee RE Jr. Molecular regulation of adipocyte differentiation. Semin Cell Dev Biol., 1999, 10, 3-10.

7. Day FR, Loos JFR. Developments in Obesity Genetics in the Era of Genome-Wide Association Studies. J Nutrigenet Nutrigenomics, 2011, 222-238.

8. Feng H, Zheng L, Feng Z, Zhao Y, Zhang N. The role of leptin in obesity and the potential for leptin replacement therapy. Endocrine, 2012, [Epub ahead of print].

9. Fernández-Galilea M, Matute-Pèrez P, Prieto-Hontoria P, Martinez A, Moreno-Aliaga M. Effects of lipoic acid on lipolysis in 3T3-L1 adipocytes. J Lipid Res, 2296-2306.

10. Freeman WM, Walker SJ, Vrana KE. Quantitative RT-PCR: pitfalls and potential. Biotechniques, 1999, 124-5.

11. Fève B. Adipogenesis: cellular and molecular aspects. Best Pract Res Clin Endocrinol Metab, 2005, 19, 483-499.

12. Friedman JM. A war on obesity, not the obese. Science, 2003, 856-858.

13. Garofalo RS, Orena SJ, Rafidi K, Torchia AJ, Stock JL, Hildebrandt AL, Coskran T, Black SC, Brees DJ, Wicks JR, McNeish JD, and Coleman KG. Severe diabetes, age-dependent loss of adipose tissue, and mild growth deficiency in mice lacking Akt2/PKB beta. J Clin Invest, 2003, 112, 197–208.

14. Green H, Kehinde O. An established preadipose cell line and its differentiation in culture II. Factors affecting the adipose conversion. Cell, 1975, 5, 19-27.

15. Greenberg AS, Shen WJ, Muliro K, Patel S, Souza SC, Roth RA, Kraemer FB. Stimulation of lipolysis and hormone-sensitive lipase via the extracellular signal-regulated kinase pathway. The Journal of Biological Chemistry, 2001, 276, 45456-45461.

16. Gregoire FM, Smas CM, Sul HS. Understanding adipocyte differentiation. Physiol Rev, 1998, 78, 783-809.

17. Haidar YM, Cosman BC. Obesity Epidemiology. Clin Colon Rectal Surg, 2011, 205-210.

18. Han KL, Jung MH, Sohn JH, Hwang JK. Ginsensoide 20(S)-Protopanaxatriol (PPT) Activates Peroxisome Proliferator–Activated Receptor γ (PPARγ) in 3T3-L1 Adipocytes. Biol Pharm Bull, 2006, 29, 110-113.

19. Hansen JB, Petersen RK, Larsen BM, Bartkova J, Alsner J, Kristiansen K. Activation of peroxisome proliferator-activated receptor gamma bypasses the function of the retinoblastoma protein in adipocyte differentiation. J Biol Chem, 1999, 274, 2386-2393.

20. Higuchi R, Fockler C, Dollinger G, Watson R. Kinetic PCR analysis: real-time monitoring of DNA amplification reactions. Biotechnology, 1993, 1026-1030.

21. Hill JO, Peters JC. Environmental contributions to the obesity epidemic. Science, 1998, 1371-1374.

22. Hossain P, Kawar B, El Nahas M. Obesity and diabetes in the developing world - a growing challenge. N Engl J Med, 2007, 213-215.

23. Hu E, Kim JB, Sarraf P, Spiegelman BM. Inhibition of adipogenesis through MAP kinase-mediated phosphorylation of PPARgamma. Science, 1996, 274, 2100-2103.

24. Jéquier E. Pathways to obesity. Int J Obes Relat Metab Disord, 2002, S12-S17.

25. Kawaji A, Ohnaka Y, Osada S, Nishizuka M, Imagawa M. Gelsolin, an actin regulatory protein, is required for differentiation of mouse 3T3-L1 cells into adipocytes. Biol Pharm Bull., 2010, 33, 773-779.

26. Kershaw EE, Hamm JK, Verhagen LA, Peroni O, Katic M, Flier JS. Adipose triglyceride lipase: function, regulation by insulin, and comparison with adiponutrin. Diabetes, 2006, 55, 148-157.

27. Jiang W, Miyamoto T, Kakizawa T., Sakuma T, Nishio SI, Tekeda T, Suzuki S, Hashizume K. Expression of thyroid hormone receptor alpha in 3T3-L1 adipocytes; triiodothyronine increases the expression of lipogenic enzyme and triglyceride accumulation. Journal of Endocrinology, 2004, 182, 295-302.

28. Kim JE and Chen J. Regulation of peroxisome proliferator-activated receptor-gamma activity by mammalian target of rapamycin and amino acids in adipogenesis. Diabetes, 2004, 53, 2748-2756.

29. Kim KJ, Lee OH, Lee BY. Fucoidan, a sulfated polysaccharide, inhibits adipogenesis through the mitogen-activated protein kinase pathway in 3T3-L1 preadipocytes. Life Sience, 2010, 86, 791-797.

30. Koopman R, Schaart G, Hesselink MK. Optimisation of oil red O staining permits combination with immunofluorescence and automated quantification of lipids. Histochem Cell Biol, 2001, 116, 63-68.

31. Livak KJ, Flood SJ, Marmaro J, Giusti W, Deetz K. Oligonucleotides with fluorescent dyes at opposite ends provide a quenched probe system useful for detecting PCR product and nucleic acid hybridization. PCR Methods Appl, 1995, 357-362.

32. Nakabayashi H, Hashimoto T, Ashida H, Nishiumi S, Kanazawa K. Inhibitory effects of caffeine and its metabolites on intracellular lipid accumulation in murine 3T3-L1 adipocytes. BioFactors, 2006, 34, 293-302.

33. Nakayama Y, Komuro R, Yamamoto A, et al. RhoA induces expression of inflammatory cytokine in adipocytes. Biochemical and Biophysical Research Communication, 2009, 379, 288-292.

34. Prusty B, Park BH, Davis KE, Farmer SR. Activation of MEK/ERK signaling promotes adipogenesis by enhancing peroxisome proliferator-activated receptor gamma (PPARgamma) and C/EBPalpha gene expression during the differentiation of 3T3-L1 preadipocytes. J Biol Chem, 2002, 29, 46226-46232.

35. Rangwala SM and Lazar MA. Transcriptional control of adipogenesis. Annu. Rev. Nutr., 2000, 20, 535-559.

36. Rosed ED, Hsu CH, Wang X, Sakai S, Freeman MW, Gonzales FJ, Spiegelman BM. C/EBPa induces adipogenesis through PPARg: a unified pathway. Genes & Development, 2002, 22-26.

37. Rosen ED, MacDougald OA. Adipocyte differentiation from the inside out. Nat Rev Mol Cell Biol, 2006, 7, 885-896.

38. Speakman JM. Obesity: the integrated roles of environment and genetics. J Nutr, 2004, 2090S-2105S.

39. Su TZ, Wang M, Oxender DL, Saltier AR. Troglitazone increases system A amino acid transport in 3T3-L1 cells. Endocrinology, 1998, 139, 832-837.

40. Sul HS. Pref-1: role in adipogenesis and mesenchymal cell fate. Mol Endocrinol. 2009, 23, 1717-1725.

41. Takai Y, Sasaki T, Matozaki T. Small GTP-binding proteins. Physiological Reviews, 2001, 81, 153-208.

42. Wang M, Wang JJ, Li J, Park K, Qian X, Ma JX, Zhang SX. Pigment epithelium-derived factor suppresses adipogenesis via inhibition of the MAPK/ERK pathway in 3T3-L1 preadipocytes. Am J Physiol Endocrinol Metab, 2009, 297, 1378-1387.

43. Youngson NA, Morris MJ. What obesity research tells us about epigenetic mechanism. Philos Trans R Soc Lond B Biol Sci, 2012, 1-13.

44. Xing Y, Yan F, Liu Y, Liu Y, Zhao Y. Matrine inhibits 3T3-L1 preadipocyte differentiation associated with suppression of ERK1/2 phosphorylation. Biochem Biophys Res Commun, 2010, 691-695.

45. Xu J, Liao K. Protein kinase B/AKT 1 plays a pivotal role in insulin-like growth factor-1 receptor signaling induced 3T3-L1 adipocyte differentiation. J Biol Chem., 2004, 279, 35914-35922.

8. PUBLICATION

cer (30) give rise to future applications of 2D pH sensors in studying tumor metabolism.

Acknowledgements

This work was supported by grants from the German Research Foundation DFG (grants BA3410/4–1 and WO669/9–1). Traumasept Wound Gel was supplied by Dr. August Wolff GmbH & Co. KG (Bielefeld, Germany).

Author contributions

S.S., R.J.M., O.S.W. and P.B. conceived the experiments. S.S., R.J.M., K.T.W., J.C. and D.F. performed the experiments. S.S., R.J.M. and D.F. analysed the data. S.S. and R.J.M. wrote the paper. S.G. helped to interpret data.

Conflict of interests

None declared.

References

1 Bickers D R, Lim H W, Margolis D *et al.* J Am Acad Dermatol 2006: **55**: 490–500.
2 Gurtner G C, Werner S, Barrandon Y *et al.* Nature 2008: **453**: 314–321.
3 Martin P. Science 1997: **276**: 75–81.
4 Schreml S, Szeimies R M, Prantl L *et al.* Br J Dermatol 2010: **163**: 257–268.
5 Schreml S, Szeimies R M, Karrer S *et al.* J Eur Acad Dermatol Venereol 2010: **24**: 373–378.
6 Dickinson B C, Chang C J. Nat Chem Biol 2011: **7**: 504–511.
7 Niethammer P, Grabher C, Look A T *et al.* Nature 2009: **459**: 996–999.
8 Yoo S K, Starnes T W, Deng Q *et al.* Nature 2011: **480**: 109–112.
9 Muller P, Schier A F. Dev Cell 2011: **21**: 145–158.
10 Bumke M A, Neri D, Elia G. Proteomics 2003: **3**: 675–688.
11 Olson E R. Mol Microbiol 1993: **8**: 5–14.
12 Borsi L, Balza E, Gaggero B *et al.* J Biol Chem 1995: **270**: 6243–6245.
13 Sharpe J R, Harris K L, Jubin K *et al.* Br J Dermatol 2009: **161**: 671–673.
14 Paradise R K, Lauffenburger D A, Van Vliet K J. PLoS One 2011: **6**: e15746.
15 Behne M J, Meyer J W, Hanson K M *et al.* J Biol Chem 2002: **277**: 47399–47406.
16 Hachem J P, Behne M, Aronchik I *et al.* J Invest Dermatol 2005: **125**: 790–797.
17 Goerges A L, Nugent M A. J Biol Chem 2003: **278**: 19518–19525.
18 Hinman C D, Maibach H. Nature 1963: **200**: 377–378.
19 Winter G D. Nature 1962: **193**: 293–294.
20 Winter G D, Scales J T. Nature 1963: **197**: 91–92.
21 Walpole G S. Biochem J 1914: **8**: 131–133.
22 Meier R J, Schreml S, Wang X D *et al.* Angew Chem Int Ed Engl 2011: **50**: 10893–10896.
23 Schreml S, Meier R J, Wolfbeis O S *et al.* Proc Natl Acad Sci U S A 2011: **108**: 2432–2437.
24 Schreml S, Meier R J, Wolfbeis O S *et al.* Exp Dermatol 2011: **20**: 550–554.
25 Fischer L H, Borisov S M, Schaeferling M *et al.* Analyst 2010: **135**: 1224–1229.
26 Borisov S M, Krause C, Arain S *et al.* Adv Mater 2006: **18**: 1511–1516.
27 Liebsch G, Klimant I, Krause C *et al.* Anal Chem 2001: **73**: 4354–4363.
28 Schaferling M. Angew Chem Int Ed Engl 2012: **51**: 3532–3554.
29 Neri D, Supuran C T. Nat Rev Drug Discov 2011: **10**: 767–777.
30 Arwert E N, Hoste E, Watt F M. Nat Rev Cancer 2012: **12**: 170–180.

Supporting Information

Additional Supporting Information may be found in the online version of this article:

Figure S1. Region of interest in a split skin donor site wound.

Figure S2. Demonstration of complete sensor removal.

Figure S3. Visualization of pH heterogeneity in wounds.

Figure S4. Visualization of bacteria-induced pH changes.

DOI: 10.1111/exd.12029
www.blackwellpublishing.com/EXD

Letter to the Editor

A specific combination of zeaxanthin, spermidine and rutin prevents apoptosis in human dermal papilla cells

Stephana Carelli[1], Danuta M. Hebda[1], Maria V. Traversa[1], Fanuel Messaggio[1], Giammaria Giuliani[2], Barbara Marzani[2], Anna Benedusi[2], Anna M. Di Giulio[1] and Alfredo Gorio[1]

[1]Department of Health Science, Laboratories of Pharmacology, University of Milan, Milan, Italy; [2]Research and Development, Giuliani SpA, Milan, Italy
Correspondence: Stephana Carelli, Department of Health Science, Laboratories of Pharmacology, University of Milan, via A. di Rudinì 8, 20142 Milan, Italy, Tel.: +390250323039, Fax: +390250323033, e-mail: stephana.carelli@unimi.it
Alfredo Gorio, Department of Health Science, Laboratories of Pharmacology, University of Milan, via A. di Rudinì 8, 20142 Milan, Italy, Tel.: +390250323032, Fax: +390250323033, e-mail: alfredo.gorio@unimi.it

Abstract: Hair follicle (HF) regression is characterized by the activation of apoptosis in HF cells. Dermal papilla cells play a leading role in the regulation of HF development and cycling. Human follicular dermal papilla cells (HFDPC) were used to investigate the protective activities of rutin, sperimidine and zeaxanthine. HFDP cell incubation with staurosporine caused apoptosis, which was completely inhibited by exposure to rutin (2.2 μM), spermidine (1 μM) and zeaxanthin (80 μM). These agents were much less effective when applied as single compounds. Moreover, treatment preserved the expression of anti-apoptotic molecules such as Bcl-2, MAP-kinases and their phosphorylated forms. In conclusion, the investigated agents may represent an effective treatment for the prevention of apoptosis, one of the leading events involved in hair bulb regression.

Key words: dermal papilla cells, hair follicle, rutin, spermidine, zeaxanthin

Accepted for publication 26 September 2012

Background

The hair follicle (HF) is a skin appendage with complex structure and functions. It is formed by an invagination of the dermis down to the hypodermis and is located in the subcutaneous tissue (1–4). Dermal papilla cells (DPCs), located in the bulbar zone of the HF, play a leading role in the regulation of HF development and cycling regeneration (5–7). DPCs are specialized cells with the ability to induce new HF formation (8,9). HF undergoes cycles in which stages of rapid growth and hair shaft formation (anagen) alternate with apoptosis-driven regression (catagen) and relative HF quiescence (telogen) (10). This cycle is regulated by factors that promote proliferation, differentiation and survival, while regression is characterized by the activation of apoptotic pathways in distinct cell populations (11–14).

Question addressed

The effects of three active compounds (sperimidine, rutin and zeaxanthin) were investigated in the counteraction of apoptosis in human dermal papilla cells (HFDPC).

Experimental design

The action of sperimidine, rutin and zeaxanthin was investigated in human follicular dermal papilla cells (HFDPC) maintained *in vitro*. Apoptosis was induced 24 h after incubation with 1 μM staurosporine added to the culture medium (15). Apoptosis was monitored by assaying caspase-3 activity and DNA fragmentation using a TUNEL assay and by examining the expression of pro- and anti-apoptotic proteins via Western blotting.

Results

Following a 24-h exposure to staurosporine (1 μM; 15), HFDPC showed marked activation of caspase-3, cytoskeletal degradation, nuclear blebbing and cellular fragmentation (Figs. S1A–C). Compounds were added at specific concentrations (details in Table SI; Fig. 1) to the growth medium together with 1 μM staurosporine, and 24 h later, caspase-3 activity was determined (see Data S1). Compounds were added alone (Fig. 1a), or in different combinations (Figs. 1–b–c). The most effective single agent was rutin, as at a concentration of 22 μM, it reduced caspase-3 activity by 50%. Sperimidine (1 μM) alone decreased caspase-3 activity by 40%, and zeaxanthin (8 μM) reduced activity by approximately 30%. Higher zeaxanthin concentrations had no protective activity; however, 8 μM of zeaxanthin co-administered with rutin (22 μM) enhanced the effect of rutin (Fig. 1b). The addition of spermidine or zeaxanthin to rutin enhanced the anti-apoptotic action of only 2.2 μM rutin (Fig. 1b). Almost all triple combinations resulted in an improved activity compared with the addition of a double combination (Fig. 1c). The most effective agent was rutin (2.2 μM), zeaxanthin (80 μM) and spermidine (1 μM). HFDPC exposed to staurosporine were subjected to apoptosis. However, when incubated with the active compounds (1 μM spermidine; 2.2 μM rutin; 80 μM zeaxanthin) and staurosporine, HFDPC maintained their normal shape and apoptosis was counteracted. Caspase-3 is normally present around the nucleus, but it increased in a diffuse manner throughout the cell after staurosporine exposure; drug treatment only mildly affected this increase. In HFDPC, treatment abolished the activation of caspase-3 (Fig. 1c) and DNA fragmentation, and the extent of cell death was reduced to almost control levels (Fig. S2A). The anti-apoptotic action of the compound mixture was also assessed in Outer Root Sheath (ORS) and mesenchymal stem cells by a TUNEL assay. We observed comparable results to those reported above for HFDPC (Fig. S2B). The expression of caspase-3 and PARP in HFDPC was enhanced by staurosporine and inhibited by treatment with spermidine, rutin and zeaxanthin (Fig. S3A). The execution of caspase-mediated apoptosis relies on the interaction between pro-apoptotic and anti-apoptotic members of the Bcl-2 family (16). The importance of the balance between Bcl-2 and Bax in the sensitivity of different hair bulb cell types to resisting DNA damage-induced apoptosis by ionizing irradiation was recently reported by Sotiropoulou et al. (14). In our study, we found that incubation with staurosporine modified the expression of Bcl-2 in HFDPC, thus creating a disequilibrium that was inhibited with treatment (Fig. S3B). The efficacy of drug treatment in counteracting apoptosis was further supported by the full preservation of Akt and ERK activities in those experimental conditions (Fig. S3C).

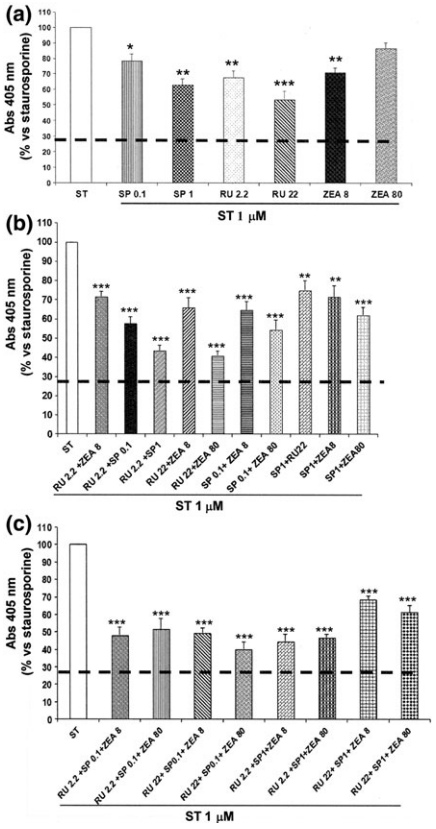

Figure 1. Reduction in caspase-3 activity and prevention of staurosporine apoptotic action in HFDP cells by active compounds. The actions of spermidine (SP), rutin (RU) and zeaxanthin (ZEA) were investigated following their addition to growth medium together with staurosporine (ST; 1 μM). (a) The effect of the compounds added as single agents; (b) and (c) the effect of different combinations. Caspase-3 activity is reported as O.D. measured at 405 nm as a percentage of the effects of ST treatment. The dashed line represents basal caspase-3 activity in untreated cells. Each experimental condition was assayed in triplicate, and reported data are the mean of three independent experiments. Values are mean ± SEM. *Significantly different from control, *$P < 0.05$; **$P < 0.01$; ***$P < 0.001$.

Conclusions

Hair follicles undergo cycles of organ transformation, in which stages of rapid growth and hair shaft formation (anagen) alternate with stages of apoptosis-driven HF regression (catagen) and relative HF quiescence (telogen) (10). The mediators responsible for regulating the cyclic action of the follicles include dozens of factors that have been studied in several cell signalling pathways, like those involved with the initiation of apoptosis (1,17). HFDPC play a major regulatory role in the complex cell biology of the hair follicle (18,19). During adult hair follicle cycling, the signalling between epithelial keratinocytes and underlying specialized mesenchymal dermal papilla cells induces stem cell proliferation and initiates the cascade of cell differentiation into the HF cell lineages. Moreover, HF regression is driven by apoptotic events that also involve DP cells during early catagen (20). For these reasons, HFDPC represent a reliable *in vitro* model system to investigate the action of potential therapeutic agents (21). In this study, we originally observed that apoptosis in DP cells was prevented by co-incubation with rutin, spermidine and zeaxanthin. The anti-apoptotic action of the compounds is likely due to suppression of caspase-3 expression, preservation of phosphorylated Akt and ERK, and counteraction of Bcl-2 loss. Previously, it was shown that flavonoids with a chemical structure similar to rutin exerted anti-apoptotic actions by blocking the activity of caspase-3 (22–25), zeaxanthin could reduce the extent of nuclear fragmentation and typical apoptotic events in photoreceptors (26), and polyamines may be involved in promotion of hair growth (27–29). Taken together, these data may explain the greater protective effects that our compounds exhibited in combination rather than as single agents. In conclusion, the combination of rutin, spermidine and zeaxanthin enhanced the survival of dermal papilla cells via the counteraction of apoptosis, one of the leading events involved in hair bulb regression.

Acknowledgements

SC designed the study, performed the research, analysed the data and wrote the paper; DMH contributed to the research; MVT contributed to the research; FM contributed to the research; GG, BM, AB and AMDG analysed the data; AG designed the study, analysed the data and wrote the paper. All authors revised the final form of the paper.

Funding sources

This work was supported in part by a grant from NIRECO to Alfredo Gorio.

Conflict of interests

GG serves as vice president of Giuliani SpA. AB and BM are employees of this company. No other relationships/conditions/circumstances present a potential conflict of interest.

References

1 Weinberg W C, Goodman L V, George C *et al.* J Invest Dermatol 1993: **100**: 229–236.
2 Soma T, Ogo M, Suzuki J *et al.* J Invest Dermatol 1998: **111**: 948–954.
3 Stenn K S, Paus R. Physiol Rev 2001: **81**: 449–494.
4 Schneider M R, Schmidt-Ullrich R, Paus R. Curr Biol 2009: **19**: 132–142.
5 Li Y, Li G Q, Lin C M *et al.* J Dermatol Sci 2005: **37**: 58–60.
6 Li Y, Lin C M, Cai X N *et al.* J Dermatol Sci 2005: **38**: 107–109.
7 Higgins C A, Richardson G D, Ferdinando D *et al.* Exp Dermatol 2010: **19**: 546–548.
8 Jahoda C A, Horne K A, Oliver R F. Nature 1984: **311**: 560–562.
9 Horne K A, Jahoda C A, Oliver R F. J Embryol Exp Morphol 1986: **97**: 111–124.
10 Paus R, Foitzik K. Differentiation 2004: **72**: 489–511.
11 Hashimoto T, Kazama T, Ito M *et al.* J Investig Dermatol Symp Proc 2001: **6**: 38–42.
12 Botchkareva N V, Ahluwalia G, Shander D. J Invest Dermatol 2006: **126**: 258–264.
13 Fulda S, Debatin K M. Recent Pat Anticancer Drug Discov 2006: **1**: 81–89.
14 Sotiropoulou P A, Candi A, Mascré G *et al.* Nat Cell Biol 2010: **12**: 572–582.
15 Ferraris C, Cooklis M, Polakowska R R *et al.* Exp Cell Res 1997: **234**: 37–46.
16 Youle R J, Strasser A. Nat Rev Mol Cell Biol 2008: **9**: 47–59.
17 Ohyama M, Zheng Y, Paus R *et al.* Exp Dermatol 2010: **19**: 89–99.
18 Reynolds A J, Jahoda C A. Development 1992: **115**: 587–593.
19 Oliver R, Jahoda C. The dermal papilla and the maintenance of hair growth. In: Rogers G E, Reis P J, Ward K A, Marshall R C, eds. The Biology of Wool and Hair. Cambridge: University Press, 1989: 51–67.
20 Kloepper J E, Sugawara K, Al-Nuaimi Y *et al.* Exp Dermatol 2010: **19**: 305–312.
21 Kwack M H, Kim M K, Kim J C *et al.* Exp Dermatol 2010: **19**: 1110–1112.
22 Boots A W, Haenen G R, Bast A. Eur J Pharmacol 2008: **585**: 325–237.
23 Bruynzeel A M, Abou El, Hassan M A *et al.* Br J Cancer 2007: **96**: 450–456.
24 Sanchez-Gonzalez P D, Lopez-Hernandez F J, Perez-Barriocanal F *et al.* Nephrol Dial Transplant 2011: **26**: 3484–3495.
25 Ahmad A, Khan M M, Hoda M N *et al.* Neurochem Res 2011: **36**: 1360–1371.
26 Chucair A J, Rotstein N P, Sangiovanni J P *et al.* Invest Ophthalmol Vis Sci 2007: **48**: 5168–5177.
27 Childs A C, Mehta D J, Gerner E W. Cell Mol Life Sci 2003: **60**: 1394–1406.
28 Ramot Y, Tiede S, Bíró T *et al.* PLoS ONE 2011: **6**: e22564.
29 Ramot Y, Pietilä M, Giuliani G *et al.* Exp Dermatol 2010: **19**: 7847–7890.

Supporting Information

Additional Supporting Information may be found in the online version of this article:

Figure S1. Induction of apoptosis in HFDP cells.
Figure S2. The counteractive effects of SP, RU, and ZEA in apoptosis and cell death.
Figure S3. SP, RU, and ZEA in combination prevent the expression of pro-apoptotic proteins and preserve Akt and MAP kinase activity.
Table SI. Concentrations of the active principles used.
Data S1. Materials and Methods.